

*THIS DELIVERABLE HAS BEEN SUBMITTED TO THE EUROPEAN COMMISSION AND IS CURRENTLY UNDER REVIEW. IT HAS NOT YET BEEN FORMALLY APPROVED AND MAY THEREFORE BE SUBJECT TO REVISION.*



## TWIN TRANSITION AND CHANGING PATTERNS OF SPATIAL MOBILITY: A REGIONAL APPROACH

### MOBI-TWIN D3.4 THE EFFECTS OF SPATIAL MOBILITY DURING TWIN TRANSITION ON REGIONAL INEQUALITY AND SUSTAINABILITY IN THE IDENTIFIED EU REGIONAL TYPOLOGIES

<b>Work package</b>	WP3: Assessing the impact of spatial mobility on EU regions. Updates and next steps
<b>Task</b>	Task 3.4: Assess the effects of spatial mobility on regional inequality and sustainability in the identified EU regional typologies
<b>Authors</b>	<b>Junyao He (RUG), Thanasis Ziogas (RUG), Jianhua Zhang (RUG), Wander Jager (RUG), Dimitris Ballas (RUG)</b> Contributors: Christina Mikropoulou (AUTH), Eleni Kalantzi (AUTH), Asya Salnikova (ESF)
<b>Lead Beneficiary</b>	RUG
<b>Reviewer(s)</b>	Asya Salnikova (ESF), Francesco Cellino (POLIMI)
<b>Status</b>	Final
<b>Version</b>	1.1
<b>Due Date</b>	28/02/2026
<b>Issue Date</b>	27/02/2026

<b>Dissemination Level</b>	PU



Funded by the  
European Union

MOBI-TWIN has received funding from the European Union's Horizon Europe Research and Innovation Programme under Grant Agreement no. 101094402. Content reflects only the authors' view and European Commission is not responsible for any use that may be made of the information it contains.

<b>Abstract</b>	<p>This document presents the simulation results and analyses produced using the MOBITWIN model, a spatial microsimulation and agent-based model (ABM) developed in the MOBI-TWIN project. It describes the modelling rationale, key design choices, and the experimental procedure used to evaluate residential mobility and population change under alternative scenarios and Twin Transition policy pathways. Building on the synthetic populations and spatial inputs prepared earlier in the project, the ABM simulates population trajectories over a ten-year horizon for five pilot systems and generates standardized outputs for post-processing and mapping. The reported outputs include pilot-wide population trajectories, population composition panels by key demographic and socioeconomic groups, and subregional indicators of population, equality, and sustainability. The report also provides delta-series maps that summarize percent changes relative to the baseline time point, enabling consistent comparison across scenarios, policy pathways, and time points. The analysis highlights policy-relevant insights on how scenario-driven risks and opportunities and transition contexts can alter mobility outcomes and population composition, and how these changes translate into evolving patterns of inequality and sustainability at the regional level. Combined with probabilistic expectations from the Delphi survey, the results support structured assessment of potential futures for left-behind regions and provide evidence that can inform regional strategy development within the MOBI-TWIN framework.</p>
-----------------	---

---

**Disclaimer**

The information and views set out in this publication are those of the author(s) and do not necessarily reflect the official opinion of the European Communities. Neither the European Union institutions and bodies nor any person acting on their behalf may be held responsible for the use which may be made of the information contained therein.

COPYRIGHT@ MOBI-TWIN CONSORTIUM 2023

---



Funded by the  
European Union

MOBI-TWIN has received funding from the European Union’s Horizon Europe Research and Innovation Programme under Grant Agreement no. 101094402. Content reflects only the authors’ view and European Commission is not responsible for any use that may be made of the information it contains.

<b>Version</b>	<b>Date</b>	<b>Partner</b>	<b>Description</b>
<b>0.1</b>	10/01/2026	RUG	Draft outline
<b>0.2</b>	01/02/2026	RUG	First draft (sent to reviewers - POLIMI and ESF)
<b>1.0</b>	21/02/2026	RUG	Second draft (sent to reviewers - POLIMI and ESF)
<b>1.1</b>	27/02/2026	RUG	Final version

## EXECUTIVE SUMMARY

This deliverable provides a systematic account of the methodological foundations, implementation, and analytical outputs of the MOBI-TWIN model which is underpinned by microsimulation and agent-based modelling (ABM) methods and tools developed within the MOBI-TWIN project under Work Package 3, Task 3.4. As a primary deliverable, it presents the ABM and the associated analytical workflow used to generate the reported simulation outputs. It builds on and extends the spatial microsimulation work produced in Task 3.1 by introducing a dynamic simulation layer to study residential mobility and to assess how population structure, inequality, and sustainability evolve over time under alternative scenarios and transition pathways. The deliverable contributes to MOBI-TWIN's broader objective of developing a policy-relevant simulation framework for understanding risks and opportunities faced by left-behind regions in the context of the Green and Digital Twin Transition. The work is connected to other project outputs through shared inputs, harmonized scenario design, and consistent reporting conventions, and it provides complementary evidence that can inform model integration and cross-task interpretation. For cross-pilot contextualisation, the five case-study regions are also referenced against the D2.3 regional typology as a high-level framing of their structural positioning.

A central contribution of this deliverable is the implementation of ABM configurations (based on spatial microsimulation output generated in task 3.1) for five pilot systems: Central Macedonia in Greece, Castilla-La Mancha in Spain, Lombardy in Italy, Groningen in the Netherlands, and North and East Finland in Finland. The models use the high-resolution synthetic populations and spatial reference inputs generated in Task 3.1 as the micro-level backbone for simulation. Individual agents are characterized by socioeconomic attributes and decision-relevant heterogeneity, including residential preferences and intention-related fields derived from MOBI-TWIN survey relationships and applied consistently within the modeling workflow. The ABM simulates monthly population trajectories over a ten-year horizon under combinations of scenarios and transition pathways and represents key demographic processes, mobility

decisions, and optional within-system relocation mechanisms. In this way, the models link micro-level decision channels to macro-level outcomes, generating trajectories of population change, spatial redistribution, and region-level distributions that are relevant for inequality and sustainability assessment. The analysis is organised around each pilot's full set of subregional spatial units. This resolution allows differences between urban cores, peri-urban belts, and more rural or peripheral areas to emerge empirically through their simulated trajectories and indicator profiles. Across the pilots, this framing spans “Structurally Lagging and Peripheral Regions” (EL52), “Economies in Structural Transition” (ES42, ITC4), and “Balanced Innovators” (FI1D, NL11), without affecting the common modelling workflow applied to all five systems.

The main outputs reported in this deliverable include the following. First, pilot-wide population trajectories under alternative scenario and policy pathway configurations, summarized across multiple random seeds to make uncertainty explicit. Second, population composition panels that track changes by age groups, sex, education tiers, and labour-force structure across time and configurations. Third, a harmonized set of subregional indicators for population, equality, and sustainability computed from agent-level snapshots and aggregated by subregion within each pilot system. These indicators include standard measures of regional inequality and dispersion, such as GINI index, alongside sustainability-relevant metrics computed consistently from the same agent-level backbone. Fourth, delta-series maps that summarize percent changes relative to the baseline time point, supporting consistent comparative visualization of regional dynamics across scenarios, policies, and time points. Fifth, initial robustness assessments based on replicated runs and pre-batch sanity checks that validate the end-to-end pipeline from simulation outputs to mapped indicators. The workflow is also structured to support comparison across regional types by using harmonized indicator definitions and consistent reporting conventions across pilots and subregional units.

The deliverable also offers initial policy-relevant insights for left-behind regions. By evaluating scenario and transition pathway combinations, the analysis identifies regional types and subregional patterns associated with elevated risks of population loss, as well as conditions under which retention capacity and population composition outcomes improve. The results support structured

comparison of alternative transition contexts and help clarify which mechanisms are most responsible for differences in trajectories across pilots. This deliverable demonstrates the feasibility and policy relevance of ABM within the MOBI-TWIN framework for evaluating medium- and long-term implications of mobility dynamics under the Twin Transition and for informing policy discussion and future model refinement. Consistent with Task 3.4, the deliverable accounts for the influence of macro-level shocks, including disruptions such as the COVID-19 pandemic and Brexit, by introducing a macro-shock noise component that incorporates both known and unknown shocks into the robustness design. At the same time, the simulation framework distinguishes between two responsive policy pathways, to reflect how the presence or absence of proactive improvement strategies can lead to materially different outcome trajectories for population change, inequality, and sustainability.

## TABLE OF CONTENTS

<b>1</b>	<b><i>List of terms and abbreviations</i></b> .....	<b>14</b>
<b>1</b>	<b><i>Introduction</i></b> .....	<b>15</b>
1.1	<b>Document structure</b> .....	<b>17</b>
<b>2</b>	<b><i>Methods: Theory, Data, Model, and Visualisation</i></b> .....	<b>19</b>
2.1	<b>Methodological Background</b> .....	<b>19</b>
2.2	<b>Overview of Methods</b> .....	<b>22</b>
2.2.1	Methodological Purposes.....	22
2.2.2	Conceptual Framework.....	23
2.3	<b>Utilising EU-SILC for ABM sampling</b> .....	<b>25</b>
2.3.1	Purpose and Role in the Workflow.....	25
2.3.2	Data sources and roles.....	25
2.3.3	Harmonization and estimation logic.....	26
2.3.4	Enriched output and sampling pool construction.....	27
2.3.5	Example of enrichment output.....	27
2.3.6	Quality controls and auditability for enrichment.....	28
2.4	<b>Data preparation for ABM runtime inputs</b> .....	<b>29</b>
2.4.1	ABM input overview.....	29
2.4.2	Spatial reference file preparation.....	29
2.4.3	Spatial weights from spatial microsimulation.....	29
2.4.4	IML based residential preference weight file.....	30
2.4.5	Out-migration timing distribution over a 120 month horizon.....	30
2.4.6	Scenario specific mg and ng inflow settings.....	31
2.4.7	Final ABM input inventory.....	31
2.5	<b>Agent-based model design and simulation</b> .....	<b>32</b>
2.5.1	Model scope, agents, and state variables.....	32
2.5.2	Time structure and execution order.....	33
2.5.3	Exit decision mechanism using a baseline timing curve and explicit modifiers.....	34
2.5.4	Policy channels and preference based response parameterization.....	35
2.5.5	Internal relocation and destination choice based on spatial weights.....	35
2.5.6	Scenario and policy configuration.....	35
2.5.7	Multi-run execution and reproducibility in simulation.....	36
2.5.8	The interface of ABM in NetLogo.....	36
2.5.9	Detailed explanation of modules.....	37
2.5.10	Model calibration and alignment strategy.....	42
2.6	<b>Analytical Outputs and mapping</b> .....	<b>44</b>
2.6.1	Output strategy and file schema.....	44
2.6.2	Simplified structure of the agent-level snapshot output.....	45
2.6.3	Pilot-wide total population trajectories.....	46

2.6.4 Regional equality and sustainability indicators computation.....	47
2.6.5 Categorized population dynamic computations for regional maps.....	49
2.6.6 Between-region inequality indices for pilot-level comparative assessment.....	50
2.6.7 Geospatial merge and map production.....	50
2.6.8 Robustness across runs and pre batch sanity checks.....	51
<b>3 Main result: population, equality, and sustainability.....</b>	<b>51</b>
<b>3.1 Greece: Central Macedonia (NUTS - EL52).....</b>	<b>51</b>
3.1.1 EL (Central Macedonia) pilot-level total population dynamics across scenarios.....	51
3.1.2 EL (Central Macedonia) pilot-level population trends over time by certain groups.....	53
3.1.3 EL (Central Macedonia) subregion-level total population dynamics across scenarios.....	55
3.1.4 EL (Central Macedonia) subregion-level indicators change across scenarios.....	56
3.1.5 EL (Central Macedonia) between-subregion inequality across scenarios and time horizons.....	57
3.1.6 EL (Central Macedonia) scenario effects on population, equality, and spatial differentiation.....	58
<b>3.2 Spain: Castilla-La Mancha (NUTS - ES42).....</b>	<b>59</b>
3.2.1 ES (Castilla-la Mancha) pilot-level total population dynamics across scenarios.....	59
3.2.2 ES (Castilla-la Mancha) pilot-level population trends over time by certain groups.....	61
3.2.3 ES (Castilla-la Mancha) subregion-level total population dynamics across scenarios.....	63
3.2.4 ES (Castilla-la Mancha) subregion-level indicators change across scenarios.....	64
3.2.5 ES (Castilla-la Mancha) between-subregion inequality across scenarios and time horizons.....	65
<b>3.3 Finland: North &amp; East Finland (NUTS - FI1D).....</b>	<b>66</b>
3.3.1 FI (North and East Finland) pilot-level total population dynamics across scenarios.....	67
3.3.2 FI (North and East Finland) pilot-level population trends over time by certain groups.....	68
3.3.3 FI (North and East Finland) subregion-level total population dynamics across scenarios.....	70
3.3.4 FI (North and East Finland) subregion-level indicators change across scenarios.....	71
3.3.5 FI (North and East Finland) between-subregion inequality across scenarios and time horizons.....	72
3.3.6 FI (North and East Finland) scenario effects on population, equality, and spatial differentiation.....	73
<b>3.4 Italy: Lombardy (NUTS – ITC4).....</b>	<b>74</b>
3.4.1 IT (Lombardy) pilot-level total population dynamics across scenarios.....	74
3.4.2 IT (Lombardy) pilot-level population trends over time by certain groups.....	75
3.4.3 IT (Lombardy) subregion-level total population dynamics across scenarios.....	78
3.4.4 IT (Lombardy) subregion-level indicators change across scenarios.....	79
3.4.5 IT (Lombardy) between-subregion inequality across scenarios and time horizons.....	80
3.4.6 IT (Lombardy) scenario effects on population, equality, and spatial differentiation.....	81
<b>3.5 Netherlands: Groningen (NUTS - NL11).....</b>	<b>81</b>
3.5.1 NL (Groningen) pilot-level total population dynamics across scenarios.....	81
3.5.2 NL (Groningen) pilot-level population trends over time by certain groups.....	83
3.5.3 NL (Groningen) subregion-level total population dynamics across scenarios.....	85
3.5.4 NL (Groningen) subregion-level indicators change across scenarios.....	86
3.5.5 NL (Groningen) between-subregion inequality across scenarios and time horizons.....	87
3.5.6 NL (Groningen) scenario effects on population, equality, and spatial differentiation.....	88
<b>4 Integration of relevant RRI pillars.....</b>	<b>89</b>
<b>5 Conclusions and Next Steps.....</b>	<b>90</b>

**6** *References*..... **93**

## LIST OF FIGURES

Figure 1. Conceptual model of ABM.....	24
Figure 2. Different scenarios and policy pathways.....	25
Figure 3. Interface example of agent-based model in NetLogo.....	37
Figure 4. EL (Central Macedonia) Total Population trends over time.....	52
Figure 5. EL (Central Macedonia) population trends over time by age group.....	53
Figure 6. EL (Central Macedonia) population change (%) after 10 years: cross-scenario comparison maps.....	55
Figure 7. EL (Central Macedonia) change in income equality indicator after 10 years: cross-scenario comparison maps.....	56
Figure 8. EL (Central Macedonia) between-subregion income equality under twin transition and no transition.....	58
Figure 9. ES (Castilla-la Mancha) total population trends over time.....	60
Figure 10. ES (Castilla-la Mancha) population trends over time by age group.....	61
Figure 11. ES (Castilla-la Mancha) population change (%) after 10 years: cross-scenario comparison maps.....	64
Figure 12. ES (Castilla-la Mancha) change in income equality indicator after 10 years: cross-scenario comparison maps.....	65
Figure 13. ES (Castilla-la Mancha) between-subregion income equality under Twin Transition and No Transition.....	66
Figure 14. FI (North and East Finland) total population trends over time.....	67
Figure 15. FI (North and East Finland) population trends over time by age group.....	69
Figure 16. FI (North and East Finland) population change (%) after 10 years: cross-scenario comparison maps.....	71
Figure 17. FI (North and East Finland) change in income equality indicator after 10 years: cross-scenario comparison maps.....	71
Figure 18. FI (North and East Finland) between-subregion income equality under Twin Transition and No Transition.....	73
Figure 19. IT (Lombardy) total population trends over time.....	74
Figure 20. IT (Lombardy) population trends over time by age group.....	76

Figure 21. IT (Lombardy) population change (%) after 10 years: cross-scenario comparison maps.....	78
Figure 22. IT (Lombardy) change in income equality indicator after 10 years: cross-scenario comparison maps.....	79
Figure 23. IT (Lombardy) between-subregion income equality under Twin Transition and No Transition.....	80
Figure 24. NL (Groningen) total population trends over time.....	82
Figure 25. NL (Groningen) population trends over time by age group.....	83
Figure 26. NL (Groningen) population change (%) after 10 years: cross-scenario comparison maps.....	85
Figure 27. NL (Groningen) change in income equality indicator after 10 years: cross-scenario comparison maps.....	86
Figure 28. NL (Groningen) between-subregion income equality under Twin Transition and No Transition.....	87

## LIST OF TABLES

Table 1. EXAMPLE OF ENRICHMENT OUTPUT.....	28
Table 2. LIST OF INPUTS.....	32
Table 3. THE OPERATIONAL STEPS OF ABM.....	33
Table 4. THE MODULES AND PARAMETERS ON THE INTERFACE.....	37
Table 5. ALIGNMENT TARGETS AND RESULT OF FIVE PILOTS.....	43
Table 6. THE DATA STRUCTURE OF THE AGENT-LEVEL SNAPSHOT OUTPUT.....	45
Table 7. PILOT-LEVEL POPULATION WITH CATEGORIES (PANELS OVER TIME).....	46
Table 8. EQUALITY, SUSTAINABILITY, AND POPULATION INDICATORS (REGION-LEVEL).....	48
Table 9. CATEGORIZED POPULATION DYNAMIC FOR REGIONAL MAPS.....	49
Table 10. BETWEEN-REGION INEQUALITY INDICES.....	50
Table 11. EL (CENTRAL MACEDONIA) POPULATION TRENDS OVER TIME BY AGE GROUP UNDER TT.....	54
Table 12. ES (CASTILLA-LA MANCHA) POPULATION TRENDS OVER TIME BY AGE GROUP UNDER TT.....	62
Table 13. FI (NORTH AND EAST FINLAND) POPULATION TRENDS OVER TIME BY AGE GROUP UNDER TT.....	69
Table 14. IT (LOMBARDY) POPULATION TRENDS OVER TIME BY AGE GROUP UNDER TT.....	77
Table 15. NL (GRONINGEN) POPULATION TRENDS OVER TIME BY AGE GROUP UNDER TT.....	84

## 1 LIST OF TERMS AND ABBREVIATIONS

ABM	Agent Based Model
EU-SILC	European Union Statistics on Income and Living Conditions
EU	European Union
TT	Twin Transition
NT	No Transition
NUTS	Nomenclature of Territorial Units For Statistics
EL	Greece
ES	Spain
FI	Finland
IT	Italy
NL	Netherlands

## 1 INTRODUCTION

This report presents Deliverable 3.4, “The Effects of Spatial Mobility During Twin Transition on Regional Inequality and Sustainability in the Identified EU Regional Typologies.” It is the main output of Task 3.4 under Work Package 3 and contributes directly to Objective 3 (Analyse the effects of spatial mobility on EU demographics, society, welfare systems and labour market using microsimulation and agent-based modelling) of the MOBI-TWIN project. Task 3.4 builds on the efforts described in Deliverable report 3.1 and it develops and applies an agent-based model (utilising the spatial microsimulation model and outputs of Task 3.1) to assess, in the context of the Twin Transition, how scenario-driven risks and opportunities for different types of left-behind regions affect residents’ spatial mobility and population composition, and how these processes shape regional inequality and sustainability over time. The report documents the conceptual model, the operational model implemented in NetLogo, and the analytical workflow used to derive indicators and maps from simulation outputs. The report documents the operational model and the post-processing workflow used to generate the reported outputs.

Task 3.4 builds on the spatial microsimulation work undertaken in Task 3.1 by using the output generated there (spatial microsimulation weights) and extends it by introducing dynamic simulation and agent-based modeling (also implementing a relevant theoretical research agenda articulated in Ballas et al., 2019). The spatial microsimulation outputs provide high-resolution synthetic populations for the pilot systems, grounded in the MOBI-TWIN survey and in European<sup>1</sup> and national statistical sources<sup>2</sup>, and designed to reproduce key distributions and small-area population structure. Task 3.4 then uses these synthetic populations as the micro-level backbone for dynamic experiments. The ABM simulates monthly population trajectories over a ten-year horizon and

---

<sup>1</sup> <https://ec.europa.eu/eurostat/web/microdata/european-union-statistics-on-income-and-living-conditions>

<sup>2</sup> <https://www.statistics.gr/en/home/>  
<https://www.ine.es/en/>  
<https://www.istat.it/en/>  
<https://opendata.cbs.nl/#/CBS/nl/>  
<https://stat.fi/fi>

evaluates how alternative scenarios and policy pathways alter retention, out-migration, internal redistribution, and population change mechanisms. This design supports systematic counterfactual comparison across scenarios and policy configurations without the costs and irreversibility associated with real-world policy trials.

In this report, spatially microsimulated units are modeled as agents. Each agent is characterized by socioeconomic attributes and decision-relevant heterogeneity that shapes mobility responses. Agents represent individual residents living in the pilot systems and are exposed to changes that arise from combinations of scenarios and policy pathways. Policy pathways represent alternative transition contexts constructed from the Digital Transition and Green Transition dimensions, including:

- No Transition
- Digital Transition
- Green Transition
- Twin Transition

Scenarios provide narrative macro contexts that modify risks and opportunities and condition how strongly policy channels operate. The primary behavioural outcome for each agent is whether to remain within the pilot system or to exit over time, with internal relocation represented as an additional mobility outcome where enabled.

A key advantage of ABM, compared with purely regression-based analysis or aggregate scenario projections, is its ability to represent explicitly the interaction between individual decision making, spatial structure, and temporal evolution. In the model, mobility decisions are shaped by personal characteristics such as age, education, employment and income status, as well as by spatial conditions such as accessibility, the distribution of opportunities, and region-level attractiveness. behavioural heterogeneity is operationalized through intention and preference fields that enter the decision rules, enabling heterogeneous responses to the same contextual change. This makes it possible to examine not only whether policies and scenarios shift mobility outcomes, but

also how and for whom these effects emerge through defined behavioural channels.

At the regional scale, the analysis focuses on pilot regions and the regional typologies developed elsewhere in the project (Task 2.4-Deliverable 2.3.). By linking synthetic populations and simulated outcomes to these typologies, the model identifies areas that face elevated risks of population loss under adverse scenarios and areas whose retention capacity could be strengthened under more favourable transition contexts. The outputs provide both numerical and geospatial evidence on how micro-level choices accumulate into pilot-level demographic trajectories, subregional patterns, and changes in inequality and sustainability indicators.

The results workflow is explicitly modular. NetLogo is used to generate consistent agent-level snapshots at multiple time points for each scenario and policy configuration and for multiple random seeds. Python is then used for post-processing and GIS-based visualization. The post-processing pipeline produces three complementary types of outputs. First, it reports pilot-wide population trajectories and uncertainty summaries across replicated runs. Second, it produces population joint panels that break down population change by age, sex, education tiers, and labour-force structure. Third, it computes regional indicator surfaces and delta-series maps that express percent change relative to the baseline time point, enabling consistent comparative mapping across scenarios, policies, and time points. Together, these outputs support both mechanism-oriented interpretation. The work presented here is closely connected to other tasks and work packages in MOBI-TWIN. Inputs to the agent-based model and the regional classification schemes build on earlier work on regional typologies, scenario design, and the preparation of survey and contextual data. The simulation outputs complement the spatial microsimulation results from Deliverable 3.1 by adding a dynamic perspective, and they provide quantitative and visual evidence that can support policy co-creation, communication, and engagement activities across the project. The conceptual design of scenarios and their expected impact channels is informed by Deliverable 3.2, which clarifies how scenario contexts are expected to shape regional risks and opportunities. These expectations guide how we distinguish preference dimensions through which agents respond to changing conditions.

Although Delphi outputs are not used as direct simulation inputs in the current runs, they are considered explicitly when interpreting the main results, particularly when emphasizing outcomes under adverse scenarios that are assessed as relatively plausible by expert judgments.

## 1.1 DOCUMENT STRUCTURE

The remainder of this report is structured as follows. Chapter 2, “Methods: Theory, Data, Model, and Visualization,” presents the methodological background and the overall workflow used in this deliverable. It then documents the behavioural enrichment procedure used to prepare the ABM sampling pool, the preparation of ABM runtime inputs, the agent-based model design and simulation logic, the calibration and alignment strategy, and the post-processing workflow used to generate analytical outputs and maps. Chapter 3 presents the main simulation outputs by pilot system, covering the Netherlands (Groningen, NL11), Greece (Central Macedonia, EL52), Spain (Castilla-La Mancha, ES42), Finland (North and East Finland, FI1D), and Italy (Lombardy, ITC4). Chapter 4 concludes with a cross-pilot summary section. The report ends with the reference list. In addition, an appendix is provided with high-resolution simulation outputs reported at finer temporal granularity and across the full set of scenarios and policy pathways, enabling more detailed inspection beyond the main report figures and tables.

## 2 METHODS: THEORY, DATA, MODEL, AND VISUALISATION

### 2.1 METHODOLOGICAL BACKGROUND

Deliverable report 3.1 included a detailed discussion of the MOBI-TWIN model approach and the techniques underpinning it: spatial microsimulation and agent-based modelling. The work in task 3.4 extended and further implemented the MOBI-TWIN model with a particular focus on utilising the agent-based modelling potential powered by small area microdata generated with the use of spatial microsimulation (Ballas et al., 2019). Both methodological approaches were introduced and discussed in deliverable report 3.1 and in the remainder of this section we elaborate further on Agent-based Modelling (ABM), given that this was a key methodological extension and application in task 3.4. ABM provides a computational approach for studying complex social and spatial systems in which aggregate outcomes arise from decentralized decision-making and interaction (Jager et al. 2000; Jager 2021). In contrast to aggregate, equation-based models that typically represent populations through average behaviour or system-level relations, ABMs implement a bottom-up logic: macro-level patterns are generated through the actions of heterogeneous agents operating under explicit behavioural rules and constraints (Blume, 2015; Macal & North, 2010; Williams, 2017). This perspective is particularly relevant for regional science questions where spatial mobility, labour and housing adjustments, and changing opportunity structures co-evolve over time, often through nonlinear dynamics and feedback loops that are difficult to capture with purely top-down approaches (Kanj, 2016; Williams, 2017; Xu, 2008). Conceptually, ABMs are composed of agents, behavioural rules, interactions, and an environment (Macal & North, 2010; Quang et al., 2018). Agents can represent individuals or households and are characterized by attributes such as age, education, employment status, income, and digital access. behavioural rules formalize how agents respond to incentives, constraints, and information, including how they form relocation intentions, evaluate potential destinations, and update decisions over time (Klabunde & Willekens, 2016; Steinbacher et al., 2021). ABMs are well suited to represent heterogeneity, allowing agents with different

characteristics to respond differently to the same contextual conditions, which is central for mobility processes and for distributional outcomes such as inequality (Dilaver, 2015; Steinbacher et al., 2021). Interactions among agents and between agents and their environment can be direct (communication, competition, social influence) or indirect (shared exposure to congestion, housing prices, labour demand, or policy environments). These interaction channels can generate emergent patterns that are not explicitly imposed at the micro level but arise from many local decisions and constraints (Dilaver & Gilbert, 2023; Williams, 2017).

Spatial mobility is a key mechanism connecting micro-level decisions to regional outcomes. It includes migration, commuting, travel, and longer-term relocation, each shaping how people access opportunities and how regions reorganise demographically and economically (Kourtiti et al., 2021; National Research Council, 2010). Migration and relocation can alter population composition, labour supply, and demand in housing markets, with consequences for regional development trajectories and spatial inequality (Hüther, 2019; Markowska-Manista & Sawicki, 2022). Commuting and broader travel behaviour reflect the spatial organisation of work, services, and amenities, influencing congestion, accessibility, and resource use (Markowska-Manista & Sawicki, 2022). Mobility is also sensitive to structural conditions such as accessibility, density, and network connectivity, as well as disruptions including climate-related risks and global economic shifts that reshape opportunity landscapes and planning priorities (Gedikli et al., 2022; Kuttler, 2020; UNECE, 2020). Because these drivers and constraints are spatially differentiated, mobility can operate as both an equalizing mechanism (by expanding access to opportunities) and a stratifying mechanism (when constraints and risks are unevenly distributed). From a regional perspective, mobility processes matter because they affect two closely related outcomes: regional development and regional resilience. Regional development concerns changes in economic, social, and environmental well-being, often reflected in employment, incomes, infrastructure quality, and quality-of-life conditions (Bevilacqua et al., 2020). Regional resilience refers to the capacity of regions to absorb shocks, adapt to changing conditions, and in some cases transform toward new trajectories rather than simply returning to a prior state (Bevilacqua et al., 2020; Martin & Sunley, 2020). Shocks can be

economic (recessions, market restructuring), environmental (disasters, climate impacts), or social (demographic shifts, public health crises, deepening inequality). Resilience is therefore increasingly treated as a policy objective, despite ongoing debates about definitions, measurement, and empirical identification of resilience mechanisms across contexts (Bruneckienė et al., 2018; Martin & Sunley, 2013; Martin & Sunley, 2020).

ABMs are a natural methodological bridge between mobility decisions and regional development and resilience because they can represent how individual choices aggregate into changes in labour markets, housing markets, accessibility, and spatial inequality, and how these macro-outcomes feed back into future decisions. Prior work has used ABMs to simulate migration and relocation choices, commuting behaviour, and transport flows, showing how micro-level preference heterogeneity and spatial constraints can produce macro-level patterns such as congestion, segregation, and uneven development (Quang et al., 2018; Steinbacher et al., 2021; Xu, 2008). ABMs can also represent reinforcing feedback loops, such as when economic growth attracts in-movers, whose arrival then changes housing demand and infrastructure pressure, thereby reshaping local conditions that influence subsequent mobility and welfare outcomes. This capacity to encode explicit behavioural channels and to explore emergent, system-level consequences is a key advantage for policy-relevant analysis (Williams, 2017).

At the same time, ABM is methodologically demanding. Key challenges include data requirements for populating agents and parameterizing behavioural rules, computational intensity for large-scale simulation experiments, and the difficulty of validation when multiple mechanisms can generate similar macro patterns (Macal & North, 2010; Troost et al., 2023). As a result, rigorous modeling practice typically emphasizes transparent specification, careful calibration, and structured robustness analysis. Widely used guidelines include explicit model documentation protocols (for example, ODD) and systematic workflows that distinguish model design, calibration, validation, scenario testing, and sensitivity analysis (Grimm et al., 2020; Ligmann-Zielinska & Jankowski, 2007). Calibration aligns model outputs with observed empirical regularities; validation assesses whether the model reproduces patterns relevant to the intended use; scenario testing supports counterfactual exploration; and

sensitivity analysis identifies which assumptions and parameters most strongly shape results (Bektaş et al., 2021; Chopra et al., 2024; McCulloch et al., 2022). Recent methodological developments highlight the potential benefits of integrating ABM with complementary tools and data sources. Coupling ABMs with GIS can strengthen spatial realism and support fine-grained representation of accessibility and spatial constraints (Brown et al., 2005). Linking ABM with econometric approaches can improve identification and interpretation of behavioural mechanisms (Woźniak, 2020). Machine learning can support surrogate modeling, calibration, and the derivation of empirically grounded decision rules, while preserving the ABM’s capacity to explore nonlinear dynamics under alternative futures (Angione et al., 2022; Turgut & Bozdağ, 2023). Together, these developments support ABM as a pragmatic “policy laboratory” for understanding how mobility interacts with regional inequality and sustainability under uncertainty, while also underscoring the importance of methodological transparency and disciplined robustness strategies (Blume, 2015; Macal & North, 2010).

In the MOBI-TWIN project, ABM is used in this spirit: to formalize mobility mechanisms at the micro level, to examine how alternative scenario and policy configurations reshape mobility and distributional outcomes, and to provide a structured basis for comparison across pilot regions. The methodological sections that follow operationalize this rationale by documenting data preparation, model specification, calibration and validation checks, and robustness procedures that support credible counterfactual analysis.

## 2.2 OVERVIEW OF METHODS

### 2.2.1 METHODOLOGICAL PURPOSES

The primary goal of the workflow is to support credible and comparable dynamic experiments across scenario and policy configurations. The overall process focuses on the out-migration dynamics of people who already reside within each pilot region, and on the implications for equality and sustainability. These implications are assessed through changes in a set of equality and sustainability indicators over time. All data preparation steps are therefore

treated as inputs for simulation. They are designed to seed a representative agent population, parameterize decision mechanisms, and ensure that outputs can be aggregated consistently for indicator computation and mapping.

A key requirement is to initialize agents with (i) a realistic baseline socioeconomic structure and (ii) empirically grounded behavioural heterogeneity. EU-SILC provides the baseline microdata backbone that anchors population structure and inequality measurement, while MOBI-TWIN survey data is used as a training source to learn behavioural relationships. These learned relationships are then applied to EU-SILC to generate model-derived behavioural fields, such as migration intentions and preference-related variables, which are appended to EU-SILC records as an enrichment layer. This approach improves the effective behavioural content available for simulation without altering EU-SILC baseline distributions, and it supports sufficient individual heterogeneity for repeated counterfactual experiments.

The chapter is organised around three ABM-centred priorities. First, it specifies the simulation inputs that shape model behaviour, including how the spatial microsimulation outputs and enriched EU-SILC sampling pool are constructed to initialize agents with both socioeconomic attributes and behaviourally relevant variables. In this context, EU-SILC defines the baseline population structure and indicator-relevant attributes, while MOBI-TWIN supports the estimation of behavioural variables that are not observed in EU-SILC. Harmonization of shared covariates and transparent, similarity-based estimation (with a K-nearest neighbours' estimator as a baseline option) are used to generate behavioural fields in an interpretable and quality-controlled manner, ensuring that the resulting sampling pool is fit for simulation rather than optimized for descriptive combination of surveys. Second, it summarizes the core model design choices that support transparent mechanisms and consistent comparisons across scenarios, especially the separation between a time-varying baseline risk structure and scenario- or policy-specific modifiers, and the organisation of scenario and policy states in a way that scales to repeated counterfactual experiments. Third, it defines the robustness strategy used in simulation and post-processing, including multiple runs with controlled random seeds, systematic scenario and policy sweeps, and pre-batch sanity checks that reduce the risk of structural errors before indicator computation and mapping.

---

## 2.2.2 CONCEPTUAL FRAMEWORK

The conceptual architecture of the agent-based model is organised as an iterative workflow that supports calibration, operation, and validation in a transparent and comparable manner. The model is structured around three interdependent layers that together govern how population trajectories and inequality outcomes emerge over time. First, the spatiotemporal layer provides fixed distributions that drive initialization and baseline dynamics, including the spatial allocation of residents across subregions within each pilot area and the monthly exit probability curves over a 120-month horizon. These inputs are derived from project data inputs and preprocessing pipelines, including Task 3.1 spatial microsimulation outputs and MOBI-TWIN-informed timing components. They determine where agents are initially located and how their baseline propensity to move out evolves with tenure. Second, the environment layer defines the external context in which agents make decisions. This layer is operationalized through alternative future scenarios and transition pathways that represent different combinations of regional risks, opportunities, and policy directions. Third, the variable layer specifies the residential preference dimensions that mediate how scenario and policy conditions translate into changes in exit propensity. This layered structure enables the model to represent mobility as an outcome of interactions between fixed spatiotemporal structures, adjustable environmental configurations, and heterogeneous individual sensitivities, and it supports controlled counterfactual comparisons across experiments.

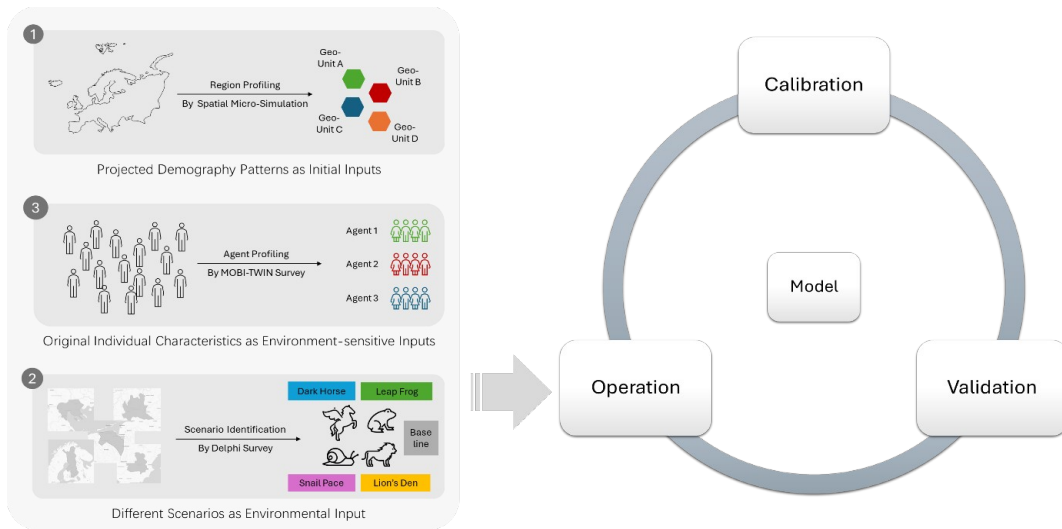


**Figure 1. Conceptual model of ABM**

The environment layer is operationalized through two orthogonal transition dimensions, Digital Transition and Green Transition, whose combinations generate four policy pathways: No Transition, Digital Transition, Green Transition, and Twin Transition. These four policy combinations are included to enable clear observation of how population mobility and related outcomes differ under alternative transition contexts, and to provide a structured comparison set that makes the effects of each transition lever interpretable. In the analytical workflow reported in this deliverable, the subsequent analysis is primarily conducted using Twin Transition as the main policy configuration because it represents the integrated transition setting in which digital and green measures jointly shape residential preference satisfaction.

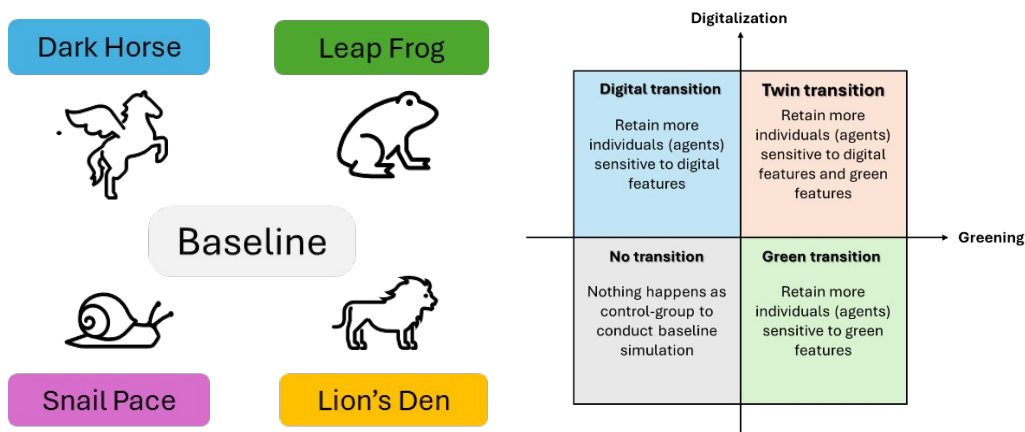


### Figure 2. Different scenarios and policy pathways

The policy pathways are evaluated under four narrative scenarios-Dark Horse, Leap Frog, Snail Pace, and Lion’s Den, while a baseline configuration represents continuation of established development trajectories without an explicit transition context. In the model, scenarios and transition pathways do not directly change individual preferences. Instead, they modify how strongly specific preference dimensions suppress or amplify exit propensity through policy strength parameters and scenario scaling coefficients. Figure 2 summarizes the scenario set and policy pathways evaluated in the simulation design.

## 2.3 UTILISING EU-SILC FOR ABM SAMPLING

### 2.3.1 PURPOSE AND ROLE IN THE WORKFLOW

The ABM focuses on out-migration dynamics among people residing within each pilot region at baseline, and on the resulting changes in equality and sustainability indicators over time. This requires two properties in the micro-level initialization data. First, the baseline population structure must be realistic so that simulated distributions of income, education, labour-market activity, household characteristics, and digital access start from a credible representation of the pilot population. Second, agents must exhibit heterogeneous intentions and preference patterns that can drive differentiated behavioural responses to scenarios and policies. EU-SILC provides the core micro-level population backbone, while MOBI-TWIN is used as a training source to learn behavioural relationships that are then applied to EU-SILC. The enrichment step generates model-derived variables capturing migration intentions and residential preferences, which are appended to EU-SILC records as additional behavioural fields. The resulting sampling pool is therefore (i) anchored to EU-SILC for socioeconomic realism and (ii) behaviourally rich for ABM decision heterogeneity. The design ensures that repeated experiments across random seeds, scenarios, and policies share a consistent micro-level foundation. Differences in simulation outcomes can be interpreted through

explicit behavioural channels and scenario or policy mechanisms, rather than through uncontrolled variation in the baseline population representation.

---

### 2.3.2 DATA SOURCES AND ROLES

The enrichment workflow relies on two micro datasets with clearly separated roles. EU-SILC is used as the baseline microdata backbone. It provides comprehensive and internally consistent socioeconomic and demographic variables that support agent initialization and the computation of equality and sustainability indicators. EU-SILC remains the authoritative source for baseline population structure and all variables required for indicator construction. MOBI-TWIN survey data is used as a behavioural training source. It contains migration intention measures and residential preference information that are not available in EU-SILC but are required to represent behavioural heterogeneity in the ABM. MOBI-TWIN is not used to replace EU-SILC records. Instead, MOBI-TWIN supports the estimation of behavioural fields as functions of shared covariates, enabling the ABM to initialize agents with intention and preference profiles that are consistent with observable socioeconomic and life-course characteristics. This separation improves interpretability and governance. EU-SILC defines the baseline population and its socioeconomic distributions, while MOBI-TWIN contributes behavioural content through model-based estimation, with clear documentation of which behavioural variables are generated and how they enter the ABM decision rules. For contextual interpretation across case-study regions, the five pilots are situated in the D2.3 regional typology as follows: EL52 is classified as “Structurally Lagging and Peripheral Regions”; ES42 and ITC4 as “Economies in Structural Transition”; and FI1D and NL11 as “Balanced Innovators”. These typological labels are used only as a high-level framing of regional positioning and do not affect the enrichment logic itself, which remains fully governed by the EU-SILC baseline and the MOBI-TWIN-based behavioural estimation.

---

### 2.3.3 HARMONIZATION AND ESTIMATION LOGIC

The enrichment pipeline consists of two coupled components: (i) harmonization of shared covariates and (ii) model-based estimation of behavioural fields. Harmonization prepares a common feature space that is comparable across EU-SILC and MOBI-TWIN. The goal is to ensure that behavioural models trained on

MOBI-TWIN can be meaningfully applied to EU-SILC without artefacts introduced by source-specific coding differences. Harmonization includes consistent data types, consistent missing-value conventions, aligned categories for key covariates, and standardized encodings for variables that appear in both datasets. Shared covariates are chosen to capture life-course and socioeconomic differences that are empirically and theoretically linked to migration intentions and residential preferences, while remaining observable in both datasets. Typical examples include age group, sex, education, labour-market status, household composition proxies, and indicators of digital access or constraints. Estimation is implemented using a similarity-based prediction model, with a K-nearest-neighbours (KNN) estimator used as a transparent non-parametric baseline. For each EU-SILC record, the estimator uses the harmonized covariates to identify a neighbourhood of similar MOBI-TWIN observations in feature space and then produces predicted behavioural values for the EU-SILC record. Depending on the variable type, predictions can be generated as (i) neighbourhood-based probability estimates for categorical outcomes, (ii) averaged or weighted scores for ordinal or continuous fields, or (iii) calibrated mappings into ABM-ready parameters. Where needed for interpretability and stability, estimation can be implemented within pre-defined strata (for example broad demographic categories), ensuring that behavioural profiles are generated under comparable population segments. Importantly, the pipeline produces model-derived behavioural fields for EU-SILC records. These fields are computed as estimator outputs, not as record-level exchanges between datasets. The objective is explicitly simulation-oriented: the enrichment is designed to generate a micro-level population that is structurally realistic and behaviourally heterogeneous, supporting repeated counterfactual experiments in the ABM.

---

#### 2.3.4 ENRICHED OUTPUT AND SAMPLING POOL CONSTRUCTION

The output of the workflow is an enriched spatial microsimulation output based on the EU-SILC sampling pool that can be read directly by the Netlogo platform. Each record corresponds to one EU-SILC individual and retains EU-SILC identifiers, and all baseline socioeconomic attributes used for agent initialization and indicator computation. Additional behavioural columns are appended as enrichment fields, including migration intention measures and preference-related variables required by the ABM decision rules. Before each

ABM run, agents are sampled from this enriched pool. The sampling procedure supports controlled scaling of population size, allowing computational experiments at different sample scales without changing the underlying EU-SILC-based distributions of core attributes. Because all runs draw from the same enriched pool, scenario and policy comparisons remain anchored to the same baseline data structure. Stochastic variability can therefore be attributed to simulation randomness and scenario or policy mechanisms, rather than to shifting micro-level inputs. This design also supports reproducibility. The enriched sampling pool constitutes a stable input contract between the microdata preparation layer and the ABM simulation layer, enabling independent versioning and inspection.

---

### 2.3.5 EXAMPLE OF ENRICHMENT OUTPUT

The table below illustrates the enrichment logic at the record level. Baseline attributes come from EU-SILC and remain unchanged. behavioural attributes are generated as model-derived estimates informed by relationships learned from MOBI-TWIN and are appended to the EU-SILC record as additional fields.

**Table 1. EXAMPLE OF ENRICHMENT OUTPUT**

Component	Role in the workflow	Example content
EU-SILC (baseline microdata)	Provides the population backbone for agent initialization and indicator computation	age, sex, education, labour-market status, household income, digital access
MOBI-TWIN (training source)	Used to learn behavioural relationships that are not observed in EU-SILC	migration intentions, preference weights, relocation considerations
Enriched EU-SILC (ABM sampling pool)	EU-SILC records with appended model-derived behavioural fields	EU-SILC baseline variables + predicted intention and preference fields

This example is illustrative. In the actual pipeline, enriched fields are defined via a structured mapping so that each behavioural variable has a clear interpretation in the ABM, either as a direct decision input, a grouping variable for heterogeneity, or a parameterization input used to compute composite scores.

---

### 2.3.6 QUALITY CONTROLS AND AUDITABILITY FOR ENRICHMENT

Enrichment quality is assessed using checks that are directly relevant for simulation validity and for responsible use of model-derived micro-level fields. First, baseline integrity is verified. EU-SILC distributions for core socioeconomic

variables must remain unchanged by construction. Nevertheless, we compare key baseline variables before and after enrichment to ensure that harmonization and processing steps did not introduce unintended recording, missingness artefacts, or type conversions. Second, estimation diagnostics are assessed. Because behavioural fields are generated by a similarity-based estimator, we summarize the distribution of neighbourhood distances and the concentration of estimator influence across the training data. These diagnostics indicate whether the estimator relies disproportionately on narrow parts of the MOBI-TWIN sample for certain strata, or whether similarity neighbourhoods are systematically poor for specific population segments. Third, structural validity of enriched fields is checked. All generated variables are validated for admissible ranges, category consistency after mapping and recording, and completeness requirements expected by the ABM. This ensures that ABM does not receive structurally invalid values that could distort decision rules or indicator computation. Auditability is supported through explicit artefacts and stable contracts. The enriched sampling pool is stored as a standalone input file that can be versioned and inspected independently from the ABM code. Harmonization rules, model configurations, covariate definitions, and the list of enriched variables are recorded so that the same output can be regenerated when inputs are updated, and so that sensitivity tests can be conducted by changing one component at a time while holding the baseline backbone fixed.

## 2.4 DATA PREPARATION FOR ABM RUNTIME INPUTS

### 2.4.1 ABM INPUT OVERVIEW

Beyond the enriched sampling pool, the ABM relies on a compact set of runtime inputs that define spatial structure, timing structure, preference-weight parameters, and scenario-specific macro inflows. These inputs are kept separate from the enrichment output because they serve different roles. The sampling pool specifies who agents are and what micro-level heterogeneity they carry at initialization, while runtime inputs specify where agents are located, how internal relocation is structured, how baseline exit risk evolves over time, and how scenario and policy mechanisms are applied during simulation. The ABM runtime package consists of six files: (1) a pilot-region shapefile with geometries

and core attributes (including `region_id` and baseline population), (2) an enriched sampling pool used for agent sampling before each run, (3) a spatial weight file from Task 3.1 used for destination choice and spatial allocation, (4) an interpretable machine learning (IML) weight file used in composite preference scoring and policy response channels, (5) a 120-month timing distribution file encoding the baseline exit CDF used to derive monthly hazards, and (6) an MG/NG inflow file specifying scenario-dependent external inflow and natural growth settings.

---

### 2.4.2 SPATIAL REFERENCE FILE PREPARATION

The shapefile defines the spatial reporting and aggregation units for the ABM. It contains pilot-region geometries and the region identifier used consistently across the workflow; `region_id` is treated as the spatial primary key and must match identifiers referenced in the spatial weight file and in any region assignments used during agent sampling and simulation. The shapefile also stores baseline region population counts, which are used to initialize region-level totals for spatial allocation at setup and to support congestion-aware mechanisms in which destination attractiveness may be adjusted using evolving population shares. Maintaining a single authoritative spatial reference prevents drift in region definitions when outputs are aggregated and mapped across multiple scenario and policy experiments.

---

### 2.4.3 SPATIAL WEIGHTS FROM SPATIAL MICROSIMULATION

The spatial weight file is produced by the spatial microsimulation work in Task 3.1 and is used as a runtime input to operationalize destination choice and spatial allocation in the ABM. The file encodes destination weights over pilot regions that can be interpreted as a structured choice distribution, enabling spatial outcomes to be interpreted relative to an explicit, documented weighting system rather than ad hoc or uniform assumptions. Weights may be provided at the group level (agents inherit the group-specific weight vector) or at the individual level (agents carry their own destination distribution). For ABM runtime use, weight vectors are additionally behaviour-normalized at the individual-agent level so that each agent's choice probabilities are comparable and consistent with the behavioural decision module. Several validity constraints are enforced: weights are nonnegative, sum to one within the

relevant unit, and reference region identifiers consistent with the shapefile; when vectors are missing or degenerate, a fallback distribution is applied to ensure every agent has a valid destination distribution for sampling-based relocation logic.

---

#### 2.4.4 IML BASED RESIDENTIAL PREFERENCE WEIGHT FILE

The ABM uses composite scoring channels that require weights for residential preference indicators, provided as a standalone runtime file derived through interpretable machine learning. The workflow trains supervised models using MOBI-TWIN intention-related outcomes and applied SHAP-based attributions to quantify global feature contributions, which are then translated into preference weights used by the ABM to compute composite preference satisfaction and to structure policy response channels. Because ABM is executed repeatedly across random seeds, scenarios, and policies, weight stability is treated as a central requirement; weights are therefore derived through repeated stratified cross-validation and aggregated using robust summaries (for example, medians) to reduce sensitivity to sampling noise and split instability. The final file is directly readable at setup and includes preference dimensions, weights, and minimal metadata required for interpretation.

---

#### 2.4.5 OUT-MIGRATION TIMING DISTRIBUTION OVER A 120 MONTH HORIZON

The ABM simulates mobility over a ten-year horizon using monthly time steps, requiring exit risk to evolve over time rather than remain constant. The timing distribution file provides this structure by storing a 120-month cumulative distribution function (CDF) that is expanded to monthly resolution through shape-preserving interpolation from anchor probabilities. Monotonicity is enforced so the CDF does not decrease across months, and values are bounded to the unit interval, ensuring that month-to-month increments are valid and that the ABM can safely convert consecutive CDF points into conditional monthly hazards. In runtime, the CDF acts as the baseline timing curve; scenario effects, policy effects, and heterogeneity modifiers are then applied on top of this baseline to produce final agent-level exit probabilities, supporting interpretable and comparable counterfactual experiments.

---

### 2.4.6 SCENARIO SPECIFIC MG AND NG INFLOW SETTINGS

Scenario differences are represented not only through micro-level decision modifiers but also through an explicit exogenous inflow and natural growth mechanism specified in an MG/NG input file. In the current model implementation, MG is interpreted as a scenario-specific annual external inflow share (expressed as a proportion) that represents exogenous in-migration from outside the pilot region; it is converted internally to a monthly compounded rate and applied to the current alive population so inflows scale dynamically with the evolving population base. NG is also used in the model and is interpreted as an annual natural growth input that is converted to a monthly compounded rate and applied to generate births during runtime, while deaths are handled in parallel through an age-specific mortality schedule; together, these processes implement natural population change within the simulation. This design is consistent with the NetLogo runtime logic, which loads scenario-specific MG/NG values, applies MG as monthly inflow, and applies NG through a monthly births process alongside a monthly deaths process. In addition to these demographic boundary conditions, scenarios are also operationalised through differentiated, stepwise coefficient schedules applied to the living-preference indicators derived from the MOBI-TWIN survey. Specifically, the full set of residential preference questions is mapped to composite preference components, and each scenario assigns a distinct set of multipliers to these components. These multipliers are designed to be tiered rather than continuous, so that scenarios correspond to discrete “levels” of preference sensitivity and policy responsiveness. In practical terms, the same underlying preference structure is retained across scenarios, but the strength of the preference-to-decision channel is adjusted using scenario-specific coefficients, creating a staircase pattern of behavioural intensities relative to the baseline configuration. This ensures that scenario narratives are reflected consistently in the ABM as systematic shifts in how strongly agents weight the survey-informed preference signals when evaluating staying, relocating, or exiting decisions. The coefficient schedules are stored in the scenario configuration and applied uniformly across pilots to ensure cross-pilot comparability, while allowing scenario contrasts to be expressed transparently as differences in parameter levels rather than changes in

## 2.4.7 FINAL ABM INPUT INVENTORY

The ABM reads a fixed package of runtime inputs that remains consistent across repeated experiments. Table 2 lists the required inputs and their roles; final file names can be inserted when preparing the deliverable package.

**Table 2. LIST OF INPUTS**

<b>ID</b>	<b>Input data (short name)</b>	<b>Purpose</b>
1	Pilot region shapefile	Spatial reference with region_id and baseline population for aggregation and mapping
2	Sampling pool	Sampling pool produced by enrichment, used for ABM sampling before each run
3	Spatial weight file (Task 3.1)	Destination weights that guide internal relocation and spatial allocation in the ABM; weights are additionally behaviour-normalized at the individual-agent level to ensure that each agent's choice probabilities are comparable and consistent with the behavioural decision module.
4	IML preference weights	Weights for residential preference indicators used in ABM composite scoring and policy-response channels. Scenario settings in Task 3.4 act as reduced-form model levers that mainly rescale the exit-probability intensity relative to baseline, rather than a direct implementation of Task 3.2 scenario narratives.
5	Exit timing distribution (120 month CDF)	Time varying baseline exit structure used to derive monthly hazards in the ABM
6	MG and NG inflow settings	Exogenous inflow settings used to represent differentiated population dynamics. NG captures natural increase and is parameterized using the latest country-level live birth rates (held constant across scenarios). MG is an externally specified migration inflow share used for calibration and cross-pilot alignment; it controls the share of incoming population and varies by scenario in a stepwise design (Leapfrog > Dark Horse > Baseline > Snail Pace > Lions' Den).

## 2.5 AGENT-BASED MODEL DESIGN AND SIMULATION

### 2.5.1 MODEL SCOPE, AGENTS, AND STATE VARIABLES

The model simulates out-migration dynamics among people who already live within the pilot region at baseline. The core unit of simulation is the individual agent sampled from the enriched sampling pool. Each agent carries baseline socioeconomic attributes used for distributional measurement and heterogeneity, together with model-derived behavioural fields that represent

intentions and residential preferences. Agents are assigned to subregions using the spatial reference system defined by `region_id`. The model evolves the population month by month over a 120-month horizon under alternative scenarios and policy configurations. Agent state variables are organised to support both behaviour and measurement: decision-relevant fields (for example, intention-related variables, preference satisfaction, policy sensitivity, and other behavioural modifiers) determine mobility responses, while measurement-relevant fields (for example, income, education, activity, and digital access) support equality and sustainability indicators. This separation keeps the decision mechanism interpretable while ensuring outcomes are computed from well-defined micro-level attributes.

---

### 2.5.2 TIME STRUCTURE AND EXECUTION ORDER

The model runs on a monthly time step over a 120-month horizon. This temporal resolution is required because exit risk is time-varying and because scenario and policy effects are evaluated through trajectories rather than single-point comparisons. A fixed execution order is applied for every month and every scenario–policy configuration to preserve counterfactual comparability: population updates, spatial reassignment, indicator computation, and exports are evaluated on the same updated system state at the same simulated time point. Setup loads the spatial environment and runtime inputs, samples agents from the enriched sampling pool, assigns baseline locations, and initializes scenario and policy parameters. During runtime, the model updates time keys, applies macro inflows (MG and NG), computes baseline exit hazards from the timing CDF, applies scenario, policy, and heterogeneity modifiers, and then executes exits and optional internal relocation. Indicators and exports are generated after population dynamics are resolved for the month, ensuring reported trajectories correspond to realised system states.

**Table 3. THE OPERATIONAL STEPS OF ABM**

Step ID	Phase	Step in a single run	Key inputs used	Purpose or meaning
1	Setup	Load spatial reference and baseline region attributes	Shapefile with <code>region_id</code> and population	Establish spatial units and baseline totals
2	Setup	Load runtime inputs	Spatial weights, IML weights, exit	Initialize fixed

			timing CDF, MG/NG inflows	parameters for this run
3	Setup	Sample agents from enriched sampling pool (enrichment output)	Spatial weights, IML weights, exit timing CDF, MG/NG inflows	Create the agent population for simulation
4	Setup	Assign baseline region locations	Shapefile region_id and population, spatial weights if used at setup	Place agents into regions consistently
5	Setup	Initialize scenario and policy configuration	Scenario coefficients, policy strengths, MG-NG inflows	Define the counterfactual setting
6	Setup	Initialize time counters and caches	Tick to calendar mapping, internal counters	Align time keeping and export schedule
7	Monthly loop	Advance simulated time by one month	Tick to calendar mapping	Move the system to the next time point
8	Monthly loop	Apply MG and NG processes for the current month (scenario-specific annual rates converted to monthly rates, applied to the current alive population base)	mgng inflow file, scenario key	Represent scenario specific inflow pressure
9	Monthly loop	Compute baseline exit hazard from timing CDF	120 month CDF	Set the time dependent baseline exit risk
10	Monthly loop	Apply scenario, policy, and heterogeneity modifiers	Scenario coefficients, policy strengths, IML weights, agent attributes	Generate agent specific exit probabilities
11	Monthly loop	Execute out migration and update alive status. Agents that exit are marked with explicit exit status variables and retained in snapshot outputs with alive = false.	Exit probabilities, random seed	Realise exits and update population
12	Monthly loop	Execute internal relocation within pilot region if scheduled	Spatial weights, congestion settings, agent state	Update within region redistribution patterns
13	Monthly loop	Allocate and place inflows if enabled (MG inflows), and apply births if enabled (NG births)	MG/NG inflow counts, spatial weights	Update population with scenario driven inflows
14	Monthly loop	Refresh region level aggregates	Current agent states	Prepare consistent regional totals for metrics
15	Monthly loop	Compute equality and sustainability indicators (alive agents)	EU SILC based attributes on alive agents	Quantify impacts at this time point
16	Monthly loop	Update monitors and plots	Current aggregates and indicators	Support in run diagnostics and calibration
17	Monthly loop	Export scheduled snapshots	Export schedule, current state	Produce traceable outputs for analysis and mapping

18	Finalization	Close run and write run summary	Run metadata, final aggregates	Enable pooling and robustness reporting
----	--------------	---------------------------------	--------------------------------	---

---

### 2.5.3 EXIT DECISION MECHANISM USING A BASELINE TIMING CURVE AND EXPLICIT MODIFIERS

Exit is the primary behavioural mechanism. The baseline timing structure is defined by the 120-month CDF input, which the model converts into a conditional monthly exit hazard representing baseline out-migration risk as a function of simulated time. Scenario and policy effects enter as explicit modifiers applied on top of the baseline hazard: scenario-level parameter sets shift background mobility pressure and condition the strength of response channels, while policy strength parameters scale intervention effects. Individual heterogeneity enters through agent-level attributes and sensitivity parameters, allowing two agents facing the same scenario and policy context to have different exit propensities. This layered structure supports clean counterfactual comparisons because the baseline timing curve remains fixed and only modifier terms vary across scenarios, policies, and individuals. An age-based mobility multiplier is applied to the effective exit probability, decreasing monotonically with age to reflect empirically observed declines in residential mobility over the life course; the same multiplier also affects internal relocation decisions so that age influences overall mobility propensity rather than a single channel.

---

### 2.5.4 POLICY CHANNELS AND PREFERENCE BASED RESPONSE PARAMETERIZATION

Policy effects are modeled through interpretable channels rather than uniform reductions in exit probability. A central channel is preference satisfaction, where policy is represented as improving conditions that matter for residential attractiveness. The relative importance of preference dimensions is provided by the IML weight file, which the model uses to compute composite scores reflecting how strongly an agent values different aspects of living conditions and how policy shifts those conditions under each scenario. Policy strength parameters scale the magnitude of improvements, while scenario-specific coefficients adjust how effectively policy translates into perceived benefits under each transition

pathway. This structure allows the same policy package to generate different behavioural effects under different scenarios and supports heterogeneous responses because agents differ in preference structure and sensitivity.

---

### 2.5.5 INTERNAL RELOCATION AND DESTINATION CHOICE BASED ON SPATIAL WEIGHTS

In addition to exit, the model can simulate internal relocation within the pilot system. When relocation occurs, destinations are not chosen uniformly; destination choice uses the spatial weight file from Task 3.1 as a structured probability distribution over regions. Spatial weights can be used directly or combined with adjustment factors such as a congestion mechanism that penalizes already dominant regions using current population shares. This discourages mechanical concentration and allows spatial patterns to respond endogenously to evolving population dynamics. Because the spatial weight structure is held constant across scenarios and policies, differences in relocation outcomes can be interpreted as consequences of behavioural and macro-condition changes rather than differences in spatial allocation assumptions.

---

### 2.5.6 SCENARIO AND POLICY CONFIGURATION

Each experiment is defined by a scenario and a policy configuration, executed over the same 120-month horizon and evaluated at aligned reporting time points. Scenarios represent alternative transformation pathways and are parameterized through scenario-specific coefficients and macro settings, including MG/NG inputs. Policies represent intervention packages or intensities and are parameterized through policy strength inputs that scale policy channels. The configuration system is designed to support systematic sweeps, so the same model structure can be executed across many combinations without code changes. This ensures that scenario and policy comparisons are performed within a consistent modelling framework and that differences in outcomes reflect configuration differences rather than implementation drift.

---

### 2.5.7 MULTI-RUN EXECUTION AND REPRODUCIBILITY IN SIMULATION

Because the model is stochastic, replicated runs are executed for every scenario–policy configuration. Multiple random seeds ensure results are not driven by single-run trajectories and support distribution-based reporting (for example, mean trajectories and percentile bands) and robustness checks on effect direction and magnitude. Reproducibility is supported by keeping inputs stable across runs, recording run identifiers and configuration keys, and exporting outputs with sufficient metadata to reconstruct experimental conditions. This makes it possible to compare outcomes across pilots using consistent definitions and to rerun specific configurations when sensitivity tests modify one input component (for example, MG/NG trajectories or policy strength values) while holding all other inputs fixed.

### 2.5.8 THE INTERFACE OF ABM IN NETLOGO

The following figure illustrates the interface of this agent-based model in NetLogo 7.0.

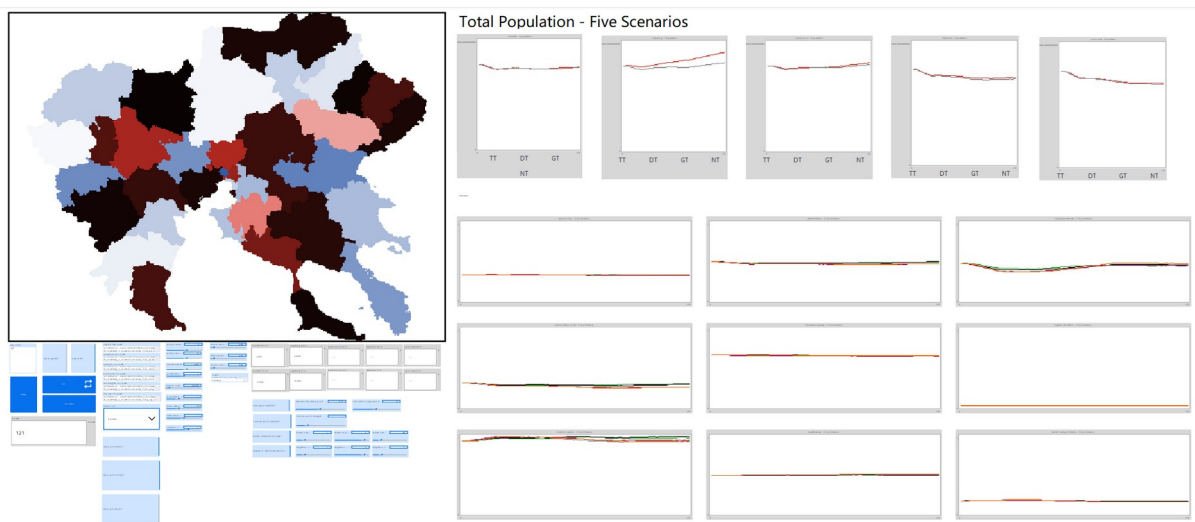


**Figure 3. Interface example of agent-based model in NetLogo**

The interface is designed as an integrated workspace that combines spatial visualization, parameter configuration, and dynamic output monitoring. The map display shows the pilot region and the distribution of agents or aggregated population patterns, enabling visual inspection of concentration, decline, and redistribution during simulation. Input panels allow users to select scenario and policy configurations and adjust key behavioural and population parameters that govern initialization, transition intensity, and the activation of exit, internal relocation, and population-change mechanisms. Multiple output windows

present time-series plots and summary indicators during runtime, supporting rapid diagnostics and parameter refinement. Final analytical results are produced through Behaviour Space batch execution, where the model is run repeatedly across random seeds and systematic scenario–policy sweeps, generating standardized agent snapshots at predefined time checkpoints for downstream processing in Python (aggregation, spatial analysis, and reporting).

### 2.5.9 DETAILED EXPLANATION OF MODULES

This section documents the simulation modules and their interface-level parameters, focusing on the runtime “input contract” that links the ABM to its external data files and configuration settings. The ABM reads a fixed set of file-based inputs at setup, including the spatial reference (region shapefile), spatial weights for allocation and relocation, the enriched sampling pool used to instantiate agents, the 120-month exit timing CDF, the IML-derived preference weights, and the MG/NG table that drives external inflows and natural growth. In addition, the interface exposes parameters that control stochasticity, scaling, policy and scenario intensity, population-change dynamics, remote-work allocation, and internal relocation. Table 4 lists these parameters in a structured manner, grouped by functional module, to support transparent documentation, reproducible batch execution, and consistent comparison across scenario–policy experiments.

**Table 4. THE MODULES AND PARAMETERS ON THE INTERFACE**

Category of Modules	Sub-category of Modules	Parameter (Interface Variable)	Meaning
Input and Output	File paths	region-shp-path	Path to the region shapefile used to load boundaries and region_id.
	File paths	spatial-probs-path	Path to the spatial probability (spatial weight) file used by spatial allocation and destination choice mechanisms.
	File paths	samples-csv-path	Path to the individual-level enriched sampling pool used to initialize agents and micro-level attributes.
	File paths	probs120-csv-path	Path to the 120-month cumulative exit probability table (CDF) used to convert tenure into a baseline monthly hazard.
	File paths	iml-weights-csv-path	Path to the interpretable ML (IML) weight table used to compute composite preference scores and policy-response channels.
	Population change	mg-ng-csv-path	Path to the CSV containing scenario-specific annual

	inputs		MG (external inflow) and NG (natural growth) rates used by the population-change module.
	Output paths	outdir	Directory where simulation outputs (CSV summaries, snapshots, and logs) are stored.
Randomness	Random seed	rng-seed	Random seed for reproducible stochastic processes (sampling, exits, relocation, noise, births, and deaths).
	Micro noise	micro-noise-scale	Strength of individual-level random disturbance in exit propensity.
	Macro noise	macro-noise-scale	Strength of macro-level stochastic shocks affecting exit propensity.
	Heterogeneity noise	heterogeneity-noise-scale	Strength of persistent heterogeneity noise representing inter-individual sensitivity differences.
Visual Setting	Track selection	only-tt-nt?	If true, only TT and NT tracks are simulated (reduces the number of scenario-policy tracks).
	Display	show-agents?	Toggle for displaying agents on the map during runtime (display-only; does not change model logic).
	Demo scenario selector (optional)	demo-scen	Chooser used for display-only demo views (e.g., selecting the scenario used in the TT vs NT percent-change overlay).
	Demo controls (optional)	show-pct-demo?	Display-only switch to show or hide the percent-change demo panel/components (UI-only; does not affect simulation results).
	Demo overlay (optional)	show-pct-overlay?	Display-only switch that enables a TT vs NT percent-change overlay map for the selected demo-scen (refreshed at annual checkpoints).
	Demo labels (optional)	show-pct-labels?	Display-only switch that toggles percent-change labels on the overlay map (labels shown on representative patches).
Sampling & scaling module	Population scale	sample-scale	Population scaling factor that changes the number of simulated agents without changing probability logic.
Policy and Scenario Setting	Policy intensity	policy-strength-dt	Strength of the Digital Transition policy channel; scales policy effects in the effective exit probability ( $p_{eff}$ ).
	Policy intensity	policy-strength-gt	Strength of the Green Transition policy channel; scales policy effects in the effective exit probability ( $p_{eff}$ ).
	Scenario intensity	scenario-impact-scale	Global multiplier that amplifies or attenuates scenario impacts and related macro mechanisms.
Population Dynamics	Exit decision rule	exit-threshold	Threshold used to trigger exit or relocation based on the effective probability ( $p_{eff}$ ).
	Macro calibration	calibration-factor	Global calibration multiplier applied to selected macro components (including MG rate conversion).
	Population growth scaling	population-growth-scale	Global multiplier scaling population-change components (MG inflows, NG births, and mortality intensity).
Remote Work	Remote-work mechanism	remote-work-enabled?	Toggle enabling the remote-work mechanism that shifts inflow allocation toward smaller or left-behind regions.
	Remote-work mechanism	remote-work-strength	Strength of the remote-work allocation shift toward smaller regions.
Internal	Relocation switch	relocation-	Toggle enabling internal relocation (moving within

Relocation		enabled?	the pilot system) as an alternative to exiting.
	Relocation probability	internal-relocation-prob	Probability that a triggered mobility event becomes relocation instead of leaving the system.
	Relocation destination model	relocation-congestion-k	Congestion penalty parameter for relocation destination choice (higher values discourage crowded regions).
Preference and Attachment	Preference satisfaction	preference-satisfaction-scale	Scaling factor for the preference-satisfaction effect in the effective exit probability.
	Place attachment	place-attachment-scale	Scaling factor for the place-attachment effect that reduces exit propensity.
	Age-sensitive mobility	(embedded in code)	Life-course adjustment implemented as an age-based multiplier that decreases with age and scales mobility propensity after other modifiers are applied.

**Input and Output module:** It defines the runtime data backbone of the simulation and the export contract used for downstream analysis. The region shapefile sets the spatial frame and the region\_id system used for allocation, relocation, and mapping. Spatial weights provide structured destination probabilities for spatial assignment processes, while the enriched sampling pool initializes agents with EU-SILC-anchored socioeconomic attributes plus model-derived behavioural and preference fields estimated from MOBI-TWIN as an enrichment layer. The 120-month exit CDF supplies the baseline timing curve used to derive monthly hazards, and the IML weights parameterize composite preference scoring and policy-response channels. Outputs are written to outdir as standardized snapshots and summaries with run metadata for reproducible post-processing.

**Randomness module:** This module controls reproducibility and the representation of stochastic variability. The random seed fixes the sequence of random draws, allowing exact replication of a configuration and controlled comparisons across scenarios and policies. Micro noise introduces short-term idiosyncratic variation in exit propensity, while heterogeneity noise introduces persistent dispersion in agent sensitivity beyond observed attributes. Macro noise adds time-varying shocks shared broadly across agents, increasing volatility in trajectories and indicator series. In batch experiments, varying seeds enables distribution-based reporting and robustness checks.

**Visual Setting module:** This module governs interactive visualization and lightweight diagnostic runs, without changing the underlying simulation logic.

Track selection (for example, TT and NT only) reduces the number of parallel tracks evaluated in a single execution and improves runtime tractability during development. Display toggles control whether agents are rendered on the map and whether optional percent-change overlays and labels are shown for a selected demo scenario. These visual controls are intended for observation, communication, and debugging, and they do not alter exported agent snapshots used for analysis. Final results are generated from BehaviorSpace batch runs where visualization is typically disabled.

**Sampling and scaling module:** This module controls the computational scale of the simulated population relative to the enriched sampling pool. The sample-scale parameter increases or decreases the number of simulated agents while preserving the same decision rules and probability logic. Larger samples reduce Monte Carlo variability and stabilize region-level indicators, especially in small subregions, at the cost of higher runtime and memory use. Smaller samples accelerate experimentation but can increase sampling noise in disaggregated outputs. Varying sample scale can therefore serve as a practical sensitivity check.

**Policy and Scenario Setting module:** This module encodes the counterfactual environment of the simulation. Policy strength parameters for Digital Transition and Green Transition scale the magnitude of policy effects within the preference-based response channels and enter the effective exit probability. The scenario impact scale adjusts the overall intensity of scenario-related modifiers and interacts with macro settings to reflect different opportunity and risk contexts. Together, these settings define differences between policy pathways within the same scenario and differences between scenarios under the same policy pathway.

The structured configuration supports systematic sweeps across scenario–policy combinations without changing code.

**Population Dynamics module:** This module controls the demographic mechanisms that translate micro-level decisions and macro rates into population trajectories. The exit threshold governs how easily an agent is

classified as leaving or relocating based on the effective probability, directly affecting population decline and compositional change. The calibration factor provides a global adjustment used to align selected macro components to external demographic references. The population growth scale modulates population-change channels, including MG inflows, NG births, and mortality intensity, and therefore shapes the balance between exits and demographic replenishment. These parameters are central for interpreting whether scenario differences manifest primarily through behavioural exits, demographic replenishment, or their interaction.

**Remote Work module:** This module modifies how external inflows are spatially allocated across subregions when remote-work conditions are enabled. When turned on, inflows generated by the MG mechanism are not allocated solely according to existing concentration patterns; instead, allocation is shifted toward smaller or left-behind subregions. The strength parameter controls the magnitude of this shift and can generate divergent spatial distributions even when total population trajectories are similar. This redistribution affects subregional indicators and can create feedback because spatial distribution influences subsequent relocation and exit dynamics. The module is therefore important for evaluating spatial equity implications of remote work.

**Internal Relocation module:** This module represents within-pilot mobility as a distinct outcome from leaving the system. When enabled, some mobility events that would otherwise result in exit are converted into internal moves across subregions, with the conversion frequency governed by the internal relocation probability. Destination choice is structured by spatial weights and can be adjusted by a congestion penalty that discourages moves into already crowded subregions. This mechanism affects net population loss, spatial sorting, and region-level inequality outcomes, even when total population change is modest. It also captures realistic adaptation behaviours where residents move within the region rather than leaving it.

**Preference and Attachment module:** This module governs the behavioural link between living conditions and mobility outcomes. Preference satisfaction aggregates multiple preference dimensions into a composite term that modifies

exit propensity, with its scaling factor controlling how responsive agents are to improvements in conditions. Place attachment represents stabilizing effects of rootedness and local ties and reduces exit propensity, potentially dampening differential policy effects if attachment dominates. Age-sensitive mobility is implemented as a life-course multiplier that decreases with age and scales mobility propensity after other modifiers are applied. Together, these mechanisms shape heterogeneous responses and therefore influence distributional outcomes over time.

Social Influence module (friends and neighbours): This module represents endogenous social influence as additional modifiers of exit propensity based on observed mobility behaviour of others. Friend-based influence captures relational effects through explicit social ties, while neighbour-based influence captures informational effects derived from the local residential environment. These signals do not replace individual decision logic; they amplify or dampen existing tendencies alongside preference satisfaction, scenario and policy modifiers, attachment, and stochastic noise. The module can generate path dependence, localized cascades, and clustering of mobility behaviour across space and time. As a result, it can shape both aggregate population trajectories and the spatial sequencing of departures and stabilization.

---

### 2.5.10 MODEL CALIBRATION AND ALIGNMENT STRATEGY

The model adopts a coarse alignment strategy to ensure that baseline simulation trajectories evolve within a plausible demographic envelope for each country–pilot system while preserving the internal causal mechanisms of the agent-based model (ABM). The goal is not to reproduce exact population forecasts, but to anchor the baseline to an external long-run reference so that subsequent scenario and policy experiments can be interpreted relative to a stable benchmark. This approach is appropriate because the ABM is designed as a comparative experimental platform rather than a forecasting tool, because population change emerges from interacting micro-level mechanisms that cannot be uniquely fitted to a single macro target without overfitting, and because overly tight calibration risks absorbing scenario signals into parameter tuning. As a result, moderate deviations from the external reference are

acceptable as long as baseline direction and magnitude remain plausible and consistent.

Within this framework, the alignment workflow follows three steps. Step 1 (base parameterization and cross-pilot consistency): we first established a stable and reproducible sampling and simulation pipeline on one pilot and then held core behavioural and policy parameters constant across all pilots. Importantly, the input sampling pool is pilot-specific because it is constrained by the available EU-SILC microdata in the target country; for example, the Groningen pilot is instantiated by sampling exclusively from the Netherlands-wide EU-SILC micro-sample. The main pilot-specific adjustment at this stage is the sampling ratio (down-sampling ratio) used to instantiate the agent population from the enriched sampling pool, which supports computational feasibility while keeping model logic unchanged. At the same time, parameter-missingness handling is kept consistent across all pilots to ensure comparable treatment of empty or unavailable parameter fields. Step 2 (alignment to an external demographic reference): baseline trajectories are aligned to the projected 10-year population change rate for 2025–2035 derived from EU population projections (PROJ\_19RP3). For each pilot, the calibration target for total population is taken from an independent EU population projection at the corresponding spatial scope, and the model aligns its baseline by calibrating exogenous population inflows (i.e., inflows external to the internal transition system) so that simulated total population change approaches the projection target as closely as possible. Because the spatial scope differs by pilot in the current workflow, the reference change rate is computed at the corresponding scope (national or pilot-area level). Table 5 summarizes the target change rate (2025–2035), the resulting aligned baseline change produced by the model, and the sampling ratio used for each country–pilot system. In addition, out-migration dynamics are primarily driven by the stated migration expectations elicited in the MOBI-TWIN survey; the model’s role is to transform these expectations under different scenario conditions rather than to re-estimate behaviour separately for each pilot.

**Table 5. ALIGNMENT TARGETS AND RESULT OF FIVE PILOTS**

Name Country and Pilot	Country Code	NUTS Code	2025 <sup>3</sup>	2035 <sup>4</sup>	10_year_change Target	Alignment Result	Sampling Ratio
------------------------	--------------	-----------	-------------------	-------------------	-----------------------	------------------	----------------

Greece (Central Macedonia)	EL	EL52	1837355	1768749	-3.734%	-2.200%	0.002
Spain (Castilla-La Mancha)	ES	ES42	2007777	1939099	-3.421%	-2.800%	0.002
Finland (North & East Finland)	FI	FI1D	1253804	1193997	-4.770%	-5.000%	0.005
Italy (Lombardy)	IT	ITC4	10179939	1037091 7	1.870%	1.600%	0.001
Netherlands (Groningen)	NL	NL11	581097	566152	-2.572%	-2.000%	0.01

Alignment is implemented by adjusting the scenario-intensity parameter MG using mean outcomes over ten stochastic runs. For each country–pilot system, we evaluate a set of candidate MG values, summarize the mean population change at the end of the simulation horizon (month 120), and fit a smooth relationship between MG and end-of-horizon population change. We then solve for the MG value that yields an aligned baseline under the No Transition setting, which represents continuation of current trends without digital-transition policies, green-transition policies, or additional scenario shocks. After obtaining the aligned baseline MG, MG values for the remaining scenarios are rescaled proportionally to preserve the predefined stepwise ordering (Leapfrog > Dark Horse > Baseline > Snail Pace > Lions’ Den) while maintaining comparable spacing across pilots. Because MG directly governs scenario-dependent external inflows, this procedure anchors the scenario ladder to an externally meaningful baseline while preserving internally consistent relative differences across scenarios.

Step 3 (final batch runs and robust reporting): after alignment, the model is executed in batch mode for each country–pilot system, scenario, and policy setting with ten stochastic replications. Reported results summarize mean trajectories and, where relevant, uncertainty bands across replications to reduce Monte Carlo variability and support cross-pilot comparison. Subsequent scenario and policy effects are interpreted relative to the aligned baseline documented in Table 5, ensuring that differences in outcomes reflect modeled

---

<sup>3</sup> [https://ec.europa.eu/eurostat/databrowser/view/proj\\_19rp3/default/table?lang=en&category=proj.proj\\_19r](https://ec.europa.eu/eurostat/databrowser/view/proj_19rp3/default/table?lang=en&category=proj.proj_19r)

<sup>4</sup> [https://doi.org/10.2908/PROJ\\_19RP3](https://doi.org/10.2908/PROJ_19RP3)

mechanisms under alternative configurations rather than differences in starting demographic envelopes.

## 2.6 ANALYTICAL OUTPUTS AND MAPPING

### 2.6.1 OUTPUT STRATEGY AND FILE SCHEMA

Simulation outputs are designed to support three needs at the same time: within-run diagnostics, cross-scenario and cross-policy comparison, and pooling across multiple seeds for robustness analysis. For this reason, outputs are saved as file-based snapshots rather than relying only on interactive monitors. Each exported record carries the minimal metadata required to reconstruct provenance, including `run_id`, `tick`, `scenario`, and `policy`, together with a stable agent identifier and key state variables. Outputs follow a long-format schema in which each row represents one agent at one time point under one scenario and one policy configuration, with explicit fields for alive status and `region_id` assignment. This design supports consistent post-processing rules, most importantly the alive-only filter for indicator computation, and enables unambiguous aggregation by `region_id` for mapping. The schema also retains explicit exit-related fields (`exit_kind`, `exit_month`, and `exit_from_rid`), which allows post-processing to distinguish active residents from agents who have exited and to support diagnostics on the timing and spatial origin of exits.

To ensure computational feasibility and comparability across pilots, simulations are executed on sampled synthetic populations using pilot-specific sampling ratios. Sampling ratios are selected to balance tractable runtime with adequate spatial coverage of agents across subregions for mapping and diagnostics, and the pilot-specific values are reported in Table 5. Reported outputs can be interpreted at the sampling scale directly and can also be rescaled to the original population magnitude for contextual understanding by applying the corresponding sampling ratio as a scalar conversion factor. For the main report, visualizations and cross-scenario comparisons are expressed primarily as percent changes relative to the baseline time point, which improves interpretability across pilots and reduces sensitivity to differences in population size and sampling scale. High-resolution outputs in absolute values at the sampling scale, including additional disaggregation and indicator panels, are provided in the Appendix to support detailed inspection and traceability. Specifically:

- Simulations for EL (Greece, Central Macedonia) are executed on a sampled synthetic population using a pilot-specific sampling ratio of 0.002.

- Simulations for ES (Spain, Castilla-la Mancha) are executed on a sampled synthetic population using a pilot-specific sampling ratio of 0.002.
- Simulations for FI (Finland, North and East Finland) are executed on a sampled synthetic population using a pilot-specific sampling ratio of 0.005.
- Simulations for IT (Italy, Lombardy) are executed on a sampled synthetic population using a pilot-specific sampling ratio of 0.001.
- Simulations for NL (Netherlands, Groningen) are executed on a sampled synthetic population using a pilot-specific sampling ratio of 0.01.

---

## 2.6.2 SIMPLIFIED STRUCTURE OF THE AGENT-LEVEL SNAPSHOT OUTPUT

The ABM exports agent-level snapshots in long format. Each row represents one agent at one simulated time point under one scenario and one policy, with explicit identifiers that support downstream filtering, aggregation, and replication-based pooling. Table 6 summarizes the snapshot schema as grouped field blocks, including run and time keys, agent identifiers, alive and eligibility flags, spatial state, exit state, core socioeconomic attributes used for indicator computation, and simulation heterogeneity fields. The snapshot also contains intention- and preference-related variables (q35 to q59) used by ABM decision channels. These fields are included as model-derived enrichment fields appended to the baseline micro attributes and are treated as standard inputs in post-processing rather than as separate external joins.

**Table 6. THE DATA STRUCTURE OF THE AGENT-LEVEL SNAPSHOT OUTPUT**

Level 1 block	Level 2 fields (examples)	Meaning for post-processing
Run and experiment identifiers	run_id, scenario, policy, source_type	Keys used to group outputs by configuration and to pool results across replicated runs; source_type flags the origin/type of the record within the simulation pipeline.
Time keys	tick, month	Aligns observations to reporting time points and supports consistent trajectory comparisons.
Agent identity	aid, eu_id	Stable identifiers for tracing agents across time and preventing double counting during aggregation (identifiers are used for internal tracking only).
Survival and activity status	alive, status, can_migrate	Defines the analytic population at each time point (alive-only rule) and captures runtime eligibility and activity labels used in filtering and diagnostics.
Spatial state	region_id, x, y	Links agents to spatial units used for aggregation and mapping and supports relocation diagnostics.
Exit state	exit_kind, exit_month, exit_from_rid	Captures whether and how an exit occurred, the time of exit, and the origin region at the moment of exit; supports separating active residents from exited agents in long-format snapshots.

Demographics and lifecycle state	age_sim, RB081_age, RB090_sexcode, tenure_months	Demographic fields and lifecycle state variables used for stratification, life-course adjustments, and time-varying mobility risk.
Core socioeconomic attributes for indicators	HY010_income, PD080_internet, PE041_edu, PH010_health, RB211_activity, PC280_ptfreq	Micro-level attributes used to compute equality and sustainability indicators; value mappings and valid-response rules are applied consistently in post-processing.
Simulation heterogeneity	heterogeneity_base	Baseline heterogeneity term used to represent inter-individual differences in sensitivity and response.
Model-derived behavioural enrichment fields	q35-q59	Intention- and preference-related variables used by ABM decision channels; included as model-derived enrichment fields appended to baseline micro attributes (not created via record-level matching or transfer).

### 2.6.3 PILOT-WIDE TOTAL POPULATION TRAJECTORIES

Pilot-wide population trajectories are computed as a core analytical output to contextualize indicator changes and to document demographic impacts of the modeled mobility dynamics. Total population at each time point is defined as the number of alive agents in the pilot system, computed for every (run\_id, tick, scenario, policy) by counting `alive == 1` in the snapshot files and then summarized across replicated runs to produce mean trajectories with uncertainty bands. Beyond the total trajectory, the post-processing pipeline also produces a set of population joint outputs that decompose population structure by key demographic and socioeconomic categories, including sex, age bins, education tiers, and labour-force structure. These breakdown panels are computed at the pilot level using alive-only snapshots and are summarized across seeds using consistent statistics such as means and quantile bands. This enables side-by-side interpretation of how scenarios and policies reshape both population size and composition over time. Table 7 lists these population output families and their computation basis.

**Table 7. PILOT-LEVEL POPULATION WITH CATEGORIES (PANELS OVER TIME)**

Output family	Breakdown group	Output unit	Key fields used (alive-only)	Computation and outputs
Total population trajectory	Total	Pilot-level	run_id, tick, scenario, policy, alive	For each (run_id, tick, scenario, policy), compute <code>pop_total = count(alive==1)</code> . Summarize across runs to produce mean trajectory and uncertainty bands (quantiles). Export by-run tables and summary tables; generate time-series figures.
Population by sex	Male / Female	Pilot-level	RB090_sexcode	Map RB090_sexcode into Male/Female (code lists), compute counts by group within each (run_id, tick, scenario, policy). Summarize across runs (mean + quantiles) and plot panel figures.

Population by age	Age bins	Pilot-level	RB081_age	Bin ages into predefined intervals (AGE_BINS/AGE_LABELS), compute group counts per (run_id, tick, scenario, policy). Summarize across runs and plot multi-line/panel figures.
Population by education	Primary / Secondary / Tertiary	Pilot-level	PE041_edu	Recode education into three buckets using top-coded logic: Primary (PE041 < 300), Secondary (300 ≤ PE041 < 500), Tertiary (PE041 ≥ 500). Compute group counts; summarize across runs; plot panel figures.
Employment structure	Labour force total; Employed; Unemployed	Pilot-level	RB211_activity	Define labour force as RB211_activity ∈ {1,2}; compute labour-force total and counts of Employed (1) and Unemployed (2) per (run_id, tick, scenario, policy). Summarize across runs and plot panel figures (employment totals + composition).

## 2.6.4 REGIONAL EQUALITY AND SUSTAINABILITY INDICATORS COMPUTATION

For each exported snapshot, the analytic population is restricted to agents flagged as alive and then grouped by region\_id to produce subregional metrics that can be compared across space and over time within a pilot. Indicator definitions rely on EU-SILC-based micro attributes carried by agents, ensuring that reported values retain a clear interpretation as distributional properties, population shares, or behavioural proxies of the simulated resident population. In the current simulation design, we do not re-assign or re-scale individual income under scenario conditions (e.g., via an explicit inflation or economic-growth module). Instead, agents are instantiated by sampling from the pilot’s overall enriched micro-sample and then “deployed” into the simulation, such that income-related indicators remain anchored to the EU-SILC-based micro distribution embedded in the sampled population. The indicator suite is computed consistently for each (run\_id, tick, scenario, policy, region\_id) combination using transparent rules: invalid or missing micro variables are excluded from denominators rather than imputed, formulas are kept stable across pilots and configurations, and outputs are produced for every run to enable robust aggregation across replications. Table 8 summarizes the region-level metrics, starting with the subregional population count (pop) and followed by equality and sustainability indicators that capture income dispersion, internet access, education and health distributions, gender balance, working-age structure, employment performance, human-capital concentration, and a public-transport-use index. Accordingly, the implicit modelling assumption is that temporal and spatial changes in these indicators are primarily driven by compositional change in the resident population, especially via differential out-migration and relocation, rather than by endogenous interactions

among indicators or within-indicator value updates during the simulation. These metrics provide the harmonized basis for mapping and for subsequent delta-series analyses described below. .

**Table 8. EQUALITY, SUSTAINABILITY, AND POPULATION INDICATORS (REGION-LEVEL)**

Category	Indicator name	Output field name	Meaning and interpretation	Computation from agent snapshot variables (alive-only, within each region_id)
Population	Population (alive agents)	pop	Subregional population size used for mapping and weighting.	pop = count(alive==1) within each region_id for a given (run_id, tick, scenario, policy).
Equality	Income equality	income_equality	Higher values indicate more equal income distribution within a subregion.	Compute Gini over positive HY010_income (>0) among alive agents; income_equality = 1 - Gini(income). If <2 valid observations, return 1.0. HY010 is total household gross income.
Equality	Internet access share	internet_share	Share of residents with home internet among valid responses.	Using PD080_internet, valid responses {1,2,3}; "has internet" is 1. internet_share = count(PD080_internet==1) / count(PD080_internet ∈ {1,2,3}).
Equality	Education equality	edu_equality	Higher values indicate a more even distribution of education codes within a subregion.	Coerce PE041_edu to numeric edu_lv (with invalid codes mapped to NaN); compute edu_equality = 1 - Gini(edu_lv). If <2 valid, return 1.0.
Equality	Health equality	health_equality	Higher values indicate more equal self-reported health (higher is better).	For valid PH010_health ∈ {1..5}, define health_good = 6 - PH010_health; compute health_equality = 1 - Gini(health_good). If <2 valid, return 1.0.
Equality	Gender balance	gender_balance	Balance between men and women among valid sex codes.	From RB090_sexcode valid {1,2}, compute shares and set `gender_balance = 1 -
Sustainability	Working-age share (15–64)	labour_share_15_64	Proxy for labour supply potential and demographic sustainability.	From RB081_age, labour_share_15_64 = count(15≤age≤64)/count(valid age).
Sustainability	Employment rate (working age)	employment_rate	Employment performance among working-age residents; denominator excludes retired.	Working age 15–64. Denominator: RB211_activity ∈ {1..8} and RB211_activity != 3; numerator: RB211_activity == 1. employment_rate = num/den.
Sustainability	Higher	higher_edu_share	Proxy for human-	Using numeric edu_lv:

y	education share		capital concentration.	higher_edu_share = count(edu_lv ≥ 500)/count(valid edu_lv). According to the EU-SILC data methodology guide, we use the code ≥500 as tertiary (high education agents).
Sustainability	Public transport index	public_transport_index	Public transport friendliness from frequency of PT use.	Map PC280_ptfreq to {1:1.00,2:0.75,3:0.50,4:0.25,5:0.00}; compute mean score within region_id.

## 2.6.5 CATEGORIZED POPULATION DYNAMIC COMPUTATIONS FOR REGIONAL MAPS

To support comparative mapping of regional dynamics, the analysis pipeline derives delta-series measures that express relative change over time rather than raw levels. The core idea is to compute percent change relative to the baseline time point (Year 0 or tick 0) for each region, and then summarize these changes across replicated runs to obtain stable, uncertainty-reduced surfaces for mapping. The workflow proceeds in three stages. First, for each run and each metric in the regional indicator set, including pop and all equality and sustainability metrics, a per-run delta percent change is computed within each (scenario, policy, region\_id) as  $(\text{value} / \text{baseline} - 1) \times 100$ , where the baseline is the metric value at Year 0 for the same run and configuration. Second, delta percent change values are aggregated across runs to produce mean delta surfaces at each time point. For population mapping, the pipeline retains both the absolute pop, which is used for masking and validity checks, and a dedicated delta field (pop\_delta\_pct), which is used as the mapped value. Third, to ensure comparability across maps, delta colour scales are defined symmetrically around zero using a robust absolute bound derived from the empirical distribution of absolute delta values, which prevents outliers from dominating visualization. Table 9 summarizes these delta-series outputs and how they are used in map production.

**Table 9. CATEGORIZED POPULATION DYNAMIC FOR REGIONAL MAPS**

Delta output family	Output field(s)	Definition	Computation basis	Notes for mapping
Delta percent change vs Year 0 (per run)	<metric>_delta_pct (intermediate)	Percent change relative to Year 0 within the same run, scenario, policy, and region.	For each (run_id, scenario, policy, region_id) and each year, compute delta_pct = $(\text{value} / \text{base\_year0} - 1) \times 100$ , where base_year0 is the metric value at Year 0 (tick 0).	Computed for all metrics in METRICS_ALL (including pop and all equality/sustainability metrics).
Delta percent change	pop_delta_pct (for pop), and <metric> (for others)	Mean delta percent change across	Compute delta percent change per run first, then aggregate across runs by	For pop, keep absolute pop as a separate column for masking and map value

(mean across runs)		replicated runs.	mean for each (tick/year, scenario, policy, region_id).	uses pop_delta_pct.
Delta map scales	vmin/vmax (per metric)	Symmetric scale around zero based on a robust absolute bound.	For each metric, compute a bound from a high quantile of `	delta

### 2.6.6 BETWEEN-REGION INEQUALITY INDICES FOR PILOT-LEVEL COMPARATIVE ASSESSMENT

In addition to region-level indicators and delta-series mapping, the pipeline quantifies inequality across subregions at the pilot level by treating region\_id units as the analytical observations. These indices summarize how unevenly population and regional metrics are distributed across subregions and support pilot-level comparison across scenarios and policies. The workflow computes inequality measures for each (run\_id, tick, scenario, policy) combination and then summarizes them across replicated runs. Table 10 lists the between-region indices, including dispersion in subregional population sizes and population-weighted inequality measures for the regional indicator set in Table 8. Weights are based on subregional population (pop) so that larger subregions contribute proportionally more to area-wide inequality estimates.

**Table 10. BETWEEN-REGION INEQUALITY INDICES**

Category	Index name	Meaning and interpretation	Computation basis
Inequality across subregions	Unweighted Gini of population across subregions	Inequality of subregional population sizes across region_id units.	Compute Gini over region_pop across subregions (finite values only).
Inequality across subregions	Unweighted coefficient of variation of population across subregions	Dispersion of subregional population sizes across region_id units.	$\text{between\_pop\_cv} = \text{std}(\text{region\_pop}) / \text{mean}(\text{region\_pop})$ (finite values).
Inequality across subregions	Population-weighted Gini across subregions (by metric)	Population-weighted inequality of a regional metric across region_id units.	For each regional metric in Table 8, compute weighted Gini over subregional values using weights region_pop (drop NaN in values).
Inequality across subregions	Population-weighted coefficient of variation across subregions (by metric)	Population-weighted dispersion of a regional metric across region_id units.	For each regional metric in Table 8, compute weighted CV over subregional values using weights region_pop (drop NaN in values).

---

### 2.6.7 GEOSPATIAL MERGE AND MAP PRODUCTION

After region-level metrics and delta-series outputs are computed, they are joined to the pilot region geometry using `region_id` as the spatial primary key, producing geospatial tables that can be mapped consistently across scenario and policy configurations. Mapping is designed to support comparative interpretation rather than isolated visualization. Indicator definitions, spatial units, and reporting time points are fixed across map sets, and delta-series maps use symmetric scales centred at zero to make increases and decreases directly comparable. Outputs are produced as static images for reporting, with file names that encode scenario, policy, tick, and metric identifiers. This naming convention supports automated assembly of result appendices and prevents accidental mixing of outputs across experiments.

---

### 2.6.8 ROBUSTNESS ACROSS RUNS AND PRE BATCH SANITY CHECKS

Robustness is addressed through replicated runs under multiple random seeds for each scenario and policy configuration. Post-processing pools outputs across runs and summarizes indicators using distribution-based statistics such as means, medians, and percentile intervals. This makes stochastic uncertainty explicit and supports claims about stable effect direction and magnitude rather than relying on single-run trajectories. To reduce the risk of silent pipeline failures during large batch processing, a lightweight quick-check routine is used as a pre-batch gate: it reads one output file, selects one observed configuration, computes region metrics, merges them with geometry, and draws a diagnostic map to validate schema consistency, filtering logic, merge integrity, and expected missingness behaviour. Once the quick check passes, the same functions are applied in batch across all outputs to produce the full set of tables and maps for reporting.

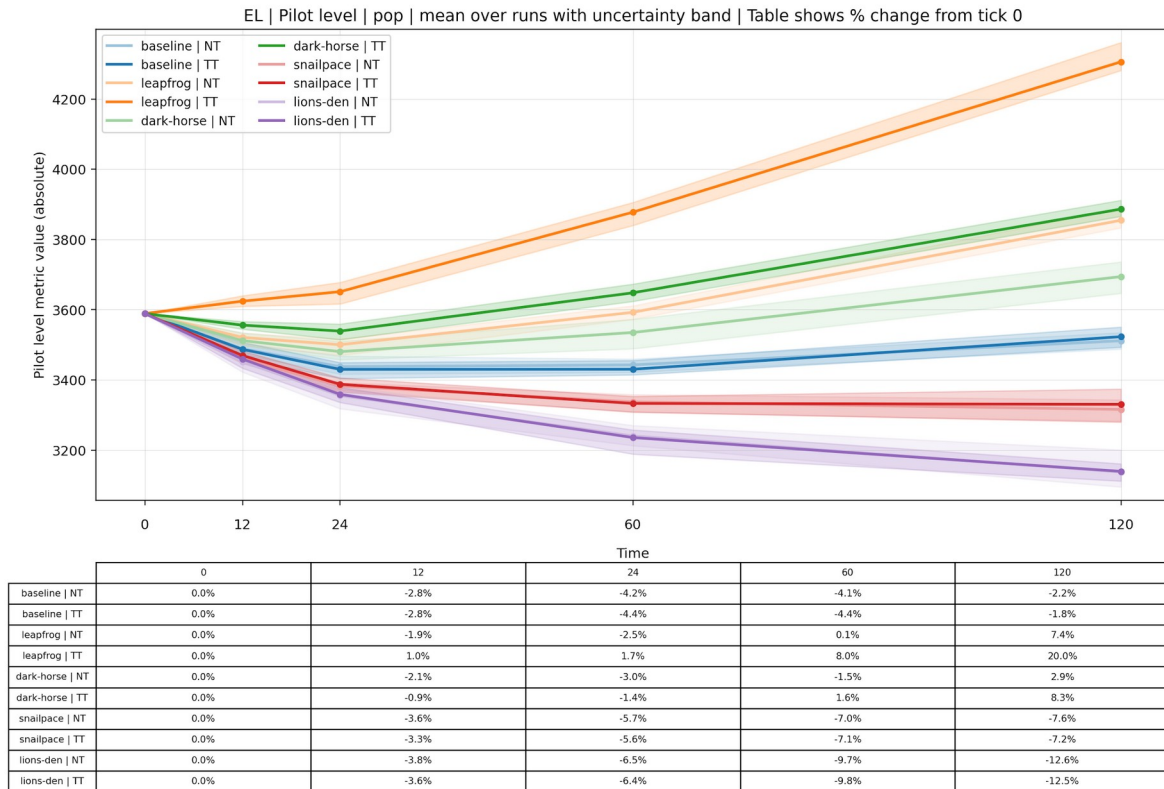
## 3 MAIN RESULT: POPULATION, EQUALITY, AND SUSTAINABILITY

### 3.1 GREECE: CENTRAL MACEDONIA (NUTS - EL52)

---

#### 3.1.1 EL (CENTRAL MACEDONIA) PILOT-LEVEL TOTAL POPULATION DYNAMICS ACROSS SCENARIOS

Figure 4 illustrates the change of total population in year 1, year 2, year 5, and year 10.



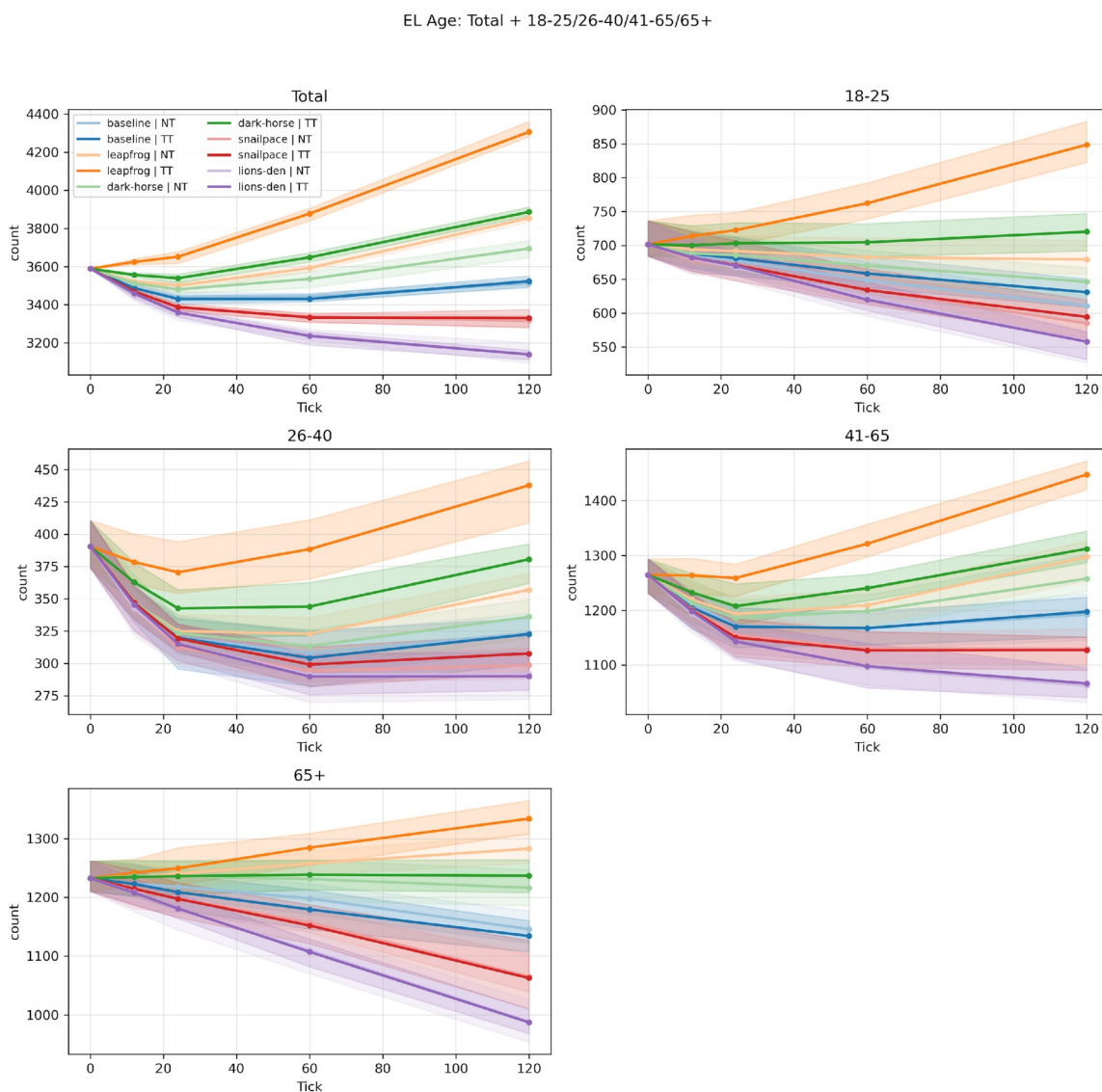
**Figure 4. EL (Central Macedonia) Total Population trends over time**

Figure 4 shows strong separation between scenarios that grows with the time horizon, indicating that scenario context is the primary driver of long-run population outcomes in EL (Greece, Central Macedonia). The reporting time points correspond to Year 1 (t = 12), Year 2 (t = 24), Year 5 (t = 60), and Year 10 (t = 120). By Year 10, Leapfrog produces sustained growth, reaching a 20.0 percent increase, while Dark Horse ends with a smaller but still positive increase of 8.3 percent. Baseline remains close to zero change and ends with a modest decline of 1.8 percent. In contrast, Snail Pace and Lion’s Den generate persistent decline trajectories that deepen over time, reaching 7.2 percent and 12.5 percent declines by Year 10, respectively. Overall, the result indicates that favourable scenarios generate a widening demographic advantage over time in Central Macedonia, while adverse scenarios dominate long-run population outcomes. The subsequent figures and tables follow the same set of reporting time points to support consistent comparison across outputs. In Deliverable D2.3, Central Macedonia (EL52) is classified as a “Structurally Lagging and Peripheral Region”, where weaknesses such as low accessibility and weaker institutions coexist with opportunities including niche tourism, decentralised energy, and rural innovation. The population trajectories in Figure 4 are consistent with this typology, as scenario context determines whether such

opportunities can translate into cumulative gains or whether structural constraints dominate. Consequently, adverse scenarios are associated with persistent decline, whereas favourable scenarios support a cumulative demographic advantage over time.

### 3.1.2 EL (CENTRAL MACEDONIA) PILOT-LEVEL POPULATION TRENDS OVER TIME BY CERTAIN GROUPS

Figure 5 shows the population trends over time by age group as an example.



**Figure 5. EL (Central Macedonia) population trends over time by age group**

Figure 5 shows that scenario differences in Central Macedonia are expressed not only in total population levels but also in age composition, with the clearest divergence emerging in younger and prime working-age cohorts. Under Leapfrog, growth becomes broad-based by the end of the horizon, with strong increases among ages 18 to 25 and clear gains among ages 41 to 65, while ages 26 to 40 show an early decline followed by recovery later in the horizon. Under Dark Horse, total growth is positive by the end of the horizon, but the cohort profile is more uneven, with limited gains among ages 18 to 25 and continued weakness in ages 26 to 40 relative to other groups. Under Snail Pace and Lion's Den, declines are widespread across cohorts, and the largest proportional losses concentrate in ages 26 to 40 and ages 18 to 25, implying disproportionate pressure on segments most closely linked to labour-force capacity and longer-term demographic sustainability. These cohort-specific trajectories help explain why the total population lines separate sharply across scenarios, since favourable contexts support retention and replenishment among working-age groups, while adverse contexts generate concentrated losses in the same segments. Results for population trends disaggregated by education, employment status, and gender are reported in the Appendix.

Table 11 provides more details of population trends over time by age group under Twin Transition.

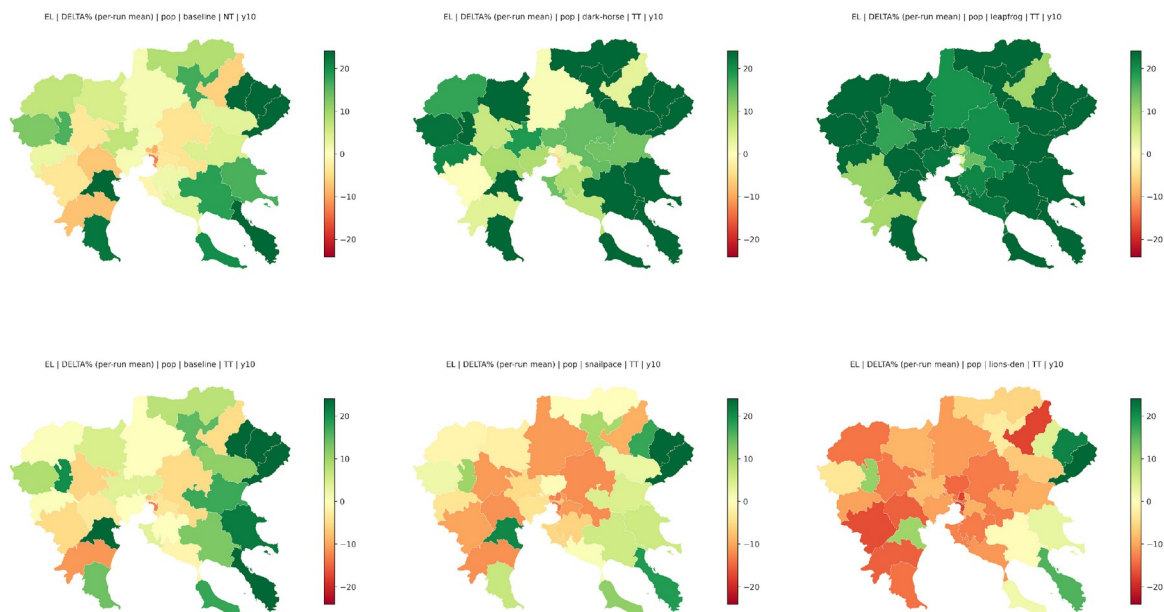
**Table 11. EL (CENTRAL MACEDONIA) POPULATION TRENDS OVER TIME BY AGE GROUP UNDER TT**
**EL TT Age: % change vs t0**

Scenario	Category	0	12	24	60	120
<b>leapfrog</b>	Total	0.000%	0.984%	1.739%	8.047%	19.980%
	18-25	0.000%	1.782%	3.008%	8.683%	20.987%
	26-40	0.000%	-3.099%	-5.122%	-0.538%	12.138%
	41-65	0.000%	-0.079%	-0.451%	4.491%	14.486%
	65+	0.000%	0.803%	1.388%	4.236%	8.252%
<b>dark-horse</b>	Total	0.000%	-0.917%	-1.390%	1.649%	8.292%
	18-25	0.000%	-0.185%	0.242%	0.442%	2.680%
	26-40	0.000%	-7.093%	-12.266%	-11.908%	-2.535%
	41-65	0.000%	-2.546%	-4.515%	-1.921%	3.764%
	65+	0.000%	0.187%	0.292%	0.503%	0.349%
<b>snailpace</b>	Total	0.000%	-3.332%	-5.612%	-7.133%	-7.205%
	18-25	0.000%	-2.737%	-4.363%	-9.595%	-15.241%
	26-40	0.000%	-11.140%	-18.259%	-23.406%	-21.229%
	41-65	0.000%	-5.140%	-9.046%	-10.904%	-10.864%
	65+	0.000%	-1.452%	-2.840%	-6.524%	-13.778%
<b>lions-den</b>	Total	0.000%	-3.608%	-6.408%	-9.838%	-12.524%
	18-25	0.000%	-2.766%	-4.477%	-11.634%	-20.459%
	26-40	0.000%	-11.549%	-19.334%	-25.787%	-25.762%
	41-65	0.000%	-5.266%	-9.615%	-13.189%	-15.672%
	65+	0.000%	-1.980%	-4.179%	-10.167%	-19.904%

Table 11 clarifies that the scenario spread observed in Figure 5 is driven primarily by divergence in younger and prime working-age cohorts. Under Leapfrog, total population increases by 19.980 percent by the end of the horizon, with ages 18 to 25 increasing by 20.987 percent and ages 41 to 65 increasing by 14.486 percent. Ages 26 to 40 decline early, reaching a 5.122 percent decrease at the second reporting point, but recover to a 12.138 percent increase by the end of the horizon, indicating delayed gains in a core working-age segment. Under Dark Horse, the total increases by 8.292 percent by the end of the horizon, but ages 26 to 40 remain below baseline even at the final reporting point at minus 2.535 percent, while ages 41 to 65 rise by 3.764 percent. Under Snail Pace and Lion’s Den, losses are concentrated in ages 26 to 40 and ages 18 to 25. By the end of the horizon, ages 26 to 40 decline by 21.229 percent under Snail Pace and 25.762 percent under Lion’s Den, and ages 18 to 25 decline by 15.241 percent and 20.459 percent, respectively. Appendix figures report the same reporting time points for population trends disaggregated by education, employment status, and gender.

### 3.1.3 EL (CENTRAL MACEDONIA) SUBREGION-LEVEL TOTAL POPULATION DYNAMICS ACROSS SCENARIOS

Figure 6 includes the four designed scenarios under Twin Transition and a Baseline comparison shown under both policy pathways.



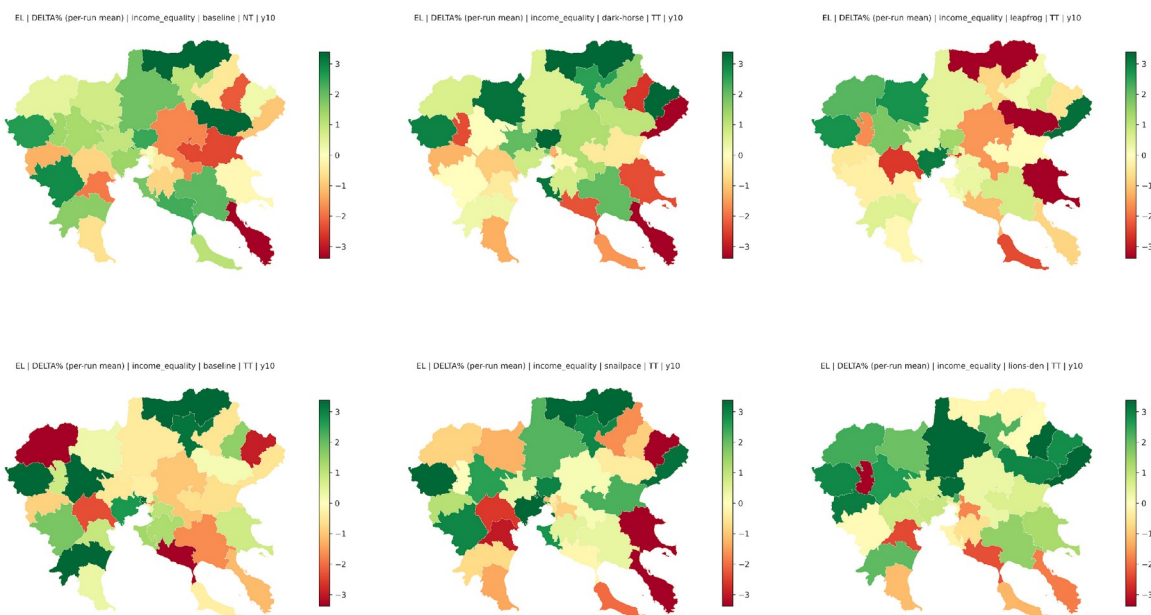
**Figure 6. EL (Central Macedonia) population change (%) after 10 years: cross-scenario comparison maps**

Figure 6 shows that scenario differences in Central Macedonia translate into distinct spatial patterns rather than uniform shifts across the pilot system. Under Leapfrog, positive population change is spatially widespread, with many subregions showing gains and only limited pockets of decline, indicating broad-based improvements in retention and population replenishment across the territory. Under Dark Horse, gains remain common, but the pattern becomes more mixed, with a larger share of subregions close to neutral change and a smaller set of localized declines, suggesting that moderate favourable conditions yield less uniform spatial improvement. Under Snail Pace and especially Lion’s Den, negative change becomes dominant across much of the pilot region, forming more continuous zones of decline rather than isolated local losses. In these adverse contexts, a limited subset of subregions still exhibits positive or less negative outcomes, indicating uneven resilience across the internal geography of Central Macedonia. Overall, the cross-scenario maps emphasize that the scenario

context is the primary driver of both the magnitude and the spatial concentration of population change in this pilot.

### 3.1.4 EL (CENTRAL MACEDONIA) SUBREGION-LEVEL INDICATORS CHANGE ACROSS SCENARIOS

Figure 7 includes the four designed scenarios under Twin Transition and the Baseline comparison maps, using the income equality indicator as an example.



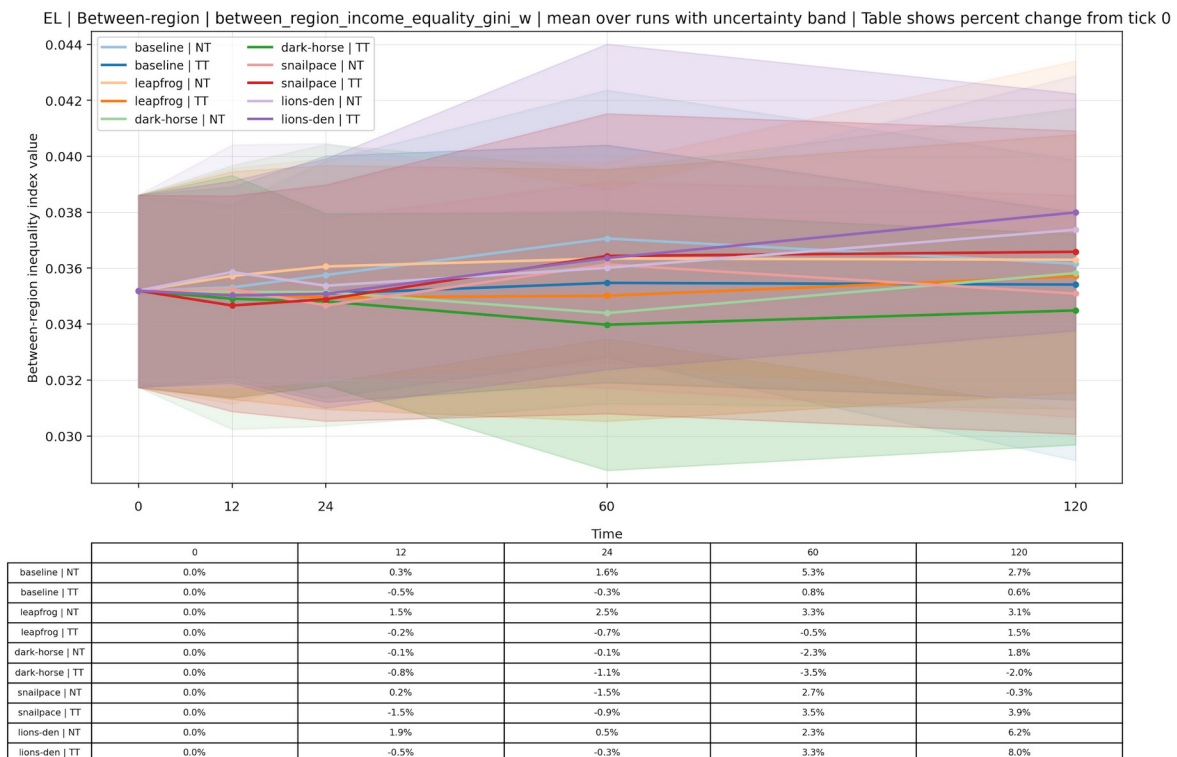
**Figure 7. EL (Central Macedonia) change in income equality indicator after 10 years: cross-scenario comparison maps**

Figure 7 shows that changes in income equality in Central Macedonia are spatially heterogeneous and do not simply mirror the population change surfaces. Across scenarios, the map patterns exhibit clear clustering, with some contiguous subregional areas showing improvement in income equality while other areas show deterioration. Under Leapfrog, the spatial surface includes both improvement clusters and deterioration clusters, suggesting that favourable population dynamics can still coincide with uneven distributional outcomes across subregions, consistent with selective retention or uneven shifts in socioeconomic composition. Under Dark Horse, the pattern remains mixed but the location and extent of improvement and deterioration clusters shift, indicating that moderate macro conditions can redistribute distributional pressure across the pilot system rather than uniformly improving

outcomes. Under Snail Pace and Lion’s Den, the configuration tends to feature broader and more contiguous areas of deterioration in parts of the pilot region, alongside smaller pockets of improvement, which is consistent with scenario contexts that generate stronger demographic stress and uneven adjustment. These results highlight that scenario context in Central Macedonia affects both demographic trajectories and distributional patterns, and that distributional impacts are mediated by spatially differentiated compositional change rather than by population totals alone. Additional cross-scenario maps for equality- and sustainability-related indicators are provided in the Appendix.

### 3.1.5 EL (CENTRAL MACEDONIA) BETWEEN-SUBREGION INEQUALITY ACROSS SCENARIOS AND TIME HORIZONS

Figure 8 illustrates the level of differentiation in income equality among subregions within the pilot area (as measured by the Gini coefficient across subregions), indicating how spatial dispersion for this indicator evolves within EL (Central Macedonia).



**Figure 8. EL (Central Macedonia) between-subregion income equality under twin transition and no transition**

Figure 8 indicates that between-subregion inequality for the income equality indicator changes only modestly in magnitude over time, but the direction of change differs

across scenarios. Under Baseline, the between-subregion index remains close to its initial value, ending with small increases by the final reporting point. Under Leapfrog and Dark Horse, the index fluctuates within a narrow range and does not show sustained divergence, suggesting relatively stable cross-subregion dispersion for this indicator under more favourable contexts. By contrast, Lion's Den shows a clearer tendency toward rising between-subregion inequality by the final reporting point, indicating that adverse scenario conditions in Central Macedonia can amplify spatial differentiation in distributional outcomes even when within-subregion changes remain mixed across the map. Uncertainty bands overlap across configurations, so these results should be interpreted as directional signals rather than sharp separations. The Appendix provides comparable between-subregion trajectories for other indicators and time points to support a consistent assessment of spatial differentiation across multiple dimensions.

---

### 3.1.6 EL (CENTRAL MACEDONIA) SCENARIO EFFECTS ON POPULATION, EQUALITY, AND SPATIAL DIFFERENTIATION

Across the five scenarios, EL (Greece, Central Macedonia) exhibits a clear scenario gradient in both the magnitude and the spatial distribution of population change. Favourable contexts generate sustained gains and a widening demographic advantage over time, while adverse contexts dominate long-run outcomes and produce persistent decline. By the end of the horizon, Leapfrog yields strong positive population change at the pilot level, while Dark Horse produces more moderate gains; Baseline remains close to neutral with a small decline, and Snail Pace and Lion's Den produce pronounced losses. These scenario differences are amplified by cohort-specific dynamics and indicate a shift in age structure that is most consequential for demographic sustainability. Younger and prime working-age cohorts account for a disproportionate share of divergence, implying that adverse contexts accelerate working-age depletion and weaken medium-term labour supply capacity.

Spatially, the cross-scenario population change maps suggest that scenario context reshapes the internal core-periphery pattern within Central Macedonia. Under favourable scenarios, gains are more spatially widespread and extend beyond the main centres, while under adverse scenarios decline becomes dominant and forms more continuous zones of negative change, with only limited pockets of resilience. This indicates that adverse contexts can deepen territorial polarization through uneven retention and uneven demographic replenishment across subregions. Distributional outcomes add another layer of spatial differentiation. Income equality changes are spatially heterogeneous and do not mechanically track population change, which is

consistent with compositional change and differential sorting across subregions. Between-subregion inequality in income equality changes only modestly in magnitude over time, but the direction differs by scenario, with the most adverse scenario showing clearer tendencies toward increased spatial dispersion by the end of the horizon.

## 3.2 SPAIN: CASTILLA-LA MANCHA (NUTS - ES42)

### 3.2.1 ES (CASTILLA-LA MANCHA) PILOT-LEVEL TOTAL POPULATION DYNAMICS ACROSS SCENARIOS

Figure 9 illustrates the change of total population in year 1, year 2, year 5, and year 10.

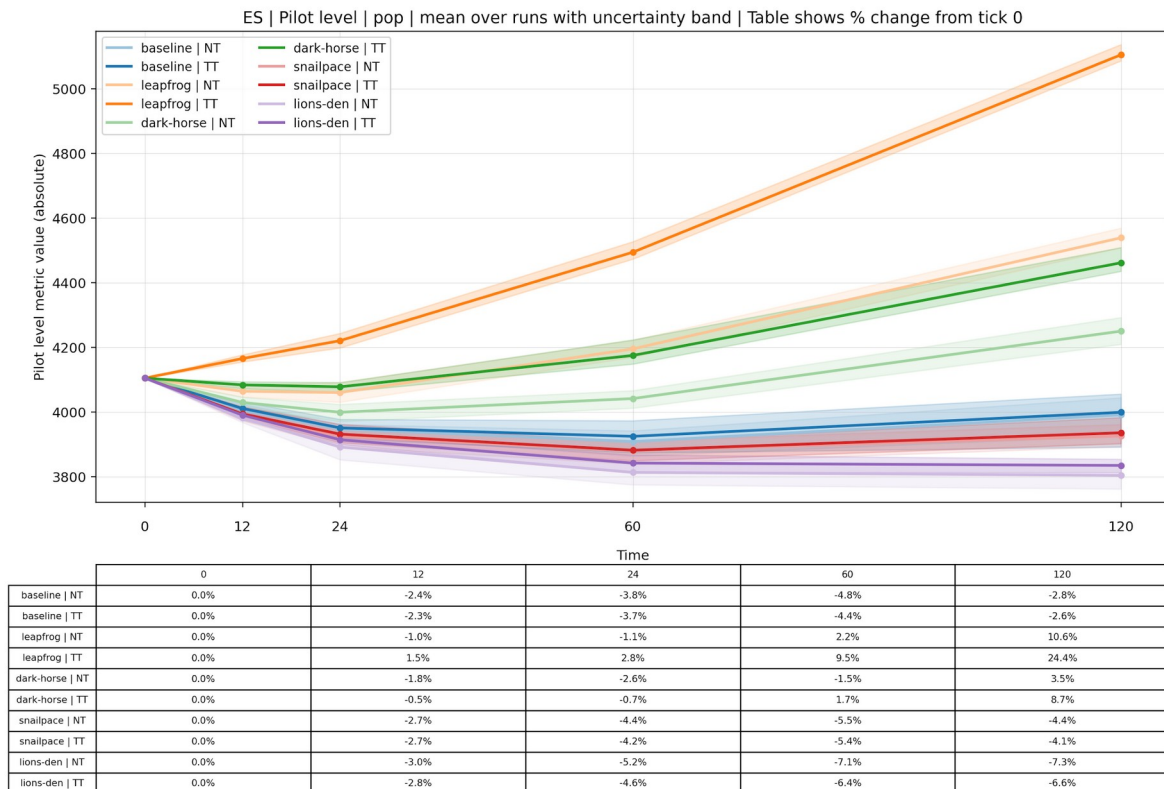


**Figure 9. ES (Castilla-la Mancha) total population trends over time**

Figure 9 shows clear separation across scenarios that expands with the time horizon, indicating that scenario context is the primary driver of long-run population outcomes in ES (Spain, Castilla-la Mancha). Leapfrog produces sustained growth and ends with the largest increase by the final reporting point at 24.4 percent, while Dark Horse ends with moderate growth at 8.7 percent. Baseline remains close to neutral and ends with a modest decline at 2.6 percent. In the adverse scenarios, Snail Pace and Lion’s Den

remain negative throughout and end with declines of 4.1 percent and 6.6 percent, respectively. The widening spread between Leapfrog and Lion's Den from the early horizon to the end of the horizon indicates that cumulative population change mechanisms dominate short-run adjustments, and that scenario-specific macro contexts create clearly differentiated demographic envelopes for interpreting later spatial and distributional outcomes. The subsequent figures and tables follow the same set of reporting time points to support consistent comparison across outputs. In Deliverable D2.3, Castilla-La Mancha (ES42) is grouped under "Economies in Structural Transition", where a relatively diverse economic base and moderate attractiveness coexist with institutional weaknesses and uneven performance across regions. The population trajectories in Figure 9 align with this diagnosis, as scenario context determines whether positive change pathways consolidate over time or whether structural constraints dominate long-run outcomes. Consequently, adverse scenarios remain associated with persistent decline, while favourable scenarios generate a cumulative demographic advantage by the final reporting point.

---

### 3.2.2 ES (CASTILLA-LA MANCHA) PILOT-LEVEL POPULATION TRENDS OVER TIME BY CERTAIN GROUPS

Figure 10 shows the population trends over time by age group as an example.

ES Age: Total + 18-25/26-40/41-65/65+

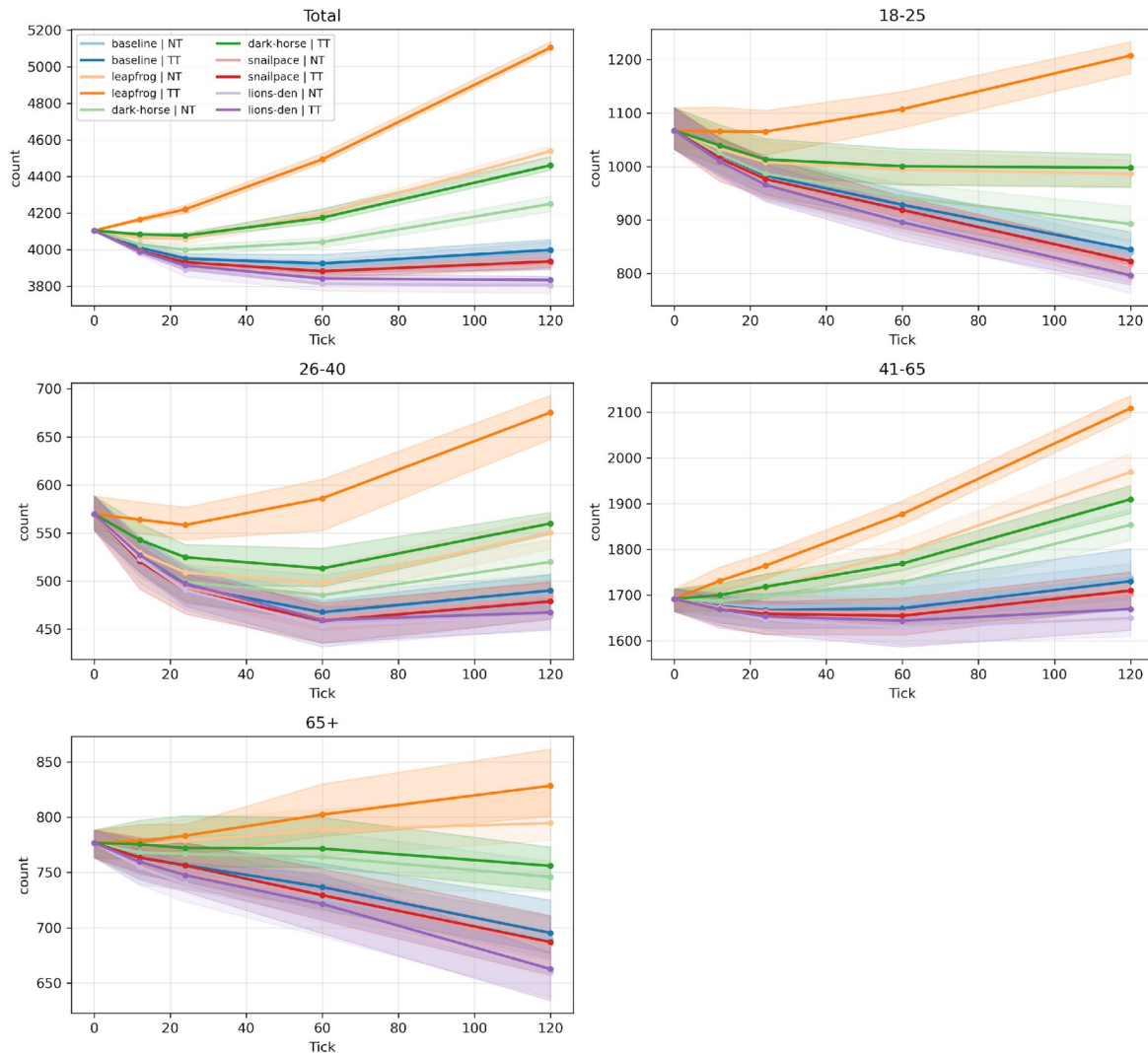


**Figure 10. ES (Castilla-la Mancha) population trends over time by age group**

In particular, Figure 10 indicates that scenario differences in Castilla-la Mancha are expressed not only in total population trajectories but also in age composition, with the clearest divergence emerging in younger and prime working-age cohorts. Under Leapfrog, total population growth is broad-based by the end of the horizon, but cohort dynamics remain differentiated. Ages 41 to 65 expand strongly and drive a large share of the overall increase, while ages 26 to 40 show early decline followed by strong recovery by the final reporting point. Ages 18 to 25 also perform substantially better under Leapfrog than under other scenarios, reversing the pervasive decline seen elsewhere. Under Dark Horse, the total increases by the final reporting point, but the age profile is mixed. Ages 41 to 65 increase strongly, while ages 18 to 25 and ages 26 to 40

remain below baseline, indicating that moderate favourable contexts stabilize overall totals primarily through older working-age growth rather than broad youth retention. Under Snail Pace and Lion’s Den, declines are widespread across cohorts and are particularly strong for ages 18 to 25 and ages 26 to 40, implying disproportionate pressure on early-career and prime working-age segments that matter for demographic sustainability and labour-force renewal. Results for population trends disaggregated by education, employment status, and gender are reported in the Appendix.

Table 12 provides more details of population trends over time by age group under Twin Transition.

**Table 12. ES (CASTILLA-LA MANCHA) POPULATION TRENDS OVER TIME BY AGE GROUP UNDER TT**

**ES TT Age: % change vs t0**

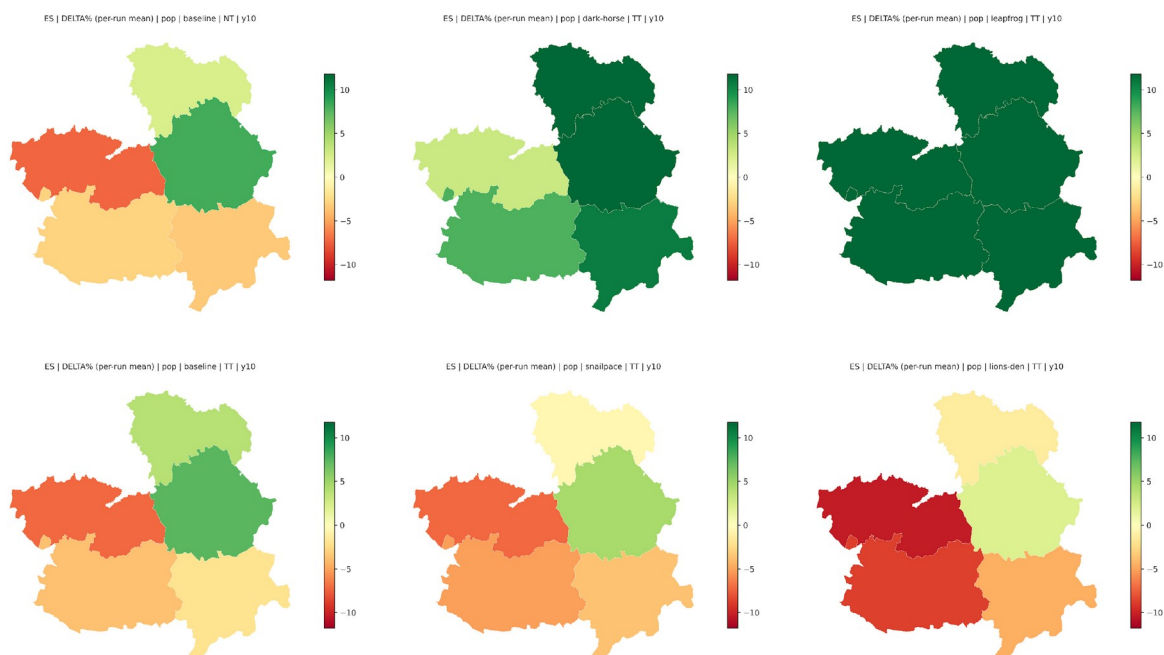
Scenario	Category	0	12	24	60	120
<b>leapfrog</b>	Total	0.000%	1.474%	2.823%	9.488%	24.363%
	18-25	0.000%	-0.150%	-0.187%	3.757%	13.145%
	26-40	0.000%	-1.018%	-2.001%	2.878%	18.533%
	41-65	0.000%	2.371%	4.316%	10.998%	24.675%
	65+	0.000%	0.245%	0.850%	3.309%	6.669%
<b>dark-horse</b>	Total	0.000%	-0.512%	-0.658%	1.710%	8.689%
	18-25	0.000%	-2.586%	-5.050%	-6.249%	-6.502%
	26-40	0.000%	-4.739%	-7.898%	-9.933%	-1.720%
	41-65	0.000%	0.520%	1.591%	4.594%	12.902%
	65+	0.000%	-0.154%	-0.592%	-0.644%	-2.665%
<b>snailpace</b>	Total	0.000%	-2.704%	-4.219%	-5.430%	-4.117%
	18-25	0.000%	-4.844%	-8.498%	-13.904%	-22.899%
	26-40	0.000%	-8.617%	-13.917%	-19.498%	-15.953%
	41-65	0.000%	-1.348%	-1.922%	-2.170%	1.094%
	65+	0.000%	-1.725%	-2.626%	-6.090%	-11.536%
<b>lions-den</b>	Total	0.000%	-2.789%	-4.648%	-6.402%	-6.577%
	18-25	0.000%	-5.397%	-9.519%	-16.050%	-25.372%
	26-40	0.000%	-7.494%	-12.654%	-19.358%	-17.971%
	41-65	0.000%	-1.366%	-2.241%	-2.809%	-1.289%
	65+	0.000%	-2.189%	-3.747%	-7.107%	-14.690%

Table 12 clarifies that cross-scenario divergence in Castilla-la Mancha is driven largely by how scenarios reshape younger and prime working-age trajectories relative to older working-age growth. Under Leapfrog, total population increases by 24.363 percent by the final reporting point, with particularly large gains in ages 41 to 65 at 24.675 percent and strong recovery in ages 26 to 40 at 18.533 percent. Ages 18 to 25 rise by 13.145

percent by the end of the horizon, indicating improved youth retention or replenishment under the most favourable scenario. Under Dark Horse, the total increases by 8.689 percent, but this growth is concentrated in ages 41 to 65 at 12.902 percent, while ages 18 to 25 decline by 6.502 percent and ages 26 to 40 remain slightly negative at minus 1.720 percent. Under Snail Pace and Lion’s Den, the total remains negative and losses are concentrated among ages 18 to 25 and ages 26 to 40. By the final reporting point, ages 18 to 25 decline by 22.899 percent under Snail Pace and 25.372 percent under Lion’s Den, while ages 26 to 40 decline by 15.953 percent and 17.971 percent, respectively. Appendix figures report the same reporting time points for population trends disaggregated by education, employment status, and gender.

### 3.2.3 ES (CASTILLA-LA MANCHA) SUBREGION-LEVEL TOTAL POPULATION DYNAMICS ACROSS SCENARIOS

Figure 11 includes the four designed scenarios under Twin Transition and a Baseline comparison shown under both policy pathways.



**Figure 11. ES (Castilla-la Mancha) population change (%) after 10 years: cross-scenario comparison maps**

Figure 11 shows that scenario differences in Castilla-la Mancha translate into distinct spatial patterns across a small number of large subregions, rather than a uniform shift across the pilot system. Under Leapfrog, positive population change is spatially

widespread across all subregions, indicating a pilot-wide improvement in retention and replenishment conditions. Under Dark Horse, the spatial pattern becomes more uneven, with some subregions showing clear gains while others remain close to neutral or slightly negative, suggesting that moderate favourable contexts do not lift all parts of the pilot region equally. Under Snail Pace and especially Lion’s Den, decline dominates across the pilot system, and negative change intensifies in the most adverse scenario. The Baseline comparison remains close to neutral overall, but shows subregional variation that indicates localized resilience or vulnerability even in the reference context. Overall, the maps highlight that scenario context drives both the magnitude and the internal spatial differentiation of population change in Castilla-la Mancha.

### 3.2.4 ES (CASTILLA-LA MANCHA) SUBREGION-LEVEL INDICATORS CHANGE ACROSS SCENARIOS

Figure 12 includes the four designed scenarios under Twin Transition and the Baseline comparison maps, using the income equality indicator as an example.



**Figure 12. ES (Castilla-la Mancha) change in income equality indicator after 10 years: cross-scenario comparison maps**

Figure 12 shows that income equality changes in Castilla-la Mancha are spatially heterogeneous and do not mechanically follow the spatial pattern of population change. Across scenarios, the map surfaces suggest a structured contrast in which some

subregions experience improvements in income equality while others experience deterioration, and the configuration shifts across scenario contexts. Under Baseline, improvements cluster in some parts of the pilot region while declines appear in others, indicating that distributional outcomes vary across subregions even when overall population change remains close to neutral. Under Dark Horse, the pattern becomes more polarized, with one subregion showing a clear improvement while at least one other subregion exhibits deterioration, suggesting uneven distributional adjustment across space. Under Leapfrog, the spatial surface remains mixed, with improvements concentrated in some subregions and weaker outcomes elsewhere, indicating that favourable demographic trajectories can still coincide with uneven distributional change across the pilot system. Under Snail Pace and Lion's Den, the maps continue to show mixed directions by subregion, which is consistent with scenario contexts that reshape socioeconomic composition unevenly across space rather than shifting all subregions in the same direction. Additional cross-scenario maps for other equality and sustainability indicators are provided in the Appendix.

---

### 3.2.5 ES (CASTILLA-LA MANCHA) BETWEEN-SUBREGION INEQUALITY ACROSS SCENARIOS AND TIME HORIZONS

Figure 13 illustrates the between-subregion inequality in income equality within ES (Castilla-la Mancha), showing how spatial dispersion evolves over time under different scenarios.

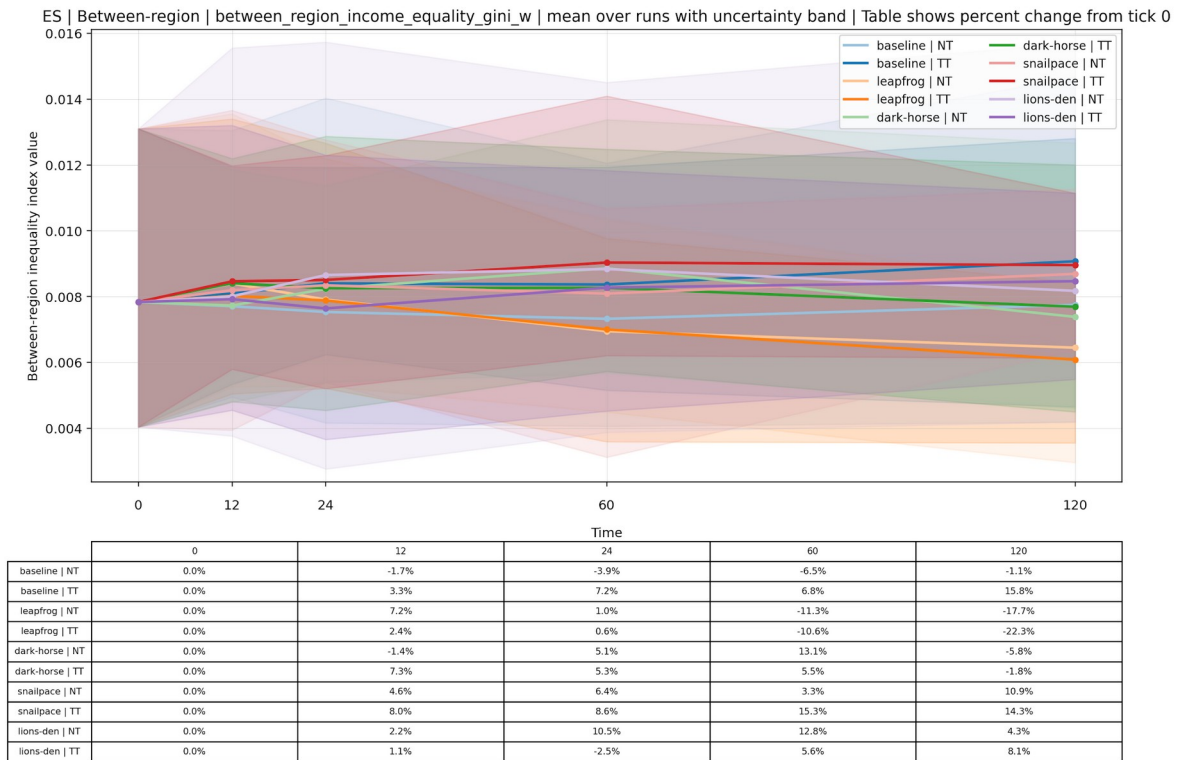


**Figure 13. ES (Castilla-la Mancha) between-subregion income equality under Twin Transition and No Transition**

In particular, Figure 13 indicates that between-subregion dispersion in income equality changes modestly at an absolute level but shows scenario-specific directionality by the end of the horizon. Under Baseline and Dark Horse, the percent-change table indicates increasing between-subregion dispersion by the final reporting point, consistent with a gradual widening of spatial differentiation in distributional outcomes under these contexts. Under Snail Pace, dispersion also increases by the final reporting point, suggesting that adverse demographic contexts can coincide with stronger spatial differentiation rather than uniform decline. By contrast, Leapfrog shows a downward trend in the between-subregion index by the end of the horizon, indicating reduced spatial dispersion in income equality under the most favourable scenario. Uncertainty bands overlap across configurations, so differences should be interpreted as directional signals rather than sharp separations. The Appendix provides comparable between-subregion trajectories for other indicators and time points to support a consistent assessment of spatial differentiation across multiple dimensions.

### 3.3 FINLAND: NORTH & EAST FINLAND (NUTS - FI1D)

#### 3.3.1 FI (NORTH AND EAST FINLAND) PILOT-LEVEL TOTAL POPULATION DYNAMICS ACROSS SCENARIOS

Figure 14 illustrates the change of total population in year 1, year 2, year 5, and year 10.

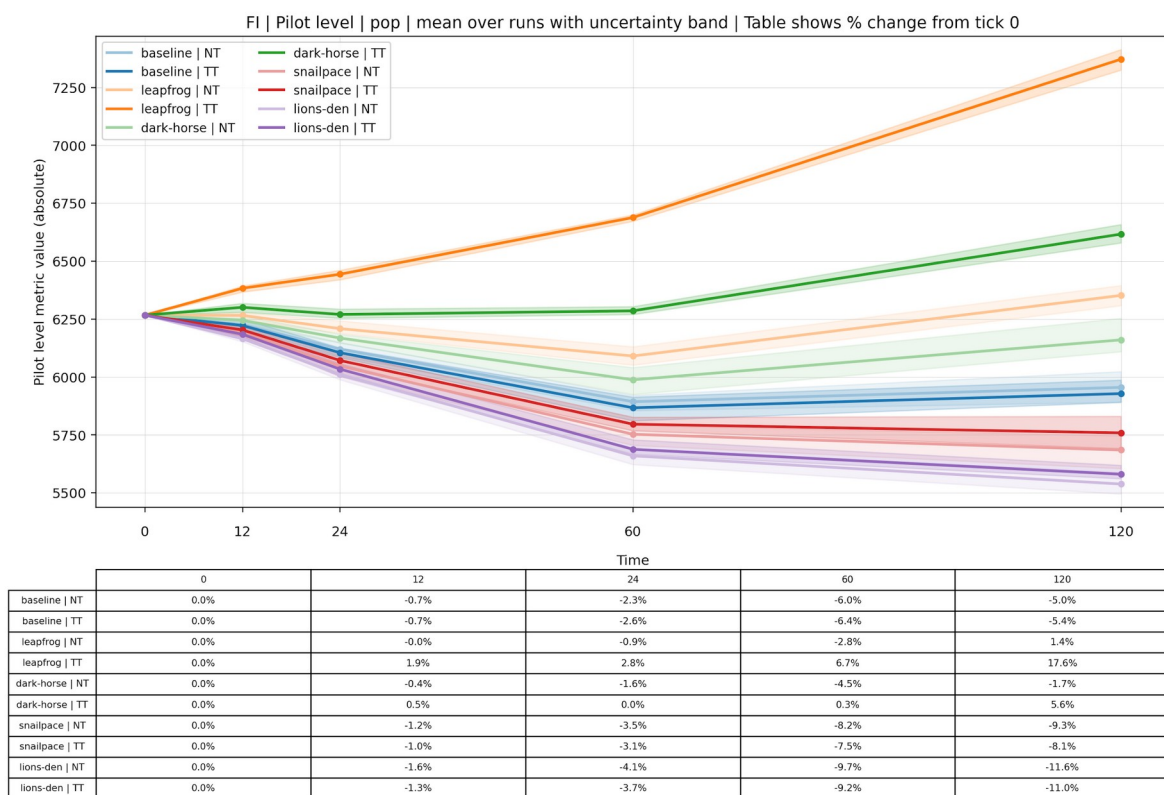


**Figure 14. FI (North and East Finland) total population trends over time**

In particular, figure 14 shows clear separation across scenarios that expands with the time horizon, indicating that scenario context is the primary driver of long-run population outcomes in FI (Finland, North and East Finland). Leapfrog produces sustained growth and ends with the largest increase by the final reporting point at 17.6 percent. Dark Horse remains mildly positive by the end of the horizon at 5.6 percent, while Baseline is negative and ends around minus 5.4 percent. The adverse scenarios show pronounced decline, with Snail Pace ending at minus 8.1 percent and Lion's Den ending at minus 11.0 percent. Overall, the scenario ladder yields a wide demographic spread by the end of the horizon, and the divergence becomes more visible after the mid-horizon reporting point, suggesting that cumulative change dominates early

adjustments. The subsequent figures and tables follow the same set of reporting time points to support consistent comparison across outputs. In Deliverable D2.3, North and East Finland (FI1D) is grouped under “Balanced Innovators”, where well-rounded performance and robust governance coexist with comparatively weaker innovation ecosystems and moderate visibility relative to metropolitan leaders. The population trajectories in Figure 14 align with this profile, as scenario context determines whether the region’s balanced strengths translate into sustained gains over time or whether longer-run structural headwinds dominate demographic outcomes. Consequently, adverse scenarios remain associated with persistent decline, whereas favourable scenarios generate a cumulative demographic advantage by the final reporting point.

---

### 3.3.2 FI (NORTH AND EAST FINLAND) PILOT-LEVEL POPULATION TRENDS OVER TIME BY CERTAIN GROUPS

Figure 15 shows the population trends over time by age group as an example.

FI Age: Total + 18-25/26-40/41-65/65+

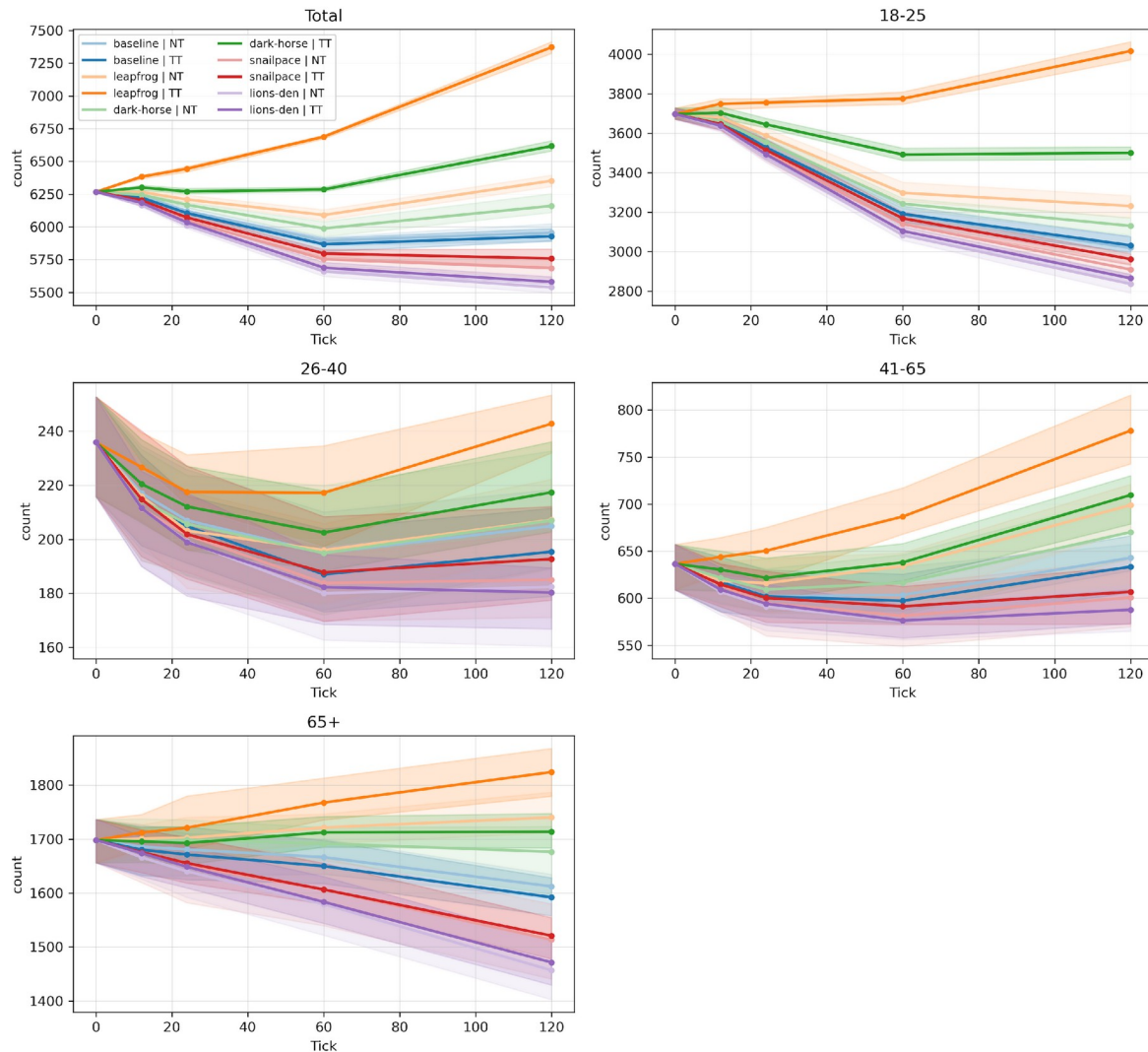


**Figure 15. FI (North and East Finland) population trends over time by age group**

Figure 15 indicates that scenario differences in North and East Finland are expressed through cohort-specific dynamics, with the strongest divergence emerging in the prime working-age group and, in favourable scenarios, in late working-age expansion. Under Leapfrog, total population growth is accompanied by strong gains in ages 41 to 65 and moderate gains in ages 18 to 25, while ages 26 to 40 decline early and recover toward the end of the horizon. Under Dark Horse, total population ends positive, but the age profile is mixed. Ages 41 to 65 increase substantially by the final reporting point, while ages 18 to 25 and ages 26 to 40 remain below baseline, indicating that moderate favourable contexts stabilize totals mainly through older working-age expansion rather than broad youth and prime-age recovery. Under Snail Pace and Lion’s Den, declines are

widespread and become most pronounced for ages 18 to 25 and ages 26 to 40, implying disproportionate pressure on early-career and prime working-age segments that matter for labour supply renewal. Results for population trends disaggregated by education, employment status, and gender are reported in the Appendix.

Table 13 provides more details of population trends over time by age group under Twin Transition.

**Table 13. FI (NORTH AND EAST FINLAND) POPULATION TRENDS OVER TIME BY AGE GROUP UNDER TT**

**FI TT Age: % change vs t0**

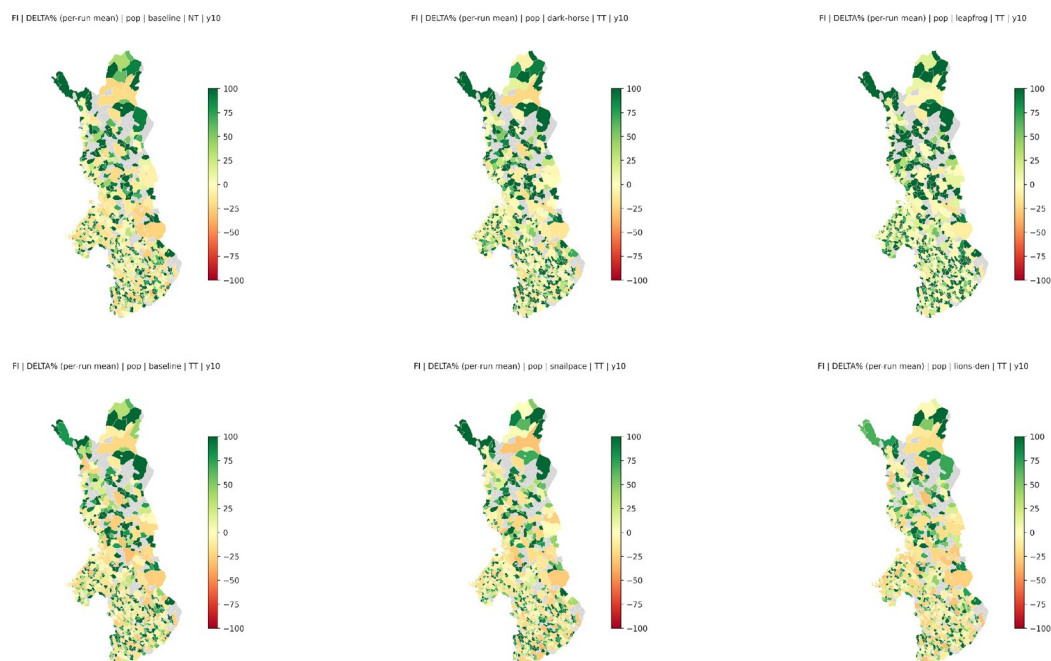
Scenario	Category	0	12	24	60	120
<b>leapfrog</b>	Total	0.000%	1.851%	2.820%	6.726%	17.629%
	18-25	0.000%	1.407%	1.580%	2.107%	8.646%
	26-40	0.000%	-3.900%	-7.800%	-7.927%	2.925%
	41-65	0.000%	1.147%	2.183%	7.886%	22.227%
	65+	0.000%	0.819%	1.349%	4.093%	7.426%
<b>dark-horse</b>	Total	0.000%	0.539%	0.048%	0.298%	5.583%
	18-25	0.000%	0.165%	-1.418%	-5.551%	-5.313%
	26-40	0.000%	-6.528%	-10.089%	-14.159%	-7.842%
	41-65	0.000%	-0.974%	-2.325%	0.236%	11.483%
	65+	0.000%	-0.153%	-0.324%	0.842%	0.901%
<b>snailpace</b>	Total	0.000%	-1.018%	-3.120%	-7.506%	-8.108%
	18-25	0.000%	-1.363%	-4.935%	-14.295%	-19.876%
	26-40	0.000%	-8.944%	-14.413%	-20.390%	-18.313%
	41-65	0.000%	-3.440%	-5.686%	-7.100%	-4.665%
	65+	0.000%	-1.313%	-2.515%	-5.394%	-10.435%
<b>lions-den</b>	Total	0.000%	-1.315%	-3.718%	-9.237%	-10.954%
	18-25	0.000%	-1.580%	-5.516%	-16.029%	-22.500%
	26-40	0.000%	-10.343%	-15.685%	-22.721%	-23.569%
	41-65	0.000%	-4.304%	-6.645%	-9.456%	-7.666%
	65+	0.000%	-1.419%	-2.909%	-6.749%	-13.344%

Table 13 clarifies that cross-scenario divergence is driven mainly by differences in prime working-age losses and the extent to which favourable contexts generate late working-age growth. Under Leapfrog, total population increases by 17.629 percent by the final reporting point, driven strongly by ages 41 to 65 at 22.227 percent and supported by gains in ages 18 to 25 at 8.646 percent. Ages 26 to 40 decline early, reaching minus 7.800 percent at the second reporting point, but recover to a 2.925 percent increase by the end of the horizon. Under Dark Horse, the total increases by 5.583 percent, but ages 18 to 25 decline by 5.313 percent and ages 26 to 40 decline by 7.842 percent at the final reporting point, while ages 41 to 65 increase by 11.483 percent.

Under Snail Pace and Lion’s Den, total population remains negative and losses concentrate in ages 18 to 25 and ages 26 to 40. By the end of the horizon, ages 18 to 25 decline by 19.876 percent under Snail Pace and 22.500 percent under Lion’s Den, while ages 26 to 40 decline by 18.313 percent and 23.569 percent, respectively. Appendix figures report the same reporting time points for population trends disaggregated by education, employment status, and gender.

### 3.3.3 FI (NORTH AND EAST FINLAND) SUBREGION-LEVEL TOTAL POPULATION DYNAMICS ACROSS SCENARIOS

Figure 16 includes the four designed scenarios under Twin Transition and a Baseline comparison shown under both policy pathways.



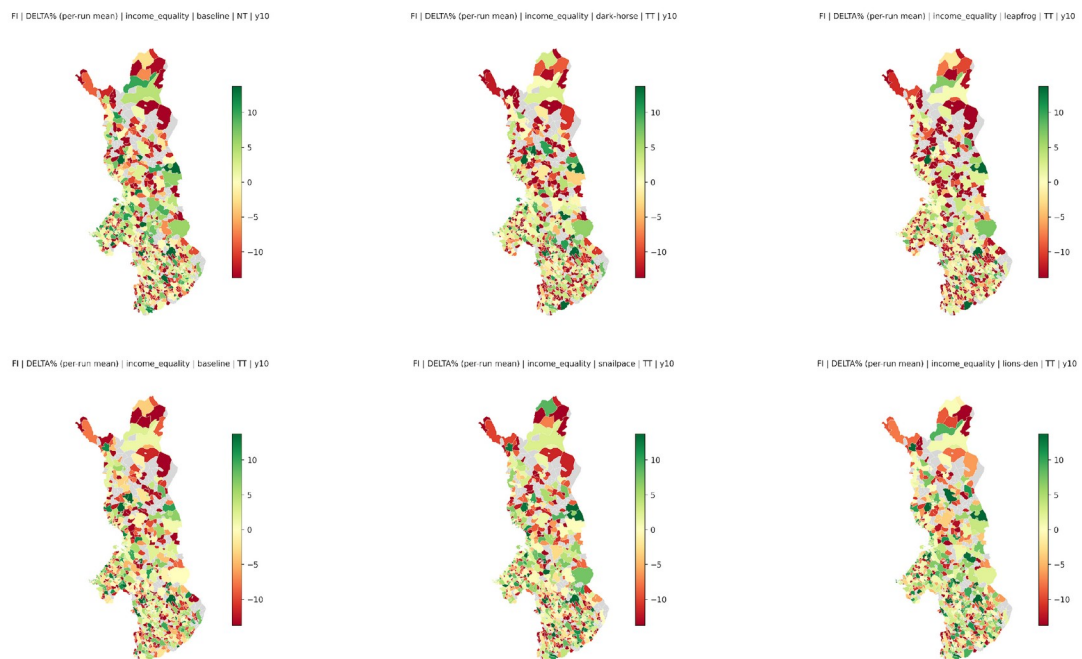
**Figure 16. FI (North and East Finland) population change (%) after 10 years: cross-scenario comparison maps**

Figure 16 shows that scenario differences translate into a highly heterogeneous spatial surface across North and East Finland, with fine-grained local variation across subregions. Under Leapfrog, positive population change is broadly visible across the map, with many local units showing gains and fewer areas of decline, indicating widespread improvement in retention or replenishment conditions. Under Dark Horse, the spatial surface remains mixed, with a wider distribution of near-neutral and modestly positive outcomes. Under Snail Pace and Lion’s Den, negative change becomes

more common and more spatially continuous, although the map still contains pockets of relative resilience where declines are weaker or outcomes remain near neutral. The Baseline comparison shows intermediate patterns, reinforcing that scenario context shapes not only the overall direction of change but also the internal geography of where gains and losses concentrate.

### 3.3.4 FI (NORTH AND EAST FINLAND) SUBREGION-LEVEL INDICATORS CHANGE ACROSS SCENARIOS

Figure 17 includes the four designed scenarios under Twin Transition and the Baseline comparison maps, using the income equality indicator as an example.



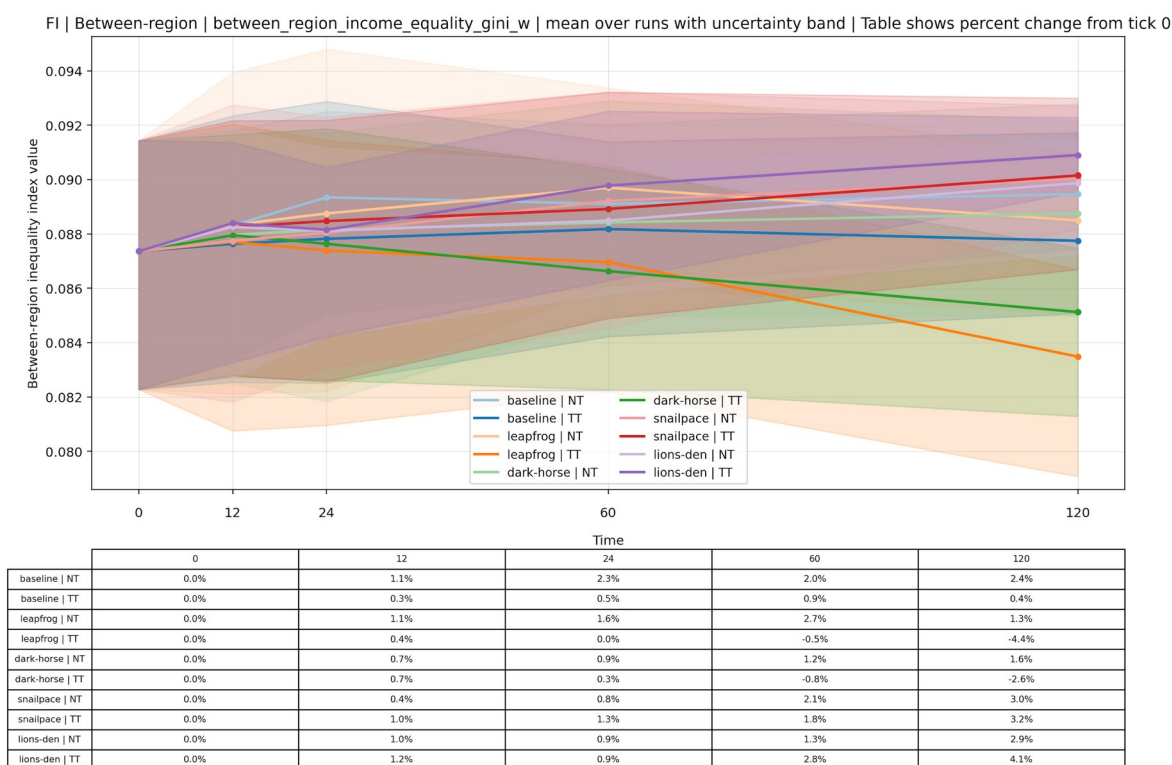
**Figure 17. FI (North and East Finland) change in income equality indicator after 10 years: cross-scenario comparison maps**

Figure 17 shows that income equality changes in North and East Finland are spatially heterogeneous and do not mechanically track the population change surface. Across all scenarios, the maps exhibit a patchwork configuration with frequent local switches between improvement and deterioration, indicating that distributional outcomes respond to compositional change in a spatially uneven way. Under Baseline, the surface includes many local units with deterioration alongside pockets of improvement, implying that near-neutral demographic change can still coincide with uneven distributional adjustment. Under Dark Horse and Leapfrog, the maps remain mixed

and do not converge toward a uniform direction, suggesting that favourable demographic trajectories can coexist with localized deterioration in distributional outcomes. Under Snail Pace and Lion’s Den, the surface continues to show both directions but includes larger clusters of deterioration in some parts of the pilot system, consistent with stronger demographic stress and uneven adjustment across subregions. Additional cross-scenario maps for other equality and sustainability indicators are provided in the Appendix.

### 3.3.5 FI (NORTH AND EAST FINLAND) BETWEEN-SUBREGION INEQUALITY ACROSS SCENARIOS AND TIME HORIZONS

Figure 18 illustrates the between-subregion inequality in income equality within FI (North and East Finland), showing how spatial dispersion evolves over time under different scenarios.



**Figure 18. FI (North and East Finland) between-subregion income equality under Twin Transition and No Transition**

Figure 18 indicates that between-subregion dispersion in income equality changes modestly in absolute level over time, but scenario-specific directionality is visible by the final reporting point. Baseline shows small increases by the end of the horizon,

remaining close to its initial level. Snail Pace and Lion's Den show clearer increases by the final reporting point, consistent with gradually widening spatial differentiation in distributional outcomes under adverse contexts. In contrast, Leapfrog under Twin Transition shows a decline by the final reporting point at minus 4.4 percent, indicating reduced dispersion in income equality under the most favourable scenario context, while Dark Horse under Twin Transition also declines modestly by the end of the horizon at minus 2.6 percent. Uncertainty bands overlap across configurations, so differences should be interpreted as directional signals rather than sharp separations. The Appendix provides comparable between-subregion trajectories for other indicators and time points to support a consistent assessment of spatial differentiation across multiple dimensions.

---

### 3.3.6 FI (NORTH AND EAST FINLAND) SCENARIO EFFECTS ON POPULATION, EQUALITY, AND SPATIAL DIFFERENTIATION

Across the five scenarios, FI (Finland, North and East Finland) exhibits a clear scenario gradient in both the magnitude and the spatial distribution of population change. Leapfrog produces strong positive growth at the pilot level and supports cohort recovery, including gains for ages 18 to 25 and eventual recovery for ages 26 to 40, while Dark Horse yields moderate positive totals that are driven primarily by growth in ages 41 to 65 and do not reverse declines among ages 18 to 25 and ages 26 to 40. Baseline remains negative, and Snail Pace and Lion's Den produce increasingly adverse demographic trajectories, with the strongest losses concentrated in early-career and prime working-age cohorts, implying pressure on labour-force renewal and medium-term demographic sustainability.

Spatially, scenario context reshapes the internal geography of outcomes across the highly disaggregated subregions in North and East Finland. Favourable scenarios generate more widespread positive change across local units, while adverse scenarios increase the prevalence and spatial continuity of decline, with remaining pockets of relative resilience. Distributional outcomes add an additional layer of spatial differentiation. Income equality changes remain mixed across space in all scenarios and do not mechanically follow population change patterns, which is consistent with uneven compositional change at fine spatial scales. Between-subregion dispersion in income equality changes modestly in level but differs in direction across scenarios, with reduced dispersion under the most favourable scenario context and increased dispersion under adverse contexts. Additional cross-scenario maps and inequality trajectories for the full set of equality and sustainability indicators are provided in the Appendix.

## 3.4 ITALY: LOMBARDY (NUTS – ITC4)

### 3.4.1 IT (LOMBARDY) PILOT-LEVEL TOTAL POPULATION DYNAMICS ACROSS SCENARIOS

Figure 19 summarizes pilot-level total population trajectories for Lombardy across the reporting time points.

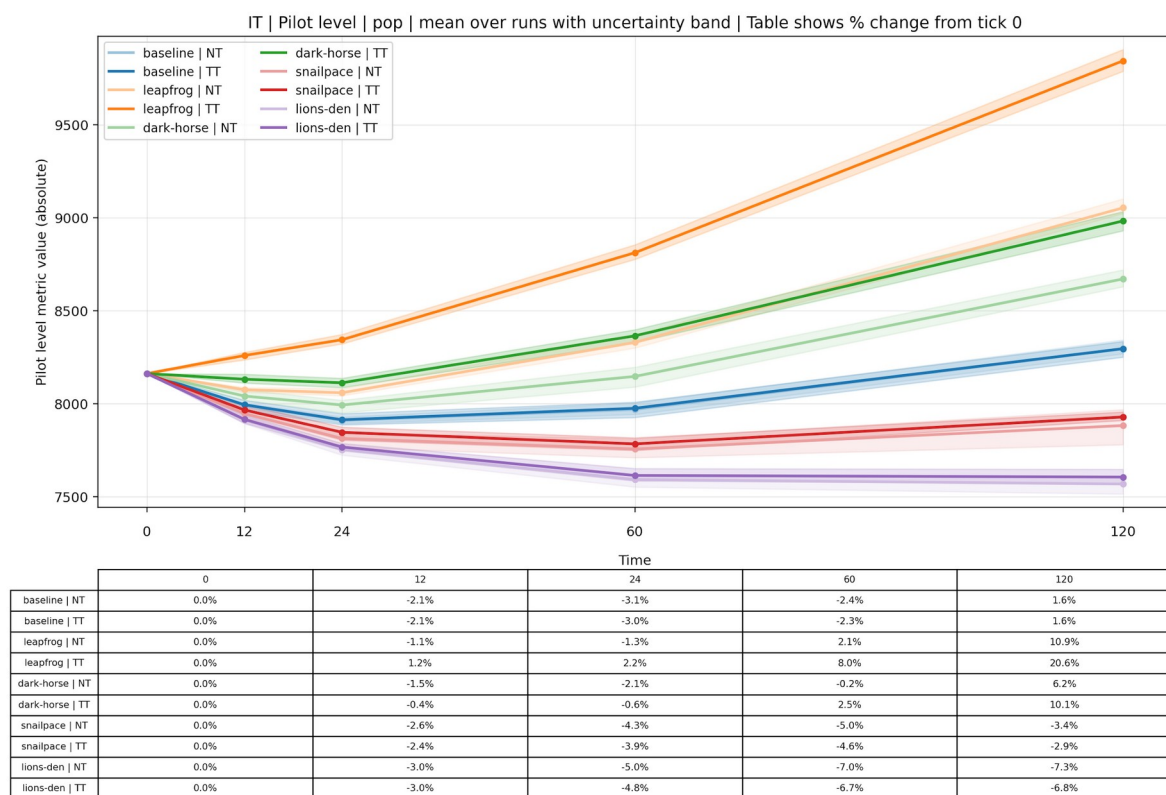


**Figure 19. IT (Lombardy) total population trends over time**

Figure 19 shows that Lombardy follows a steep scenario ladder by the end of the horizon. Leapfrog delivers the strongest growth and ends at 20.6 percent above the baseline time point, while Dark Horse also finishes clearly positive at 10.1 percent. Baseline turns slightly positive by the final reporting point at 1.6 percent, indicating near-neutral outcomes in the reference context. In contrast, Snail Pace and Lion’s Den remain negative and end at minus 2.9 percent and minus 6.8 percent, respectively. Compared with other pilots, Lombardy exhibits a notable split between moderately favourable and strongly favourable scenarios, where Leapfrog pulls away decisively after the mid-horizon reporting point, suggesting that cumulative inflow and retention advantages compound strongly in the most favourable context. The subsequent figures

and tables follow the same set of reporting time points to support consistent comparison across outputs. In Deliverable D2.3, Lombardy (ITC4) is grouped under “Economies in Structural Transition”, where a diverse economic base and moderate attractiveness coexist with institutional weaknesses and uneven performance across regions. The population trajectories in Figure 19 align with this diagnosis, as scenario context determines whether demographic gains consolidate into sustained growth or whether structural constraints dominate long-run outcomes. Consequently, adverse scenarios remain associated with persistent decline, whereas favourable scenarios generate a cumulative demographic advantage by the final reporting point.

---

### 3.4.2 IT (LOMBARDY) PILOT-LEVEL POPULATION TRENDS OVER TIME BY CERTAIN GROUPS

Figure 20 shows population trends over time by age group as an example.

IT Age: Total + 18-25/26-40/41-65/65+

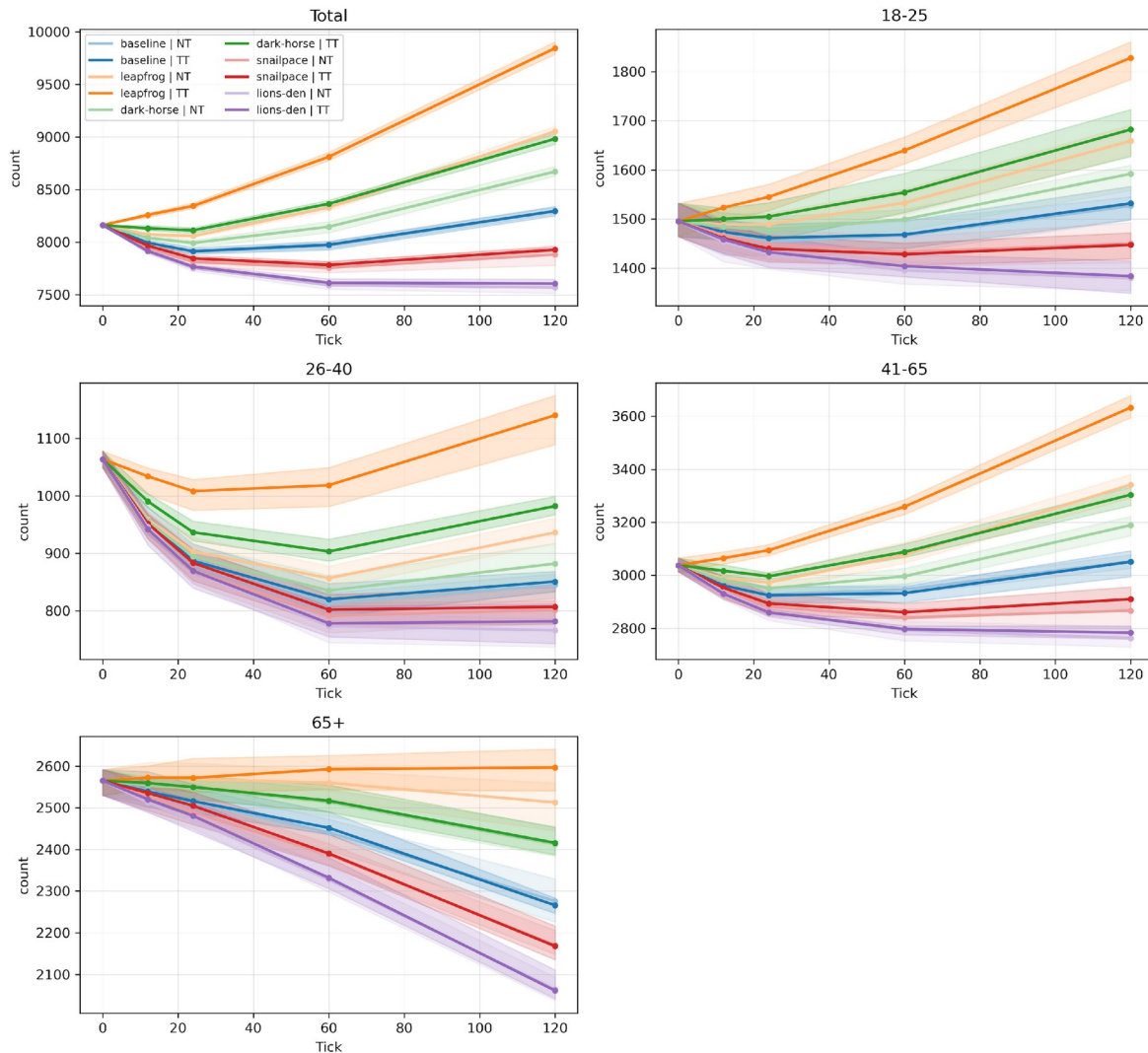


**Figure 20. IT (Lombardy) population trends over time by age group**

Figure 20 indicates that scenario differences in Lombardy are expressed through both level changes and compositional shifts, with the most pronounced divergence emerging in ages 18 to 25 and ages 26 to 40. Under Leapfrog, growth becomes broad-based by the end of the horizon. Ages 18 to 25 increase strongly, ages 41 to 65 expand steadily, and ages 26 to 40 show a sharp early contraction followed by recovery later in the horizon. Under Dark Horse, total population ends positive, but the cohort pattern is uneven. The increase is driven primarily by ages 18 to 25 and ages 41 to 65, while ages 26 to 40 remain below baseline. Under Snail Pace and Lion’s Den, losses persist across cohorts, and the sharpest declines concentrate in ages 26 to 40, indicating strong pressure on

prime working-age retention. Results for population trends disaggregated by education, employment status, and gender are reported in the Appendix.

Table 14 provides more details of population trends over time by age group under Twin Transition.

**Table 14. IT (LOMBARDY) POPULATION TRENDS OVER TIME BY AGE GROUP UNDER TT**

**IT TT Age: % change vs t0**

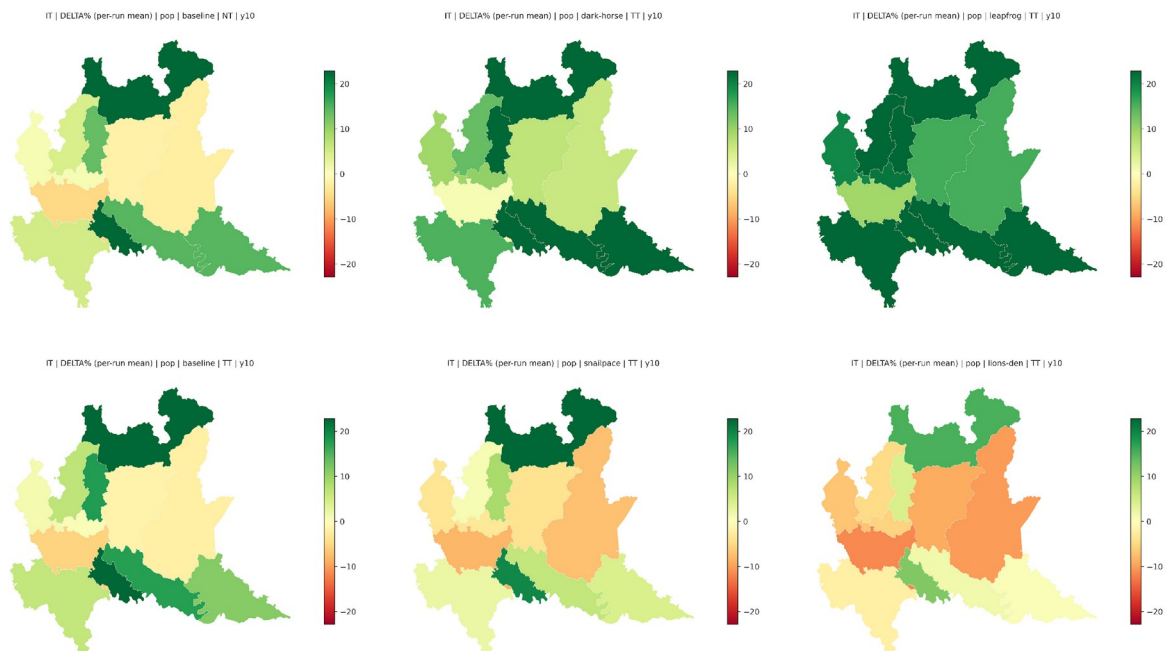
Scenario	Category	0	12	24	60	120
<b>leapfrog</b>	Total	0.000%	1.192%	2.232%	7.969%	20.615%
	18-25	0.000%	1.859%	3.317%	9.644%	22.236%
	26-40	0.000%	-2.820%	-5.235%	-4.267%	7.171%
	41-65	0.000%	0.892%	1.870%	7.279%	19.584%
	65+	0.000%	0.292%	0.261%	1.072%	1.228%
<b>dark-horse</b>	Total	0.000%	-0.372%	-0.606%	2.488%	10.059%
	18-25	0.000%	0.314%	0.642%	3.926%	12.486%
	26-40	0.000%	-6.908%	-11.964%	-15.103%	-7.679%
	41-65	0.000%	-0.681%	-1.356%	1.653%	8.763%
	65+	0.000%	-0.226%	-0.600%	-1.875%	-5.817%
<b>snailpace</b>	Total	0.000%	-2.399%	-3.873%	-4.635%	-2.861%
	18-25	0.000%	-2.327%	-3.745%	-4.494%	-3.210%
	26-40	0.000%	-10.517%	-16.974%	-24.624%	-24.164%
	41-65	0.000%	-2.785%	-4.737%	-5.827%	-4.201%
	65+	0.000%	-1.146%	-2.351%	-6.811%	-15.474%
<b>lions-den</b>	Total	0.000%	-3.019%	-4.841%	-6.715%	-6.821%
	18-25	0.000%	-2.474%	-4.220%	-6.112%	-7.470%
	26-40	0.000%	-11.447%	-18.280%	-26.861%	-26.532%
	41-65	0.000%	-3.542%	-5.853%	-7.920%	-8.365%
	65+	0.000%	-1.750%	-3.287%	-9.088%	-19.634%

Table 14 shows that scenario divergence in Lombardy is driven mainly by how scenarios reshape working-age replenishment and youth retention. Under Leapfrog, total population increases by 20.615 percent by the final reporting point, with ages 18 to 25 increasing by 22.236 percent and ages 41 to 65 increasing by 19.584 percent. Ages 26 to 40 decline early and remain negative at the mid-horizon reporting point, but recover to a 7.171 percent increase by the end of the horizon. Under Dark Horse, the total increases by 10.059 percent. Ages 18 to 25 rise by 12.486 percent and ages 41 to 65 rise by 8.763 percent, while ages 26 to 40 remain negative at minus 7.679 percent by the final reporting point, indicating incomplete recovery in the core working-age segment. Under Snail Pace and Lion's Den, the total remains negative and prime working-age losses dominate. By the end of the horizon, ages 26 to 40 decline by 24.164 percent under Snail Pace and 26.532 percent under Lion's Den, while ages 65 plus also fall sharply,

especially under Lion's Den at minus 19.634 percent. Appendix figures report the same reporting time points for population trends disaggregated by education, employment status, and gender.

### 3.4.3 IT (LOMBARDY) SUBREGION-LEVEL TOTAL POPULATION DYNAMICS ACROSS SCENARIOS

Figure 21 includes the four designed scenarios under Twin Transition and a Baseline comparison shown under both policy pathways.



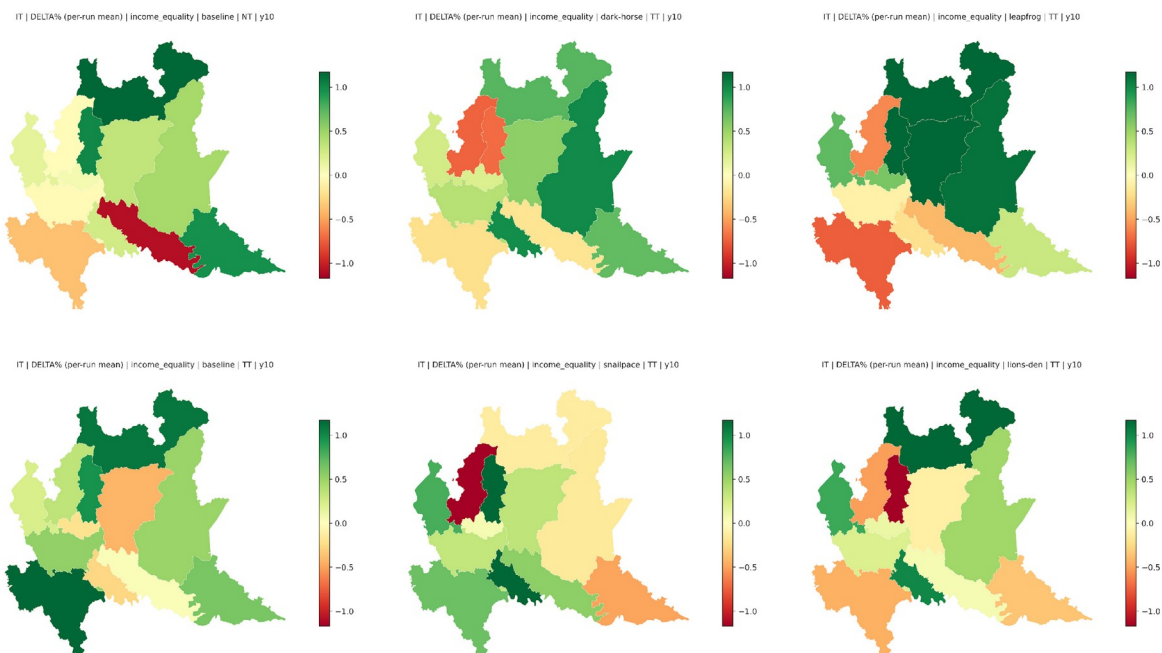
**Figure 21. IT (Lombardy) population change (%) after 10 years: cross-scenario comparison maps**

Figure 21 shows a clear spatial contrast across scenarios within Lombardy, with the most favourable context producing broad-based gains and adverse contexts producing widespread decline with localized resilience. Under Leapfrog, population change is positive across nearly all subregions, indicating a pilot-wide expansion pattern. Under Dark Horse, positive change remains dominant, but the magnitude varies across space and the map suggests a more uneven subregional gradient than under Leapfrog. Under Baseline, the surface is mixed. Some subregions show moderate gains while others remain near neutral or slightly negative, indicating uneven retention and replenishment even in the reference context. Under Snail Pace and especially Lion's Den, declines become more prevalent and more spatially continuous across the pilot

system, with only a subset of subregions remaining near neutral. Overall, the maps indicate that scenario context shapes both the scale and the internal geography of demographic change in Lombardy.

### 3.4.4 IT (LOMBARDY) SUBREGION-LEVEL INDICATORS CHANGE ACROSS SCENARIOS

Figure 22 includes the four designed scenarios under Twin Transition and the Baseline comparison maps, using the income equality indicator as an example.



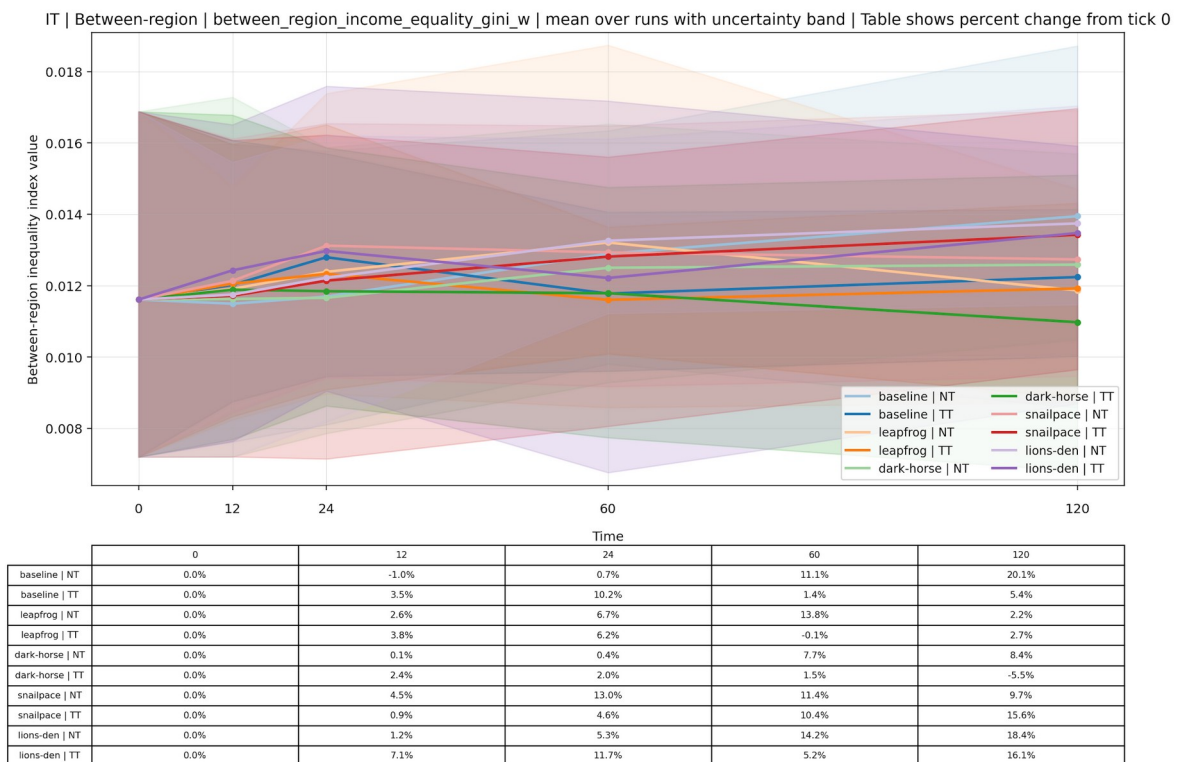
**Figure 22. IT (Lombardy) change in income equality indicator after 10 years: cross-scenario comparison maps**

Figure 22 indicates that income equality changes in Lombardy are spatially differentiated and only partially aligned with population change. Under Baseline, the map shows a mixed surface with both improvements and deterioration, including at least one subregion with a clearly negative shift in income equality, implying that near-neutral demographic outcomes can still coincide with uneven distributional change across space. Under Dark Horse, the pattern becomes more polarized, with one or more subregions improving while others deteriorate, suggesting that moderate favourable contexts can redistribute distributional pressure rather than producing uniform gains. Under Leapfrog, improvements are more prominent in several subregions, but deterioration remains visible in parts of the pilot region, indicating that broad

demographic expansion does not automatically translate into uniform distributional improvement. Under Snail Pace and Lion’s Den, the map continues to show mixed directions, with deterioration clustering in parts of the pilot region, consistent with scenario contexts that generate uneven compositional adjustment across subregions. Additional cross-scenario maps for other equality and sustainability indicators are provided in the Appendix.

### 3.4.5 IT (LOMBARDY) BETWEEN-SUBREGION INEQUALITY ACROSS SCENARIOS AND TIME HORIZONS

Figure 23 illustrates the between-subregion inequality in income equality within IT (Lombardy), showing how spatial dispersion evolves over time under different scenarios.



**Figure 23. IT (Lombardy) between-subregion income equality under Twin Transition and No Transition**

Figure 23 shows that between-subregion dispersion in income equality generally increases over time in Lombardy across most configurations, but the magnitude and direction differ by scenario. Baseline increases strongly by the final reporting point at 20.1 percent, indicating rising spatial differentiation in income equality even in the

reference context. Snail Pace and Lion's Den also increase substantially by the end of the horizon, reaching 15.6 percent and 16.1 percent under Twin Transition, consistent with stronger spatial dispersion under adverse contexts. Dark Horse is mixed, with a moderate increase under No Transition and a decline under Twin Transition by the final reporting point, suggesting that policy context can influence the direction of dispersion under some scenarios even when it does not dominate the demographic trajectory. Leapfrog remains comparatively stable, with only small increases by the final reporting point, implying that strong growth contexts may dampen the expansion of spatial dispersion in income equality. Uncertainty bands overlap across configurations, so differences should be interpreted as directional signals rather than sharp separations. The Appendix provides comparable between-subregion trajectories for other indicators and time points to support a consistent assessment of spatial differentiation across multiple dimensions.

---

### 3.4.6 IT (LOMBARDY) SCENARIO EFFECTS ON POPULATION, EQUALITY, AND SPATIAL DIFFERENTIATION

Across the five scenarios, IT (Italy, Lombardy) exhibits a strong scenario gradient in both the magnitude and the spatial distribution of population change. Leapfrog generates the largest long-run growth and supports broad-based cohort expansion, including strong gains in ages 18 to 25 and eventual recovery in ages 26 to 40. Dark Horse produces moderate growth that is driven mainly by youth and late working-age gains, while prime working-age recovery remains incomplete. Baseline is close to neutral and slightly positive by the final reporting point, but still exhibits uneven subregional outcomes. Snail Pace and Lion's Den generate persistent decline, with the strongest proportional losses concentrated in ages 26 to 40, implying pressure on labour-force renewal and medium-term demographic sustainability.

Spatially, the population change maps suggest that scenario context reshapes the internal geography of outcomes within Lombardy. Favourable scenarios produce broadly positive change across subregions, while adverse scenarios generate more widespread decline and a clearer contrast between resilient and vulnerable subregions. Distributional outcomes add a separate layer of spatial differentiation. Income equality changes remain mixed across scenarios and do not mechanically track population change, which is consistent with uneven compositional adjustment and differential sorting across subregions. Between-subregion dispersion in income equality tends to rise over time in several contexts, indicating that spatial differentiation in distributional outcomes can increase even when overall population change remains

close to neutral. Additional cross-scenario maps and inequality trajectories for the full set of equality and sustainability indicators are provided in the Appendix.

## 3.5 NETHERLANDS: GRONINGEN (NUTS - NL11)

### 3.5.1 NL (GRONINGEN) PILOT-LEVEL TOTAL POPULATION DYNAMICS ACROSS SCENARIOS

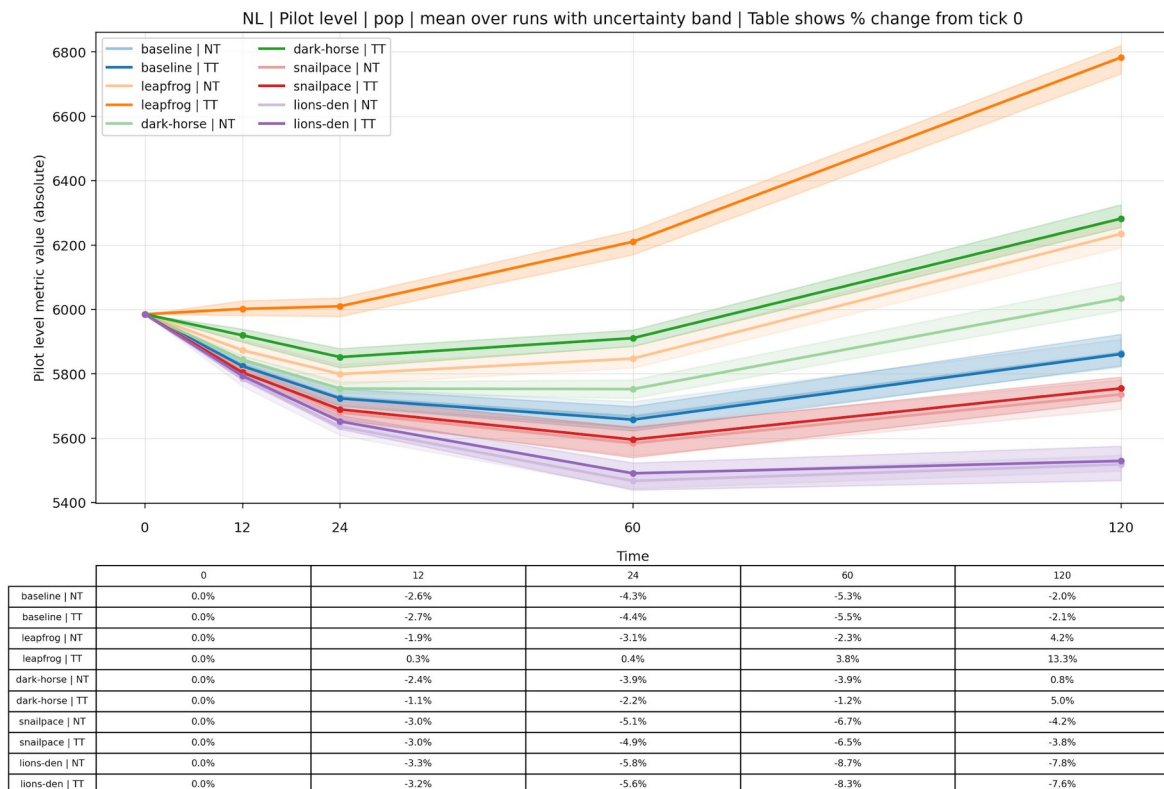


**Figure 24. NL (Groningen) total population trends over time**

Figure 24 summarizes pilot-level total population trajectories for Groningen across the reporting time points. In particular, it shows a pronounced scenario gradient in Groningen that widens steadily over time. Leapfrog is the only context that generates large long-run growth, ending at 13.3 percent above the baseline time point. Dark Horse ends positive but much smaller at 5.0 percent, while Baseline remains negative and ends around minus 2.1 percent. The adverse scenarios show stronger decline, with Snail Pace ending at minus 3.8 percent and Lion’s Den ending at minus 7.6

percent. Compared with the pilots where Baseline stays near neutral, Groningen's Baseline remains on the negative side, indicating that the reference context already implies net population pressure. The scenario ladder therefore separates favourable contexts that reverse or offset this pressure from adverse contexts that amplify it. The subsequent figures and tables follow the same set of reporting time points to support consistent comparison across outputs. In Deliverable D2.3, Groningen (NL11) is grouped under "Balanced Innovators", where well-rounded performance and robust governance coexist with comparatively weaker innovation ecosystems and moderate visibility relative to metropolitan leaders. The population trajectories in Figure 24 align with this profile, as scenario context determines whether Groningen's balanced strengths are sufficient to offset baseline demographic pressure or whether longer-run structural headwinds dominate outcomes. Consequently, adverse scenarios remain associated with persistent decline, whereas favourable scenarios generate a cumulative demographic advantage by the final reporting point.

---

### 3.5.2 NL (GRONINGEN) PILOT-LEVEL POPULATION TRENDS OVER TIME BY CERTAIN GROUPS

Figure 25 shows population trends over time by age group as an example.

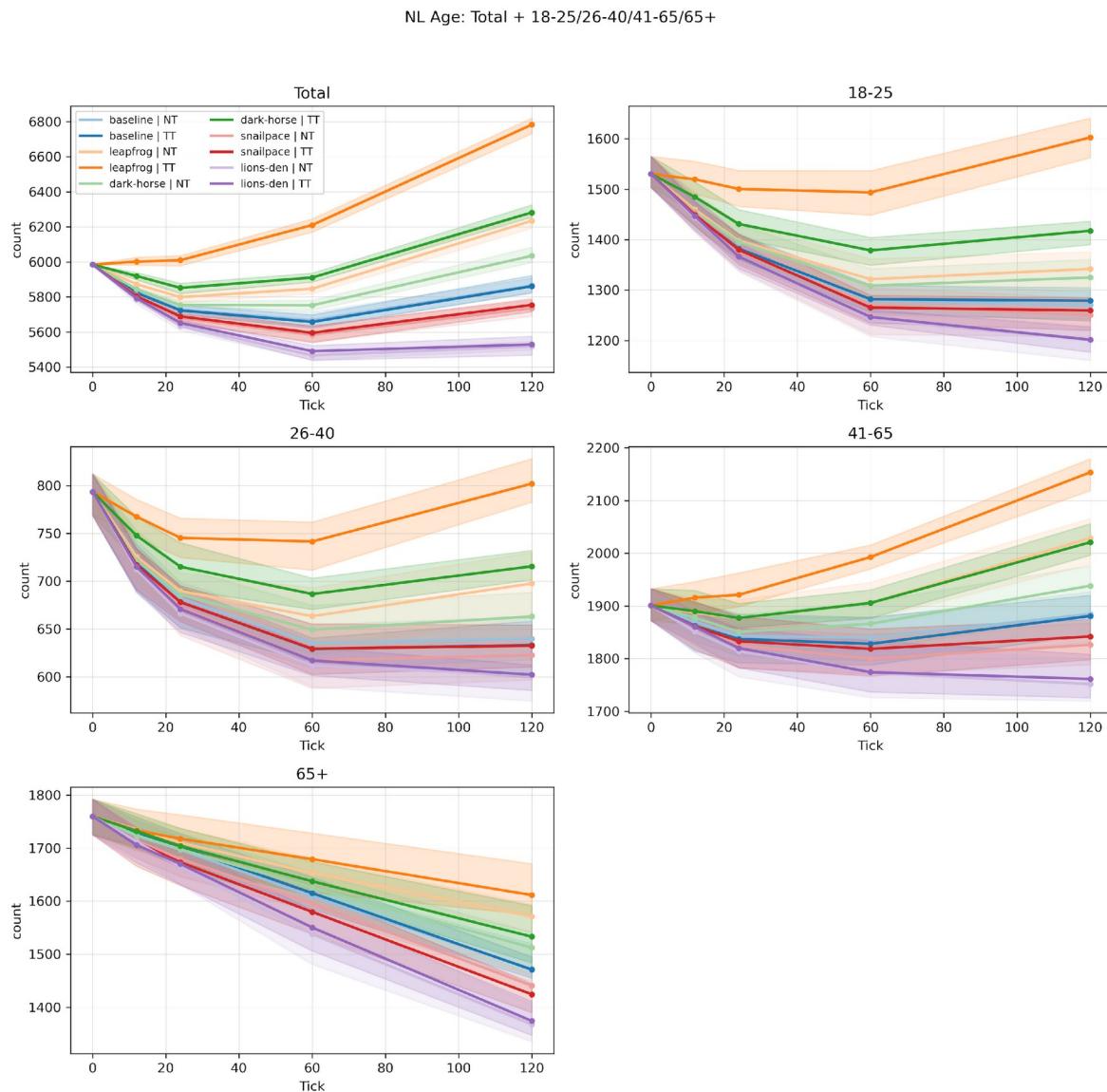


**Figure 25. NL (Groningen) population trends over time by age group**

Figure 25 indicates that the scenario spread in Groningen is strongly linked to cohort-specific dynamics, particularly the behaviour of younger and prime working-age groups. Under Leapfrog, total population growth is accompanied by clear gains in ages 41 to 65 and a late recovery for ages 18 to 25 and ages 26 to 40 by the final reporting point, despite early declines for both groups. Under Dark Horse, total population ends positive, but the age profile is uneven. Ages 41 to 65 increase clearly, while ages 18 to 25 and ages 26 to 40 remain negative at the end of the horizon, indicating incomplete recovery for early-career and prime working-age segments. Under Snail Pace and Lion’s Den, losses persist across all cohorts and become most pronounced for ages 18 to 25 and ages 26 to 40, implying that adverse contexts disproportionately reduce the segments

most closely linked to labour-force renewal. Results for population trends disaggregated by education, employment status, and gender are reported in the Appendix.

Table 15 provides more details of population trends over time by age group under Twin Transition.

**Table 15. NL (GRONINGEN) POPULATION TRENDS OVER TIME BY AGE GROUP UNDER TT**

**NL TT Age: % change vs t0**

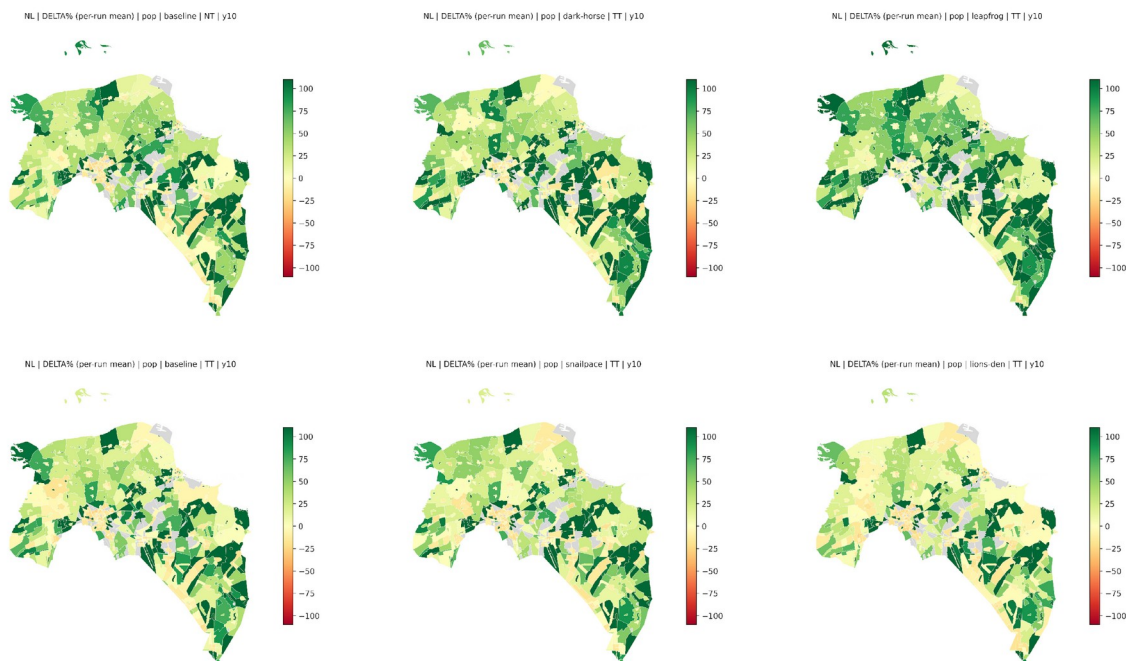
Scenario	Category	0	12	24	60	120
<b>leapfrog</b>	Total	0.000%	0.277%	0.413%	3.763%	13.328%
	18-25	0.000%	-0.699%	-1.947%	-2.392%	4.731%
	26-40	0.000%	-3.276%	-6.085%	-6.564%	1.071%
	41-65	0.000%	0.784%	1.063%	4.835%	13.288%
	65+	0.000%	-1.511%	-2.392%	-4.596%	-8.437%
<b>dark-horse</b>	Total	0.000%	-1.093%	-2.226%	-1.240%	4.964%
	18-25	0.000%	-2.973%	-6.489%	-9.907%	-7.365%
	26-40	0.000%	-5.783%	-9.890%	-13.494%	-9.840%
	41-65	0.000%	-0.573%	-1.252%	0.253%	6.308%
	65+	0.000%	-1.585%	-3.187%	-6.966%	-12.903%
<b>snailpace</b>	Total	0.000%	-3.021%	-4.939%	-6.506%	-3.846%
	18-25	0.000%	-5.280%	-9.835%	-17.323%	-17.696%
	26-40	0.000%	-9.638%	-14.552%	-20.713%	-20.310%
	41-65	0.000%	-2.083%	-3.561%	-4.335%	-3.099%
	65+	0.000%	-2.767%	-4.926%	-10.244%	-19.084%
<b>lions-den</b>	Total	0.000%	-3.201%	-5.564%	-8.257%	-7.614%
	18-25	0.000%	-5.456%	-10.723%	-18.539%	-21.486%
	26-40	0.000%	-9.903%	-15.472%	-22.250%	-24.140%
	41-65	0.000%	-2.120%	-4.251%	-6.660%	-7.328%
	65+	0.000%	-3.074%	-5.108%	-11.914%	-21.936%

Table 15 clarifies that Groningen’s long-run divergence is driven by whether scenarios can halt or reverse the decline in younger and prime working-age groups. Under Leapfrog, total population increases by 13.328 percent by the final reporting point, with ages 41 to 65 increasing by 13.288 percent. Ages 18 to 25 and ages 26 to 40 both decline early and remain negative at the mid-horizon reporting point, but recover slightly by the end of the horizon to 4.731 percent and 1.071 percent, respectively. Under Dark Horse, total population increases by 4.964 percent, but ages 18 to 25 decline by 7.365 percent and ages 26 to 40 decline by 9.840 percent by the final reporting point, while ages 41 to 65 increase by 6.308 percent. Under Snail Pace and Lion’s Den, total population remains negative and losses concentrate in ages 18 to 25 and ages 26 to 40. By the end of the horizon, ages 18 to 25 decline by 17.696 percent under Snail Pace and

21.486 percent under Lion’s Den, while ages 26 to 40 decline by 20.310 percent and 24.140 percent, respectively. Appendix figures report the same reporting time points for population trends disaggregated by education, employment status, and gender.

### 3.5.3 NL (GRONINGEN) SUBREGION-LEVEL TOTAL POPULATION DYNAMICS ACROSS SCENARIOS

Figure 26 includes the four designed scenarios under Twin Transition and a Baseline comparison shown under both policy pathways.



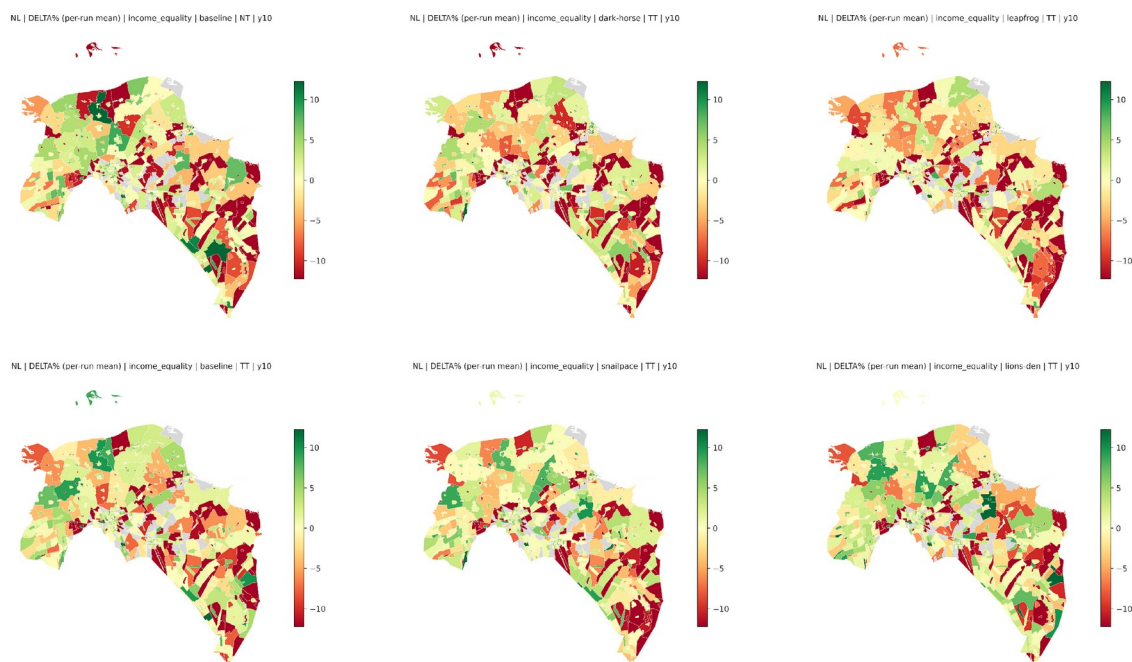
**Figure 26. NL (Groningen) population change (%) after 10 years: cross-scenario comparison maps**

Figure 26 shows that scenario differences translate into a heterogeneous spatial surface across Groningen, with localized pockets of stronger gain or loss within the pilot system. Under Leapfrog, the surface is dominated by positive change across many local units, indicating broad-based improvement in retention or replenishment conditions. Under Dark Horse, positive and near-neutral outcomes remain visible, but the surface is more mixed, suggesting that moderate favourable contexts do not lift all places equally. Under Baseline, the spatial pattern remains mixed with many units close to neutral and some pockets of decline, consistent with the pilot-level Baseline trajectory remaining negative. Under Snail Pace and Lion’s Den, negative change becomes more prevalent and more spatially continuous, indicating that adverse contexts amplify decline across a larger share of the internal geography of Groningen. Overall, the cross-scenario maps

indicate that scenario context affects both the magnitude of population change and the degree to which gains and losses concentrate spatially within the pilot.

### 3.5.4 NL (GRONINGEN) SUBREGION-LEVEL INDICATORS CHANGE ACROSS SCENARIOS

Figure 27 includes the four designed scenarios under Twin Transition and the Baseline comparison maps, using the income equality indicator as an example.



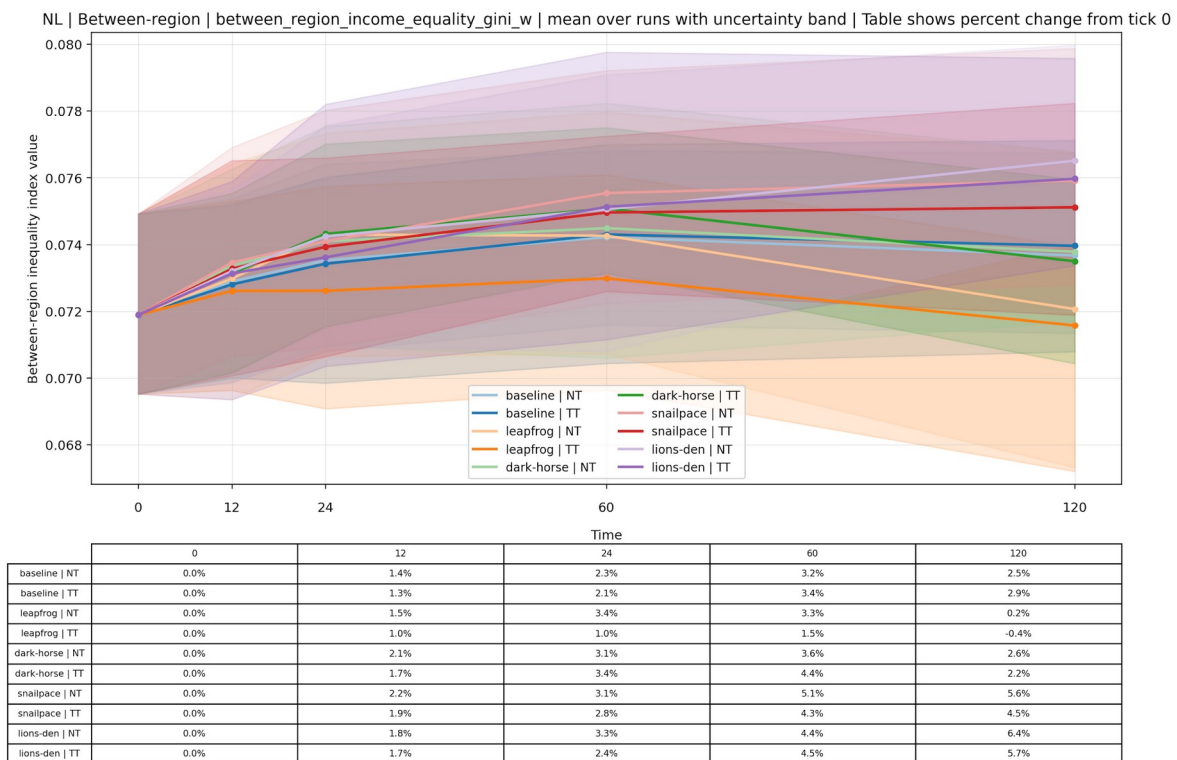
**Figure 27. NL (Groningen) change in income equality indicator after 10 years: cross-scenario comparison maps**

Figure 27 indicates that income equality changes in Groningen are spatially heterogeneous and do not mechanically track the population change surface. Across scenarios, the maps show a patchwork configuration with frequent local switches between improvement and deterioration, indicating uneven compositional adjustment across space. Under Baseline, deterioration appears widely distributed across the pilot system with pockets of improvement, suggesting that a near-neutral demographic surface can still coincide with uneven distributional change. Under Dark Horse and Leapfrog, the pattern remains mixed and does not converge to a single direction, implying that favourable demographic trajectories can coexist with localized deterioration in income equality. Under Snail Pace and Lion’s Den, deterioration remains prevalent and continues to appear in clusters, consistent with scenario

contexts that generate stronger demographic stress and uneven distributional adjustment across the internal geography of Groningen. Additional cross-scenario maps for equality and sustainability indicators are provided in the Appendix.

### 3.5.5 NL (GRONINGEN) BETWEEN-SUBREGION INEQUALITY ACROSS SCENARIOS AND TIME HORIZONS

Figure 28 illustrates the between-subregion inequality in income equality within NL (Groningen), showing how spatial dispersion evolves over time under different scenarios.



**Figure 28. NL (Groningen) between-subregion income equality under Twin Transition and No Transition**

Figure 28 shows that between-subregion dispersion in income equality increases gradually over time in Groningen across most scenarios, but differences remain moderate in magnitude. Baseline shows a small increase by the final reporting point, and Dark Horse and Snail Pace also show increasing dispersion by the end of the horizon. Lion’s Den shows one of the larger increases by the final reporting point, consistent with stronger spatial differentiation under the most adverse context. Leapfrog remains comparatively stable and ends close to its initial level, with very small

net change by the final reporting point, suggesting that the most favourable scenario context does not amplify spatial dispersion in income equality and may slightly dampen it relative to adverse contexts. Uncertainty bands overlap across configurations, so differences should be interpreted as directional signals rather than sharp separations. The Appendix provides comparable between-subregion trajectories for other indicators and time points to support a consistent assessment of spatial differentiation across multiple dimensions.

---

### 3.5.6 NL (GRONINGEN) SCENARIO EFFECTS ON POPULATION, EQUALITY, AND SPATIAL DIFFERENTIATION

Across the five scenarios, NL (Netherlands, Groningen) exhibits a strong scenario gradient in long-run population change, separating contexts that reverse baseline decline from contexts that amplify it. Leapfrog generates the strongest positive trajectory and supports cohort recovery, including late-horizon improvements for ages 18 to 25 and ages 26 to 40, while Dark Horse yields moderate growth driven primarily by gains in ages 41 to 65 and does not reverse declines in younger and prime working-age groups. Baseline remains negative, and Snail Pace and Lion's Den generate increasingly adverse demographic outcomes, with the largest proportional losses concentrated in ages 18 to 25 and ages 26 to 40, indicating pressure on labour-force renewal and medium-term demographic sustainability.

Spatially, the population change maps indicate that scenario context reshapes the internal geography of gains and losses across Groningen. Favourable scenarios produce more widespread positive change, while adverse scenarios increase the prevalence and spatial continuity of decline, with localized pockets of relative resilience. Distributional outcomes add an additional layer of spatial differentiation. Income equality changes remain mixed across space in all scenarios and do not mechanically follow population change patterns, which is consistent with uneven compositional adjustment at fine spatial scales. Between-subregion dispersion in income equality changes modestly in level but tends to rise under adverse contexts, while remaining relatively stable under the most favourable scenario. Additional cross-scenario maps and inequality trajectories for the full set of equality and sustainability indicators are provided in the Appendix.

## 4 INTEGRATION OF RELEVANT RRI PILLARS

MOBI-TWIN places the societal dimension of spatial mobility at the core of its research activities. It aligns the project's activities with the pillars of Responsible Research and Innovation (RRI) — science education, gender equality, governance, open science, public engagement and ethics — to ensure that outcomes, outputs and impacts meet as much as possible the needs of society (MOBI-TWIN D4.1).

The RRI pillars mainstreamed into the activities described in this report are gender equality, open science and ethics.

### *The integration of the gender dimension*

Gender is systematically integrated in the empirical analysis. In addition to age, education, and employment status, population trends are disaggregated by gender in the model outputs and reported in the Appendix. This ensures that scenario-driven spatial mobility dynamics are assessed not only in aggregate demographic terms but also in terms of differential impacts on women and men. Where relevant, gender-specific trajectories are examined in relation to working-age cohorts, labour-force renewal, and retention dynamics, recognizing that spatial mobility and regional inequality can affect women and men differently due to structural labour-market segmentation, care responsibilities, and differential exposure to economic shocks.

Population-weighted Gini and coefficient of variation measures are interpreted alongside gender-disaggregated demographic trends, preventing the conflation of spatial convergence with social equity.

Overall, integrating the gender dimension ensures that scenario comparisons do not treat population and inequality outcomes as socially neutral aggregates, but as processes embedded in gendered demographic and labour-market structures.

### *The integration of open science*

Standardized maps, tables, and visual comparisons make spatial differences clear and support transparent communication with stakeholders. Using fixed reporting points and consistent indicators allows systematic comparisons across scenarios, helping regional actors identify patterns of resilience, vulnerability, and divergence within their territories.

The use of EU-SILC as the baseline microdata backbone reinforces open science practices. EU-SILC provides a harmonized and publicly documented dataset capturing key socioeconomic attributes and inequality measures, enabling reproducible initialization of the agent population. Behavioural enrichment from MOBI-TWIN adds migration intentions and preference variables to EU-SILC records without altering baseline distributions, ensuring simulations are both transparent and behaviourally realistic.

All outputs - produced as static maps, tables, and aggregated indicators suitable for public reporting - adhere to FAIR principles, ensuring that results can be reused, methods replicated in other regional contexts, and stakeholders can verify findings while fully respecting data protection requirements.

#### *The integration of ethics*

The work carried out in T3.4 followed the ethical standards set by the GA article 14 (Ethics and Values), specific ethics rules are set out in Annex 5.

All analyses are conducted at aggregated regional and subregional levels, with no processing of personal-level data. Where microdata inform simulations, anonymization and GDPR-compliant procedures are applied.

## **5 CONCLUSIONS AND NEXT STEPS**

Across the five pilot regions, the results indicate a consistent scenario gradient in long-run population outcomes, with widening divergence over the ten-year horizon. In Central Macedonia (EL52), Leapfrog ends with a 20.0 percent population increase while Lion's Den ends with a 12.5 percent decline, forming a spread exceeding 30 percentage points by the final reporting time point. Similar ordering appears in Castilla-la Mancha (ES42), where Leapfrog reaches 24.4 percent and Lion's Den reaches minus 6.6 percent, and in Lombardy (ITC4), where Leapfrog reaches 20.6 percent and Lion's Den reaches minus 6.8 percent. In North and East Finland (FI1D), the gradient is also pronounced, with Leapfrog ending at 17.6 percent and Lion's Den at minus 11.0 percent. Groningen (NL11) shows the same ordering but with a different baseline position. Baseline remains negative at minus 2.1 percent in NL11, while Leapfrog is positive at 13.3 percent and Lion's Den reaches minus 7.6 percent, indicating that in this pilot, favourable contexts primarily act to offset an underlying declining reference trajectory rather than to create immediate growth. These cross-pilot gradients are also consistent with the regional typologies reported in Deliverable D2.3: EL52 is classified as a "Structurally Lagging and Peripheral Region", ES42 and ITC4 as "Economies in

Structural Transition”, and FI1D and NL11 as “Balanced Innovators”. In this sense, the typologies provide a concise contextual baseline for interpreting why the same scenario ladder can yield different baseline positions and different magnitudes of long-run divergence across pilots.

Cohort-specific dynamics explain a large share of scenario divergence and clarify why favourable pilot-level trajectories can still carry demographic risks. Across pilots, adverse scenarios concentrate losses in ages 18 to 25 and ages 26 to 40. For example, under the most adverse context, ages 18 to 25 fall by 20.5 percent in EL52, 25.4 percent in ES42, 22.5 percent in FI1D, and 21.5 percent in NL11, while ages 26 to 40 fall even more sharply, including 25.8 percent in EL52, 18.3 percent in FI1D, 26.5 percent in ITC4, and 24.1 percent in NL11. Favourable contexts show more varied patterns of recovery. In ES42, Leapfrog generates positive end-of-horizon changes for both ages 18 to 25 at 13.1 percent and ages 26 to 40 at 18.5 percent, while in FI1D the same scenario yields strong total growth but only modest recovery for ages 26 to 40 at 2.9 percent, indicating that some pilots can improve totals mainly through older working-age expansion. A similar asymmetry appears in NL11 under Dark Horse, where total population ends positive at 5.0 percent but ages 18 to 25 and ages 26 to 40 remain negative at minus 7.4 percent and minus 9.8 percent, respectively. These patterns imply that demographic sustainability risks can persist even when pilot-level totals improve, especially when youth and prime working-age recovery remains incomplete.

Spatially, scenario context reshapes the internal geography of gains and losses within each pilot rather than shifting outcomes uniformly. The cross-scenario population change maps show that favourable contexts tend to generate more widespread positive change, while adverse contexts expand the prevalence and spatial continuity of decline, leaving only localized pockets of relative resilience. At the same time, distributional outcomes do not mechanically track population change, and favourable scenarios can coincide with persistent or intensified internal differentiation. This is visible in the income equality change maps, which remain spatially heterogeneous across all pilots, including under favourable scenarios. It is also reflected in the between-subregion dispersion trajectories. In some cases, dispersion rises under adverse contexts, as in EL52 where Lion’s Den shows a clearer increase by the end of the horizon, and in NL11 where the most adverse context ends with one of the larger increases. In other cases, dispersion can decline under favourable contexts, as in ES42 where Leapfrog shows a downward trend by the final reporting point, and in FI1D where Leapfrog under Twin Transition ends at minus 4.4 percent. These contrasts indicate that scenario-driven demographic improvement does not guarantee reduced spatial dispersion in

distributional outcomes, and that pilots can exhibit different trade-offs between aggregate retention and within-pilot spatial equity.

From the perspective of preference structure, the interpretation of policy leverage in this deliverable relies on the empirical preference weights derived from MOBI-TWIN data. These weights define how strongly different preference dimensions enter the modeled response channels and therefore shape how transition pathways translate into behavioural change. The report does not present separate results for single digital transition or single green transition pathways, so the preference discussion is grounded in the empirical weight structure rather than in direct pathway comparisons. In this sense, the weights provide a consistent empirical rationale for why policy contexts that target higher-weighted preference dimensions can produce larger changes in mobility outcomes within the same scenario, while contexts that target lower-weighted dimensions may yield slower or more spatially uneven effects.

Finally, the temporal profile of impacts suggests that proactive transition contexts should be interpreted as medium- to long-term strategies rather than short-term interventions. Across pilots, scenario differences and policy-related differences are typically modest at early time points and become more pronounced toward the end of the horizon, reflecting cumulative effects on retention, compositional change, and subregional redistribution. This is particularly important for pilots with an underlying declining reference trajectory, such as NL11, where early stabilization is more plausible than rapid reversal. The Appendix provides higher-resolution and multi-dimensional evidence supporting these conclusions, including disaggregated population results by education, employment status, and gender, as well as additional cross-scenario maps and between-subregion inequality trajectories for the full indicator set across scenarios, time points, and policy pathways.

## 6 REFERENCES

Angione, C., Silverman, E., & Yaneske, E. (2022). Using machine learning as a surrogate model for agent-based simulations. *PLOS ONE*, 17(2), e0263150.

<https://doi.org/10.1371/journal.pone.0263150>

Ballas, D., Broomhead, T., & Jones, P. (2019). Spatial Microsimulation and Agent-Based Modelling. In H. Briassoulis, D. Kavroudakis, & N. Soulakellis (Eds.), *The Practice of Spatial Analysis: Essays in memory of Professor Pavlos Kanaroglou* (pp. 69-84). Cham: Springer, [https://link.springer.com/chapter/10.1007/978-3-319-89806-3\\_4](https://link.springer.com/chapter/10.1007/978-3-319-89806-3_4)

Bektaş, A., Piana, V., & Schumann, R. (2021). A meso-level empirical validation approach for agent-based computational economic models drawing on micro-data: A use case with a mobility mode-choice model. *SN Business & Economics*, 1, Article 80.

<https://doi.org/10.1007/s43546-021-00083-4>

Bevilacqua, C., Ou, Y., Pizzimenti, P., & Anversa, G. (2020). Contextualizing transition: A multiscale approach to making resilience-oriented and place-sensitive strategies. In C. Bevilacqua, F. Calabrò, & L. Della Spina (Eds.), *New metropolitan perspectives* (pp. 47–67). Springer. [https://doi.org/10.1007/978-3-030-52869-0\\_5](https://doi.org/10.1007/978-3-030-52869-0_5)

Blume, L. (2015). Agent-based models for policy analysis. In the Committee on the Assessment of Agent-Based Models to Inform Tobacco Product Regulation, *Assessing the use of agent-based models for tobacco regulation* (Appendix B). National Academies Press.

Brown, D. G., Riolo, R., Robinson, D. T., North, M., & Rand, W. (2005). Spatial process and data models: Toward integration of agent-based models and GIS. *Journal of Geographical Systems*, 7, 25–47. <https://doi.org/10.1007/s10109-005-0148-5>

Bruneckienė, J., Palekienė, O., Simanavičienė, Ž., & Rapsikevičius, J. (2018). Measuring regional resilience to economic shocks by index. *Engineering Economics*, 29(4), 418–427. <https://doi.org/10.5755/j01.ee.29.4.18731>

Chopra, A., Kumar, S., Giray-Kuru, N., Raskar, R., & Quera-Bofarull, A. (2024). On the limits of agency in agent-based models (arXiv:2409.10568). *arXiv*.

<https://doi.org/10.48550/arXiv.2409.10568>

Dilaver, Ö. (2015). From participants to agents: Grounded simulation as a mixed-method research design. *Journal of Artificial Societies and Social Simulation*, 18(1), 15.

<https://www.jasss.org/18/1/15.html>

Dilaver, Ö., & Gilbert, N. (2023). Unpacking a black box: A conceptual anatomy framework for agent-based social simulation models. *Journal of Artificial Societies and Social Simulation*, 26(1), 4. <https://doi.org/10.18564/jasss.4998>

Gedikli, A., Taş, N. B., & Yalçın, A. K. (2022). Breaking the vicious cycle between migration and environmental degradation: The role of government. In *Analyzing sustainability in peripheral, ultra-peripheral, and low-density regions* (pp. xx–xx). IGI Global. <https://doi.org/10.4018/978-1-6684-4548-8.ch009>

Grimm, V., Railsback, S. F., Vincenot, C. E., Berger, U., Gallagher, C., DeAngelis, D. L., Edmonds, B., Ge, J., Giske, J., Groeneveld, J., Johnston, A. S. A., Milles, A., Nabe-Nielsen, J., Polhill, J. G., Radchuk, V., Rohwäder, M.-S., Stillman, R. A., Thiele, J. C., & Ayllón, D. (2020). The ODD protocol for describing agent-based and other simulation models: A second update to improve clarity, replication, and structural realism. *Journal of Artificial Societies and Social Simulation*, 23(2), 7. <https://doi.org/10.18564/jasss.4259>

Hüther, M. (2019). Wozu Regionalpolitik? Wo liegt das Problem? *Wirtschaftsdienst*, 99(Suppl. 1), 3–9. <https://doi.org/10.1007/s10273-019-2425-9>

Jager, W., Janssen, M. A., De Vries, H. J. M., De Greef, J., & Vlek, C. A. (2000). Behaviour in commons dilemmas: Homo economicus and Homo psychologicus in an ecological-economic model. *Ecological economics*, 35(3), 357-379. [https://doi.org/10.1016/S0921-8009\(00\)00220-2](https://doi.org/10.1016/S0921-8009(00)00220-2)

Jager, W. (2021). Using agent-based modelling to explore behavioural dynamics affecting our climate. *Current opinion in psychology*, 42, 133-139. <https://doi.org/10.1016/j.copsyc.2021.06.024>

Kanj, H. (2016). *Contribution to risk analysis related to the transport of hazardous materials by agent-based simulation* (Doctoral dissertation, Université Grenoble Alpes). <https://tel.archives-ouvertes.fr/tel-01447765>

Klabunde, A., & Willekens, F. (2016). Decision-making in agent-based models of migration: State of the art and challenges. *European Journal of Population*, 32, 73–97. <https://doi.org/10.1007/s10680-015-9362-0>

Kourtit, K., Nijkamp, P., & Suzuki, S. (2021). The science of space: New endeavours in regional science. *Asia-Pacific Journal of Regional Science*, 5(1), 149–153. <https://doi.org/10.1007/s41685-020-00188-y>

Kuttler, T. (2020). The spatial dimension of mobility poverty. In T. Kuttler & M. Moraglio (Eds.), *Re-thinking mobility poverty* (pp. 1–20). Routledge.

- Ligmann-Zielinska, A., & Jankowski, P. (2007). Agent-based models as laboratories for spatially explicit planning policies. *Environment and Planning B: Planning and Design*, 34(2), 316–335. <https://doi.org/10.1068/b32088>
- Macal, C. M., & North, M. J. (2010). Tutorial on agent-based modelling and simulation. *Journal of Simulation*, 4(3), 151–162. <https://doi.org/10.1057/jos.2010.3>
- Markowska-Manista, U., & Sawicki, K. (2022). Introduction. *Polish Journal of Educational Studies*, 74(1), 1–4. <https://doi.org/10.2478/poljes-2022-0001>
- Martin, R., & Sunley, P. (2015). On the notion of regional economic resilience: Conceptualization and explanation. *Journal of Economic Geography*, 15(1), 1–42. <https://doi.org/10.1093/jeg/lbu015>
- Martin, R., & Sunley, P. (2020). Regional economic resilience: Evolution and evaluation. In *Handbook of regional and urban economics* (pp. 10–35). Edward Elgar Publishing. <https://doi.org/10.4337/9781785360862.00007>
- McCulloch, J., Ge, J., Ward, J., Heppenstall, A., Polhill, J. G., & Malleson, N. (2022). Calibrating agent-based models using uncertainty quantification methods. *Journal of Artificial Societies and Social Simulation*, 25(2), 1. <https://doi.org/10.18564/jasss.4791>
- National Research Council. (2010). *Understanding the changing planet: Strategic directions for the geographical sciences*. National Academies Press. <https://doi.org/10.17226/12860>
- Quang, L. A., Jung, N., Cho, E. S., Choi, J. H., & Lee, J. W. (2018). Agent-based models in social physics. *Journal of the Korean Physical Society*, 72, 1272–1280. <https://doi.org/10.3938/jkps.72.1272>
- Steinbacher, M., Raddant, M., Karimi, F., Camacho Cuena, E., Alfarano, S., Iori, G., & Lux, T. (2021). Advances in the agent-based modeling of economic and social behavior. *SN Business & Economics*, 1, Article 99. <https://doi.org/10.1007/s43546-021-00103-3>
- Troost, C., Huber, R., Bell, A. R., van Delden, H., Filatova, T., Bao Le, Q., Lippe, M., Niamir, L., Polhill, J. G., Sun, Z., & Berger, T. (2023). How to keep it adequate: A protocol for ensuring validity in agent-based simulation. *Environmental Modelling & Software*, 159, 105559. <https://doi.org/10.1016/j.envsoft.2022.105559>
- Turgut, Y., & Bozdağ, C. E. (2023). A framework proposal for machine learning–driven agent-based models through a case study analysis. *Simulation Modelling Practice and Theory*, 123, 102707. <https://doi.org/10.1016/j.simpat.2022.102707>

United Nations Economic Commission for Europe. (2020). Spatial planning for sustainable urban mobility and accessibility. In *A handbook on sustainable urban mobility and spatial planning* (pp. 15–56). United Nations.

<https://doi.org/10.18356/6ca66c92-en>

Williams, R. A. (2018). Lessons learned on development and application of agent-based models of complex dynamical systems. *Simulation Modelling Practice and Theory*, 83, 201–212. <https://doi.org/10.1016/j.simpat.2017.11.001>

Woźniak, M. (2020). Virtualising space: New directions for applications of agent-based modelling in spatial economics. *Acta Universitatis Lodzianae. Folia Oeconomica*, 1(346), 7–26. <https://doi.org/10.18778/0208-6018.346.01>

Xu, J. (2008). *A multi-agent based multi-layer distributed hybrid planning model for demand responsive transport systems* (Doctoral dissertation, INSA de Rouen).

<https://tel.archives-ouvertes.fr/tel-00558769>



## TWIN TRANSITION AND CHANGING PATTERNS OF SPATIAL MOBILITY: A REGIONAL APPROACH

The Partners of the MOBI-TWIN Consortium:

Name	Country
White Research SRL	Belgium
Aristotelio Panepistimio Thessalonikis	Greece
Rijksuniversiteit Groningen	The Netherlands

Universitat de Barcelona	Spain
Helsingin Yliopisto	Finland
Fondation Europeene de la Science	France
Politecnico di Milano	Italy
Erevnitiko Panepistimiako Institouto Periferiakias Anaptixis	Greece
Acceligenca Ltd.	Cyprus

**CONNECT WITH MOBI-TWIN FOR MORE UPDATES:**

[LinkedIn](#), [Twitter](#), [Website](#)